Impact of irrigation frequency and substrate composition on green canopy cover of extensive and intensive green roofs in Manhattan, Kansas (USA)

by

Muhaiminul Islam

B.Arch., Khulna University, 2016

M.Sc., Khulna University, 2018

A THESIS

submitted in partial fulfillment of the requirements for the degree

MASTER OF LANDSCAPE ARCHITECTURE

Department of Landscape Architecture and Regional & Community Planning

College of Architecture, Planning and Design

KANSAS STATE UNIVERSITY
Manhattan, Kansas

2026

Approved by:

Major Professor
Associate Professor Lee R. Skabelund

Copyright

Abstract

Supporting the vegetation while minimizing supplemental irrigation is one of the major goals of sustainable green roof maintenance. Within the tallgrass prairie of the Flint Hills ecoregion (Great Plains, USA), supplemental irrigation and vegetation cover dynamics are critical due to the hot summers, high evaporative demand, and multi-week dry spells. In addition to supplemental irrigation, substrate depth and substrate type or mix are also critical variables influencing vegetation performance. There is insufficient research on how these variables influence vegetative cover. This thesis evaluates the canopy cover performance of shallower (extensive: ~10 cm deep) and deeper (intensive: ~20 cm deep) green roofs with two substrate types (lighter and denser) managed under two types of minimal supplemental irrigation (78 total gallons versus 26 total gallons added), using a mature, in-situ experimental green roof planted with prairie vegetation at Kansas State University. Collecting green canopy cover data is a methodological challenge in green roof research. This study applied multiple methods of green canopy cover analysis (NDVI data from UAS images, green cover data from UAS and iPhone images, and visual observations) to explore the strengths and shortcomings. In addition, this study explored substrate temperature and moisture dynamics and their relationships with green canopy cover. The methods did not always agree, and the disagreement extended to which factors appeared most influential. In the green-cover analyses, substrate type and irrigation frequency were the dominant controls and substrate depth was secondary, whereas the NDVI analysis of all 72 plots identified substrate depth as a major factor for vegetation health. This divergence, which reflects both the larger plot count available for NDVI and the different property each method measures, shows that the choice of measurement method materially affects the conclusions drawn and points to clear directions for future monitoring.

Table of Contents

List of Figures

List of Tables

List of Abbreviations

Abbreviation	Definition
AI	Artificial intelligence
ANOVA	Analysis of variance
APD-EGR	College of Architecture, Planning and Design Experimental Green Roof
ASTM	American Society for Testing and Materials (ASTM International)
AUC	Area under the (cover) curve
DJI	Da-Jiang Innovations (manufacturer of the Mavic 3 Multispectral system)
FAO	Food and Agriculture Organization of the United Nations
FVC	Fractional Vegetation Cover
GSD	Ground sampling distance
KSU / K-State	Kansas State University
METER	METER Group, Inc. (sensor and data-logger manufacturer)
MLA	Master of Landscape Architecture
NDVI	Normalized Difference Vegetation Index
NIR	Near-infrared
NRES	Natural Resources and Environmental Sciences
PAW	Plant-available water
PAWC	Plant-available water capacity
QGIS	Quantum Geographic Information System
RGB	Red, green, blue (visible-spectrum imagery)
TEROS	Soil moisture and temperature sensor (Teros 12, METER Group)
UAS	Unmanned aircraft system (also unmanned aerial system)
UHI	Urban heat island
U.S. / USA	United States of America
VWC	Volumetric water content
ZENTRA (ZL6)	Data logger (ZENTRA ZL6, METER Group)

Definition of Key Terms

The following green roof and soil-water literature-related terms are used throughout this thesis with the specific meanings defined below:

Extensive green roof: A green roof with a shallow substrate profile, typically on the order of 7 to 15 cm (approximately 3 to 6 inches) deep, supporting low-growing, drought-tolerant vegetation and requiring minimal maintenance. In this study, the extensive treatment corresponds to the 4-inch (~10 cm) plots.

Intensive green roof: A green roof with a relatively deep substrate profile, generally exceeding 20 to 30 cm (8-12 inches), capable of supporting a wider palette of vegetation but imposing greater structural loading and maintenance demands. In this study, the deeper 8-inch (~20 cm) plots represent the intensive end of the tested range.

Semi-intensive green roof: A green roof of intermediate substrate depth, roughly 15 to 20 cm (6 to 8 inches), combining characteristics of extensive and intensive systems. The 6-inch plots assessed by unmanned aircraft system imagery in this study fall within this category.

Green canopy cover: The proportion of a plot's surface area occupied by living green vegetation when viewed from above, expressed as a percentage. It is the primary response variable of this study. A critical indicator of vegetation performance and ecosystem-service delivery.

Substrate: The engineered growing medium of a green roof, distinct from natural soil, formulated for low weight, adequate drainage, and sufficient water retention. This study compares a designed substrate (Kansas BuildEx) and a commercial substrate (Rooflite).

Volumetric water content (VWC): The volume of water held per unit volume of substrate, expressed as a percentage or as cubic centimeters of water per cubic centimeter of substrate. VWC was monitored hourly in every instrumented plot.

Field capacity: The volumetric water content a substrate retains after free drainage under gravity has effectively ceased, representing the upper limit of water readily available to plants.

Wilting point: The volumetric water content below which plants can no longer extract water from the substrate quickly enough to meet demand, representing the lower limit of plant-available water.

Plant-available water capacity (PAWC): The quantity of water a substrate can store and release to plants, defined as the difference between field capacity and wilting point. It expresses a substrate's capacity to buffer plants against dry intervals.

In-situ water behavior: The way a substrate stores and supplies water under actual rooftop field conditions, as opposed to its water retention measured on isolated samples in the laboratory. A central finding of this study is that in-situ behavior can diverge from laboratory retention, as the substrate with lower laboratory retention held more water on the APD-EGR.

Evapotranspiration: The combined loss of water from a vegetated surface through evaporation from a substrate and transpiration from plant foliage. Evapotranspiration underlies the cooling benefit of a green roof and depletion of substrate moisture between water inputs.

Factor: An independent variable that is deliberately manipulated across defined levels, magnitudes, or types to test its effect on the response. This study has three factors, each with two levels/magnitudes or types: substrate depth (shallower and deeper), substrate type (two distinct types of green roof growing media), and irrigation frequency (more and less).

Factorial design: An experimental design that tests every combination of the levels of two or more factors, allowing both the individual effect of each factor and the interactions among factors to be estimated. This study uses a 2^3 factorial design of three two-level factors.

Marginal (main) effect: The average effect of one factor on the response, taken across the levels of the other factors. The reported differences between depth, substrate, and irrigation levels are marginal effects.

Area under the cover curve (AUC): A summary measure that integrates green canopy cover over the full measurement period, so that vegetation sustaining cover over time is distinguished from vegetation reaching a brief peak. AUC complements the seasonal mean as a response variable.

The irrigation gap: The 39-day interval from 2 July to 10 August 2025 during which the less-irrigated plots received no supplemental water. Coinciding with peak summer heat, it is treated in this study as the central explanatory event of the growing season.

Senescence: The natural late-season decline and browning of vegetation associated with the onset of dormancy, as distinct from mid-season decline driven by moisture and heat stress. This study adopts 1 October as the functional end-of-season endpoint to separate senescence from stress-driven decline.

Tallgrass prairie and Flint Hills ecoregion: The regionally characteristic grassland ecosystem of the study area that lies within the U.S. Great Plains. The Flint Hills ecoregion is marked by hot summers, high summer evaporative demand, and episodic drought. This climatic setting is the context in which minimal-irrigation green roof performance is evaluated.

Acknowledgements

This thesis would not have been possible without the guidance of my major professor, Associate Professor Lee R. Skabelund. He introduced me to the College of Architecture, Planning and Design Experimental Green Roof and shaped this research at every stage through his questions, his patience, and his long commitment to green roof scholarship in the tallgrass prairie. This study was supported principally through his two Mary K. Jarvis Research Chairs in Landscape Architecture (2015-2018 and 2022-2026) and my Jarvis Fellowship (July 2023 to June 2026), and it forms one part of the wider research program that the Mary K. Jarvis funding has sustained. Thank you to Mary K. Jarvis and to all who made this funding possible, including Jody Hodges and Huston Gibson!

I am deeply grateful to the members of my committee. Dr. Mary Beth Kirkham, Distinguished Professor in the Department of Agronomy, brought to this work a depth of understanding of soil, plant, and water relations that improved my thinking well beyond the pages that follow. Her course in "Plant Water Relations" gave me the terminology and the physical concepts governing the movement of water through soil and plant that this thesis depends upon. Dr. Andres Patrignani, Associate Professor in the Department of Agronomy, opened his soil-water laboratory to this project, questioned the substrate properties that had been carried forward from earlier studies, and recommended both the re-sampling of the two media and the development of substrate-specific sensor calibrations. Those two recommendations reshaped the methodology of this thesis, while the calibration equations that underlie every moisture measurement reported here are the direct result of his patient instruction and his generosity in sharing his wisdom and time.

I owe further debt to Professor Anne Beamish, whose “Research Methods” course gave this project its intellectual shape. The literature review presented in Chapter 2 grew directly out of that class, as did my thesis proposal, along with an early version of the methodology presented in Chapter 3.

This thesis stands on the work of the three researchers who studied this roof before me, and I am fortunate that Lekhon and Allyssa each gave their time to me. Dr. M. M. Lekhon Alam reviewed my research proposal and offered comments that sharpened it. Dr. Alyssa Decker responded generously whenever I brought her any technical difficulty I faced, and her experience proved decisive on questions of sensor calibration and of canopy cover measurement. The thesis by Priyasha Shrestha influenced the structure and writing style of this thesis.

The fieldwork of a single growing season is not the work of a single person. Anika Roy volunteered with the APD-EGR research throughout the 2025 season and carried out the irrigation on many of the irrigation days, working plot by plot as I timed each application, while I managed the pump and hose. She also volunteered on a pilot investigation of the un-irrigated green roof north of the experimental beds, recording the moisture and temperature readings at each flagged point as I placed a portable TEROS 12 sensor. She also assisted with the irrigation of the green roof on the second-floor balcony of Regnier Hall. Puja Mallick took up the same work for two weeks during her visit in the summer, assisting with irrigation on both the experimental green roof and the balcony green roof. April Hough, a fellow Master of Landscape Architecture student and a mentee of Professor Skabelund through the Developing Scholars Program, assisted with the irrigation of the balcony green roof and with the collection of data from it. I am thankful to all three for the hours given freely on hot rooftops.

Kaden Spencer, Graduate Research Assistant in the Department of Agronomy, flew the unmanned aircraft system on all four flight dates, processed the imagery, and extracted the vegetation indices analyzed in Chapter 4.

Jeff Taylor, botanist, volunteered his time on several occasions across the course of this study to assist with the identification of the plants growing on the roof and the vegetation survey reported in Chapter 4.

The Kansas State University Soil Testing Laboratory conducted substrate composition and chemistry and irrigation-water analyses reported in Chapter 3. Christopher (Chip) Redmond, Manager of the Kansas Mesonet, provided guidance on the APD-EGR (Ekdahl) weather station records used to characterize the 2025 season.

I also thank Dr. Isis S. P. C. Scott and the Natural Resources and Environmental Sciences capstone team, along with Wyatt Gillman, Rory Jenkins, Jimmy Owen, and Jett Schmidt, whose independent NRES Capstone Project and study of the APD-EGR offered a valuable point of comparison for the findings presented here.

I am deeply grateful to my classmates in the Master of Landscape Architecture program: especially Alida Elliott, Ava Morrisey, Catalina Cuevas, David Roscerro, David Spencer, Emma Zurek, Joseph Hazard, Lucy Harrison, Nick Stone, Rebecca Gray, Spenser Eisele, Stephanie, Trinity Miles, and Zander Kehoe. Over these three years, they became my family and their friendship made the studio a place of joy.

I also owe heartfelt thanks to the entire Bangladeshi student community at Kansas State University, whose unconditional support helped me build a new life far from home. Their kindness turned a foreign place into one where I truly felt at home.

I thank the Department of Landscape Architecture and Regional and Community Planning, the College of Architecture, Planning and Design, and Kansas State University for supporting this research and my MLA studies, and helping us maintain the experimental green roof and its surroundings.

Last but certainly not least, I thank my mother, Mahfuza Hasnin, and my father, Md. Saiful Islam, and my sister, Maisha Hasnin, for their wonderful and persistent support during this academic and research adventure in "The Little Apple" and the USA.

Chapter 1 - Introduction

Background and Statement of the Problem

Green roofs are rooftops planted with vegetation over an engineered growing medium. Cities adopt them to reduce the urban heat island effect, manage stormwater, improve air quality, support biodiversity, and lower building energy use. Green roofs are conventionally grouped into three types. Extensive green roofs have a shallow substrate (often 6-12 cm in depth) and typically cover a large part of a rooftop. They are the most common type because they require less structural support and are typically much lower in cost to build and maintain than deeper green roofs. Intensive roofs have deeper substrates (typically 20 cm or more). Intensive green roofs can support a wider range of plants (sometimes they include trees and shrubs) and may offer greater stormwater, biodiversity, and cooling benefits depending on vegetative types and canopy cover. Semi-intensive roofs fall between these two types in both depth and capability.

The vegetative cover that a green roof sustains is central to these benefits. A fuller, healthier canopy shades the roof surface, increases evapotranspiration, and lowers rooftop and near-surface air temperatures compared to a bare roof (Bevilacqua et al. 2015, 305; Lee and Jim 2018, 8). The amount and condition of the vegetation therefore govern how well a green roof reduces urban heat. Sustaining that canopy over time depends on how the plants, the weather, and the substrate interact. Both the type of substrate and its depth shape that interaction (Nektarios et al. 2011, 1208; Thuring et al. 2010, 395).

Sustaining canopy cover with minimal supplemental irrigation is difficult in regions with hot summers, high evaporative demand, and long dry spells. The Flint Hills ecoregion of the U.S. Great Plains is one such region, and it lies within the tallgrass prairie where a range of green roofs have been implemented (Dvorak 2015, 394; Dvorak and Skabelund 2021). In this climate, supplemental irrigation becomes a key determinant of plant performance and of the long-term success of a green roof. This is true even where minimal irrigation and maintenance are important design goals. Drought-tolerant and adaptive green roof plant selection can lower the need for water (Van Mechelen et al. 2015; Rivière et al. 2024).

Plant performance on green roofs also depends on the growing medium. Substrate depth sets the volume of water and rooting space available to the plants. Substrate type establishes how much of that water is held and released to the roots (Farrell et al. 2013, 112). The water a substrate holds under real field conditions can differ from the water it holds in a laboratory test, and it is the field behavior that the plants experience (Conn et al. 2020, 1; Szota et al. 2017, 1–2). Expanding green roof use in demanding climates such as the Flint Hills ecoregion therefore depends on finding combinations of depth, substrate type, and irrigation frequency that sustain cover under low-input management.

Despite a large body of green roof research, one gap remains clear. It is not well understood how these three factors (substrate type, depth, and moisture levels) combine to govern vegetative cover on mature, in-situ green roofs through summer heat and dry spells for rooftops using tallgrass prairie plants. Much prior work has used newly planted or modular test systems (VanWoert et al. 2005, 660; Durhman et al. 2007, 589; Szota et al. 2017, 3), single extensive depths (Nawaz et al. 2015, 66), or milder climates (e.g. Bevilacqua et al. 2015; Lee and Jim 2018). The combined influence of depth, substrate type, and irrigation frequency on an operating prairie green roof in Kansas is therefore still unclear. This knowledge gap limits the development of evidence-based green roof design and maintenance guidance for the region.

Plant selection also shapes how mixed vegetation types withstand stress (Ndayambaje et al. 2024; Oberndorfer et al. 2007). Different plant communities respond to summer heat and drought in different ways. The mix of grasses, forbs, and succulents on a roof can determine how much living vegetation remains following a period of stress (Ndayambaje et al. 2024). This matters when designing roofs meant to function on minimal water inputs.

K-State's Memorial Stadium and Architecture, Planning & Design Green Roofs

Kansas State University (K-State) hosts several demonstration and experimental green roofs. Research at the university has addressed green roof vegetation and soil moisture monitoring on the K-State Seaton Upper Green Roof (Skabelund et al. 2015) and at the two K-State Memorial Stadium green roofs (Skabelund et al. 2017), plant survival and growth and canopy cover on K-State's College of Architecture, Planning and Design Experimental Green Roof (APD-EGR) (Shrestha 2019; Liu et al. 2019; Decker 2021), and carbon sequestration and climate mitigation on the APD-EGR (Alam et al. 2024; 2025; 2026). Very relevant to this study is work on the in-situ substrate, moisture, and vegetation behavior of the APD-EGR by Alam et al. (2025). That study found that the denser, sandier Kansas BuildEx (BuildEx) substrate held more water by volume than the porous Rooflite medium. This was true even though Rooflite held more water in laboratory substrate analyses. This in-situ moisture pattern makes the APD-EGR a useful site for studying how substrate type, depth, and irrigation together shape canopy cover. The present study examines whether the greater water availability of the BuildEx substrate translates into greater canopy cover than the Rooflite substrate.

Scope of the Study

This study is complementary to the wider green roof research program led by Professor Lee R. Skabelund on the APD-EGR. It was funded mainly through Professor Skabelund's Mary K. Jarvis Fellowship between 2023 and 2026. A central aim of APD-EGR research is to track changes in the green roof's vegetation over time, by assessing species richness, dominance, and cover, and to develop design, irrigation, monitoring, and weed management guidance for green roofs in similar climates (Skabelund et al. 2022). The present study supports that aim. It focuses on canopy cover performance under two irrigation frequencies, across two substrate types, and two substrate depths.

The focus of this thesis is the irrigated experimental green roof referred to as the APD-EGR (or EGR). There are 12 more-irrigated and 12 less-irrigated plots in each of the extensive (~4-inch or ~10 cm) and intensive (~8-inch or ~20 cm) beds. TEROS 12 soil moisture and temperature sensors were installed in a parallel layout across eight plots within the middle (east to west) on the extensive and intensive beds. The study was meant to be a direct comparison of the plots associated with the deepest and shallowest APD-EGR depths. It is important to note that the ~6-inch (~15 cm) semi-intensive beds followed the same irrigation pattern (with 12 more irrigated plots and 12 less irrigated plots). However, this bed was not part of the instrumented sensor experiment, and it received no TEROS 12 soil moisture/temperature sensors. Data for all three beds are included in the UAS-derived Normalized Difference Vegetation Index (NDVI) analysis. That analysis covers all 72 plots on the APD-EGR and allows a supplementary look at vegetation health across all three depth categories.

Soil moisture data and four sets of UAS images were also collected from the non-irrigated green roof areas to the north of the three APD-EGR beds. This area is part of Professor Skabelund's wider Jarvis green roof research and maintenance activities. These non-irrigated plots were not fitted with fixed sensors, so their soil moisture was measured with a portable TEROS 12 soil moisture and temperature probe during 2025. Lessons learned from studying this area are used to provide a point of comparison (briefly mentioned in Chapter 5) for how canopy cover changed over the season on extensive green roofs that received no supplemental water in 2024 and 2025 and no or very limited irrigation between 2019 and 2023. The analytical focus of this thesis is the more-irrigated and less-irrigated APD-EGR plots, with the most attention given to the extensive (shallowest) and intensive (deepest) beds and their associated plots.

Goals of the Study

The primary goals of this single-season (2025) green roof study were threefold:

1. To better understand how the two substrate types on the APD-EGR support vegetative canopy cover under different irrigation frequencies on the extensive (~4-inch or ~10 cm) and intensive (~8-inch or ~20 cm) green roof beds, and also determine the relative influence of substrate depth, substrate type, and irrigation frequency on APD-EGR vegetative cover.

2. To provide a baseline for the long-term study of vegetative canopy cover, vertical canopy structure, plant survival, and species diversity on extensive and intensive green roofs managed with minimal irrigation and maintenance within the tallgrass prairie ecoregion.

3. To help develop a minimal-irrigation strategy for extensive and intensive green roofs in Manhattan, Kansas (and hopefully comparable continental climates).

Research Questions

The study is built around a set of primary research questions on canopy cover performance. These are supported by secondary questions on plant community, resilience, and canopy structure.

Primary research questions.

1. How do substrate depth (~10 cm extensive versus ~20 cm intensive), substrate type (Kansas BuildEx versus Rooflite), and irrigation frequency (more versus less frequently irrigated) influence green canopy cover on the APD-EGR during the 2025 growing season, and how is that cover related to volumetric water content and substrate temperature dynamics?
2. To what extent do ground-based (iPhone Canopeo) and aerial (UAS/drone Canopeo and multispectral NDVI) methods provide accurate measurements of vegetation cover and health on the APD-EGR, what are the strengths and limitations of each, and how does NDVI-based vegetation health vary across all three substrate-depth categories?

Secondary research questions.

1. Which native grasses, forbs, and sedums are present within the 16 studied plots? How does functional cover composition (grasses, forbs, sedum, and bare soil) vary with substrate depth and east and west plant communities?

2. How did plant community composition affect canopy resilience through the peak-summer stress period? What does the contrast between the grass-dominant and sedum–forb communities imply for species selection on minimally irrigated prairie green roofs?
3. How does the end-of-season canopy height of the dominant warm-season grasses relate to horizontal canopy cover, and what does this vertical dimension add to the assessment of green roof vegetation performance?

Project Objectives

The main objective is to evaluate the canopy cover performance of extensive (~4-inch or ~10 cm) and intensive (~8-inch or ~20 cm) green roofs under minimal supplemental irrigation in the tallgrass prairie ecoregion. This main objective is supported by four specific objectives:

- Quantify the effects of substrate depth, substrate type, and irrigation frequency on green canopy cover under the climate of the Flint Hills ecoregion and the APD-EGR microclimate during the 2025 growing season.
- Characterize the substrate moisture and temperature dynamics of 16 experimental plots and the canopy cover consequences of the 39-day irrigation gap.
- Compare ground-based (Canopeo) and aerial (UAS/drone Canopeo and NDVI) measures of vegetation performance, characterizing what each method captures, how they diverge, and how their strengths complement one another.
- Assess vegetation health across all substrate depths, including the ~6-inch or ~15 cm semi-intensive plots, using UAS-derived NDVI.

The study also pursues three secondary objectives tied to the dominant plant community associated with each examined EGR green roof plot. The first is to characterize vegetative community composition and functional green roof cover groupings. The second is to evaluate how plant community mediated canopy resilience through the peak-summer stress period. The third is to quantify the end-of-season canopy height of the dominant grasses and its relationship to vegetative cover. These objectives draw on the species planted or seeded on the roof between fall 2017 and summer 2024 and on the 2025 vegetation survey performed by Lee Skabelund and Muhaiminul Islam.

How to best measure canopy cover on a green roof is an important research objective. The 2025 study of the APD-EGR combined multiple methods to measure canopy cover. Canopy cover was estimated by eye through (i) ocular survey (Lönnqvist et al. 2021, 1–3), (ii) using digital photography and automated image analysis tools (Rodrigues et al. 2024, 3–10; Patrignani and Ochsner 2015, 2312), and (iii) analyzing photos and NDVI from unmanned aerial systems (UAS, or drones). These methods allowed me to get a complete picture as well as compare the methods. The height of selected dominant grasses at the end of the 2025 growing season was also measured so they could be related to vegetation cover. How these measures compare, and what each one contributes, is a second question this study addresses.

To address the research questions noted above, this study evaluated the canopy cover performance of extensive (4-inch, ~10 cm) and intensive (8-inch, ~20 cm) green roofs under limited supplemental irrigation. The work was carried out during the 2025 growing season on the APD-EGR. Sixteen (16) plots were instrumented and analyzed, eight (8) extensive and eight (8) intensive. The design is a three-factor experiment. This study assessed substrate depth (~10 cm versus ~20 cm), substrate type (BuildEx versus Rooflite), and irrigation frequency (more versus less frequently irrigated). The pre-existing east versus west plant community distinction (with native grasses dominating the east-side plots and forbs dominating the west-side plots in 2025) was a pre-existing difference described rather than treated as an experimental factor. This difference influences canopy cover, but because the study has a limited number of replicates and is focused on the influence of substrate depth and type on canopy cover, the community distinction is accounted for observationally rather than analyzed as a treatment. The most important feature of the 2025 season was a 39-day-period, from July 2 to August 10, when the less-irrigated plots received no supplemental water. This interval fell during peak summer heat (recorded air temperatures on the APD-EGR). It serves as the central explanatory event for the canopy cover, soil moisture, and substrate temperature results discussed throughout the thesis.

Chapter 2 - Literature Review

This chapter reviews the research that frames the present study of canopy cover performance on extensive and intensive green roofs managed under minimal supplemental irrigation in the tallgrass prairie ecoregion of the U.S. Great Plains. The review moves from general themes toward specific ones. It begins by defining green roofs and summarizing their main types and ecosystem services. It then discusses conditions, materials, and measurement approaches that bear directly on the study and irrigation experiment described in Chapter 3.

Two subjects receive particular attention. The first is the continental, drought-prone climate of the Great Plains as it relates to green roof performance, which deserves attention in the green roof literature. The second is the established APDesign Experimental Green Roof (APD-EGR) at Kansas State University, where this study and several preceding studies have been conducted.

The literature is examined under related themes. These include the classification and functions of green roofs; their performance in continental and water-limited climates; the influence of substrate depth on vegetation and moisture dynamics; the role of substrate composition and the difference between laboratory and in-situ water retention; the effect of irrigation frequency and the philosophy of minimal-input management; key relationships between vegetation, plant communities, and canopy cover; the thermal performance and urban heat island mitigation that green roof vegetation provide; and the methods available for assessing canopy cover and vegetation health, including near surface image analysis and unmanned aircraft system (UAS) remote sensing.

The chapter consolidates prior research conducted on the Kansas State University APD-EGR and identifies the specific issues that the present study addresses. Throughout, the study by Alam et al. (2025), conducted on the EGR, serves as a primary point of reference since that study clearly established for an international audience the site characteristics, substrate properties, plant communities, and moisture relationships on which the present work builds.

Green Roofs: Definitions, Types, and Ecosystem Services

A green roof is a rooftop surface supporting living vegetation growing in an engineered substrate. The substrate sits over a series of functional layers. These typically include a waterproofing membrane, a root barrier, a drainage layer, a filter fabric, and the growing medium or soil/substrate (Dunnett and Kingsbury 2008; Shafique et al. 2018). Green roofs are variously described as vegetated roofs, eco-roofs, living roofs, or roof gardens. They are conceptually distinct from non-vegetated reflective or “cool” roofs, even though the two share certain thermal objectives (Francis and Lorimer 2011; Hoffman and McDonough 2005; Xu et al. 2012). Vegetated roofs have antecedents in both monumental and vernacular architecture across many regions and centuries (Abass et al. 2020; Osmundson 1999). The modern green roof, however, emerged in Germany in the latter half of the twentieth century. There, the systematic development of construction standards, materials, and maintenance guidelines established the country as an early leader in the field (Herman 2003; Shafique et al. 2018). From this origin, the practice spread internationally. Over the past several decades, green roofs have been adopted across North America, East Asia, Australia, and elsewhere. In some jurisdictions this adoption has been driven by regulatory mandates that require vegetated coverage on a proportion of qualifying roof area (Chen 2013; Shafique et al. 2018).

Green roofs are conventionally classified into three types according to substrate depth. Depth in turn governs the weight, plant palette, maintenance demand, and structural requirements of the system (Abass et al. 2020; Li and Yeung 2014; Vacek et al. 2017). Intensive green roofs have the deepest substrate profiles, generally about 20 cm (8 inches) or deeper. They can support a broad range of plants, including shrubs and trees comparable to ground-level gardens. They also impose the greatest structural loading, irrigation, and maintenance demands, which has limited both their construction and the research devoted to them (Abass et al. 2020; Jim and Tsang 2011; Karachaliou et al. 2016). Semi-intensive green roofs occupy an intermediate range of roughly 15 to 20 cm (6 to 8 inches). They support ornamental species, meadow vegetation, turf grasses, and woody perennials at a substantially lower cost than fully intensive systems (Abass et al. 2020; Vacek et al. 2017). Extensive green roofs are the shallowest, typically on the order of 7 to 15 cm (2.5 to 6 inches) deep. They are the lightest and least costly to construct and maintain, and they are planted with low, drought-tolerant, mat-forming, or succulent species. They are by far the most widely implemented type, owing to their structural simplicity and low input requirements (Abass et al. 2020; Getter and Rowe 2006; Li and Yeung 2014). The boundaries for these three categories are conventional rather than absolute. Many systems span the transition between the extensive and intensive ends of the spectrum. The experimental green roof examined in this study is one such system, incorporating 4-inch (~10 cm), 6-inch (~15 cm), and 8-inch (~20 cm) beds.

Interest in green roofs across all three types reflects the range of ecosystem services they provide. Green roofs reduce and retain stormwater runoff, moderate building energy demand, mitigate the urban heat island effect, improve air quality, support biodiversity, and add aesthetic and amenity value to the built environment (Getter and Rowe 2006; Liu and Minor 2005;

Shafique et al. 2018). More recently, attention has extended to their capacity to sequester carbon within the substrate and vegetation. This capacity positions green roofs as one component of building-scale climate change mitigation (Alam et al. 2024, 2025). The literature also identifies a set of recurring barriers to wider adoption. These include elevated construction and maintenance costs, technical complexity, limited public awareness, and a shortage of policy incentives for owners and developers (Liu and Minor 2005; Zhang et al. 2012). One of these challenges is especially pertinent to the present study. The cost and burden of long-term maintenance and irrigation, particularly in climates with hot, dry summers, bears directly on the goal of sustaining vegetation under deliberately minimal supplemental water.

Green Roofs in Continental and Water-Limited Climates

A persistent limitation of the green roof literature is its concentration in temperate maritime, Mediterranean, and humid subtropical settings. Comparatively little research has been conducted in the continental interior of North America. Reviews of green roof performance and of growing-media effects draw predominantly on European and East Asian studies. The U.S. Great Plains, with its extreme swings of drought, intense summer heat, and large temperature range, remains notably underrepresented (Alam et al. 2025; Kazemi and Mohorko 2017). This gap is consequential because green roof performance is strongly climate dependent. Substrate, depth, plant/vegetation, and irrigation combinations that succeed in mild or evenly watered climates perform comparably under the conditions of the central grasslands (Sims et al. 2016; Akther et al. 2018).

Tallgrass prairie ecoregion that surrounds the present study site is a distinctive and demanding context for green roof vegetation. Before European settlement, tallgrass, mixed-grass, and shortgrass prairies together covered tens of millions of hectares of central North America, extending from the present-day Canadian provinces to the southern Great Plains. Only fragments of the tallgrass prairie remain today, following widespread conversion to agriculture and urban development (Dvorak and Skabelund 2021; Steinauer and Collins 1996). These prairie ecosystems were shaped by the climatic, topographic, and soil conditions of the region. They produced assemblages of dry, mesic, and wet habitats whose thin ridgeline soils are in several respects analogous to the shallow, well-drained substrates of green roofs (Dvorak and Skabelund 2021; Schramm 1990). The "drought-tolerant prairie analogy" underlies the interest in prairie and grassland species as candidates for green roof vegetation in this region.

The climate of the Flint Hills tallgrass prairie ecoregion combines hot, frequently dry summers with cold winters. Summer maxima commonly exceed 35 to 40 degrees Celsius in July and August. Precipitation is distributed across most months, but the late-summer period from late July through September tends to be drier and more drought-prone than late spring and early summer (Dvorak and Skabelund 2021). Northern portions of the ecoregion, including Manhattan, Kansas, also experience snow cover and freezing winter temperatures. For green roofs in this setting, high summer evapotranspiration demand and episodic drought make supplemental irrigation a central determinant of vegetation survival and performance. At the same time, the cost and sustainability of that irrigation argue for minimizing it (Dvorak 2015; Dvorak and Skabelund 2021). This tension motivates the present study. The challenge is to maintain adequate canopy cover under minimal supplemental water during the hottest, driest parts of the growing season.

A small but valuable body of work has begun to document green roof practice in the Flint Hills Ecoregion and other U.S. Great Plains tallgrass prairie ecoregions. Sutton et al. (2012)

reviewed the ecological literature on prairie and grassland communities adapted to stressed environments and examined prairie-based vegetation analogs on twenty-one existing green roofs. They concluded that many, though not all, prairie and grassland species survive and thrive on green roofs, especially when adequate substrate depth is provided or supplemental irrigation is supplied as needed. Dvorak (2015) presented case studies of nine ecoregional green roofs in the Coastal Plains and Interior Lowlands of North America, three of them within tallgrass prairie ecoregions. That work documented 145 plant species native to tallgrass prairies growing on green roofs across Kansas, Nebraska, Texas, and Missouri—showing that the diversity of prairie habitats can inspire a corresponding diversity of green roof vegetation.

These studies establish the feasibility and ecological logic of prairie-based green roofs. They also make clear that controlled investigations of the specific effects of substrate depth, substrate type, and irrigation frequency in this ecoregion remain scarce. Recent long-term modeling reinforces the primacy of climate over design in water-limited settings. Comparing temperate and semi-arid climates across thirty years, Soni et al. (2025) found that climate exerted a stronger influence than green roof design on both rainfall retention and plant drought stress. In semi-arid climates, neither reducing plant density nor increasing substrate depth relieved drought stress, so supplemental irrigation or additional water storage below a green roof substrate, was typically required to maintain plant/vegetation cover (Soni et al. 2025). This conclusion directly supported the present study’s focus on supplemental irrigation as the decisive management variable in a hot, drought-prone continental climate.

Substrate Depth and Green Roof Performance

Substrate depth is among the most extensively studied design variables in green roof research (Durhman et al. 2007; VanWoert et al. 2005; Vandegrift et al. 2019). It simultaneously governs water storage, thermal mass, structural load, and the range of plant species a system can support (Getter and Rowe 2006; Oberndorfer et al. 2007; Cascone 2019). The general expectation that deeper substrates improve plant performance is supported by many studies (Durhman et al. 2007; Nektarios et al. 2011; Vandegrift et al. 2019). The literature also makes clear, however, that the relationship is mediated by climate, irrigation, and plant type (Thuring et al. 2010; Nektarios et al. 2011; Sims et al. 2016). Depth interacts with water availability rather than acting independently of it (Lu et al. 2015; VanWoert et al. 2005; Thuring et al. 2010).

In an influential semi-extensive experiment in Sheffield, United Kingdom, Dunnett and Nolan (2004) examined the growth of nine herbaceous perennials across contrasting substrate depths under limited or no supplementary irrigation. In the absence of supplemental irrigation, increasing substrate depth produced relatively few significant improvements in plant performance. Supplemental irrigation, by contrast, promoted growth in most species at both depths. Low-growing species tended to perform comparatively less well under the more productive, better-watered conditions. This early result foreshadows a theme that recurs throughout the green roof substrate depth literature (VanWoert et al. 2005; Thuring et al. 2010; Nektarios et al. 2011; Lu et al. 2015; Vandegrift et al. 2019). The benefit of additional substrate depth is expressed most clearly together with water inputs, or as a buffer against their absence, rather than as a uniform main effect. Subsequent research has reinforced the importance of depth and moisture interactions. A study of extensive green roofs in the temperate monsoonal climate of Beijing, Zhang et al. (2021) identified substrate depth and soil moisture as the two most significant determinants of plant performance under unirrigated conditions, with stress-tolerant species performing best, followed by ruderal species. Controlled experiments that vary substrate type and depth together under a range of drought conditions have likewise found that plant responses to depth are strongly conditioned by drought severity and by the substrate in which the plants are grown, rather than being uniform across watering regimes (Thuring et al. 2010; Nektarios et al. 2011; Papafotiou et al. 2013; Ondoño et al. 2016).

As discussed by Alam et al. (2025), a useful way to interpret these findings is to distinguish two roles for substrate depth. The first is depth as a source of additional average moisture. The second is depth as a buffer against moisture extremes. Deeper substrates hold a larger total volume of water. They therefore take longer to draw down to critically low levels during dry periods. Shallower substrates hold less total water. They reach low-moisture thresholds more rapidly and rebound more sharply after rainfall or irrigation. Under this interpretation, the principal value of greater depth in a drought-prone climate is the damping of the extreme low-moisture episodes that cause irreversible plant damage. Greater depth does not so much provide much sustained increase in routinely available water. This buffering role is consistent with the moisture-stability patterns reported on the EGR by Alam et al. (2025) and is examined directly in Chapter 4.

The green roof substrate depth literature explores whether the deepest, most resource-intensive systems are warranted in every context. Studies of semi-intensive depths suggest that intermediate profiles can capture much of the vegetation benefit of greater depth at substantially lower structural and maintenance cost (Kotsiris et al. 2012; Vacek et al. 2017). Hydrological modeling and field studies of extensive systems likewise indicate that substrate depth and plant cover jointly govern runoff retention. Depth contributes both to storage capacity and to the persistence of vegetation that sustains evapotranspiration (Soulis et al. 2017). For the tallgrass prairie ecoregion, a key question remains insufficiently resolved. It is how much depth is necessary to sustain adequate canopy cover under minimal irrigation, and whether intermediate, semi-intensive depths might offer a favorable balance of performance and cost. The present study is positioned to contribute to this question through its inclusion of 4-inch (~10 cm), 6-inch (~15 cm), and 8-inch (~20 cm) beds in the broader analysis.

Key Concepts in Plant-Soil-Water Relations

This study incorporates several key concepts from soil physics. These key concepts are soil volumetric water content (VWC), field capacity, permanent wilting point, plant-available water capacity (PAWC), plant-available water (PAW), fraction of plant available water, and management allowable depletion. The substrate comparison and the irrigation protocol were dependent on these key concepts. Each concept is discussed below.

The amount of water in the substrate is quantified using VWC, the volume of water held per unit bulk volume of substrate (Kirkham 2014). When a substrate is thoroughly wetted and allowed to drain freely under gravity, the water content it retains once rapid drainage has effectively ceased is termed its field capacity (Veihmeyer and Hendrickson 1931; Kirkham 2014; Allen et al. 1998). As plants withdraw water, the substrate progressively dries until it reaches field capacity or the water content below which plants can no longer extract water rapidly enough to meet transpirational demand and from which they do not recover (Kirkham 2014). The difference between these two limits defines the PAWC, the maximum reservoir of water a medium can hold and make available to vegetation (Kirkham 2014; Allen et al. 1998). PAWC is a static property of a given substrate profile; the quantity of that reservoir actually present at any moment, which declines as the substrate dries between wetting events, is the PAW (Allen et al. 1998).

Normalizing the dynamic quantity by the static capacity yields the fraction of available water (FAW = PAW / PAWC), a dimensionless index that rescales substrate moisture onto a common zero-to-one scale in which a value of 1.0 corresponds to field capacity and 0.0 to the permanent wilting point (Allen et al. 1998). Crops do not, however, deplete the full available reservoir before experiencing stress. The fraction of plant-available water that can be withdrawn before the substrate can no longer supply water rapidly enough to meet transpiration demand is the depletion fraction (Allen et al. 1998). The proportion of available water permitted to deplete before irrigation is applied is known as the management allowable depletion; the two are equivalent, and a value near 0.50 is widely adopted as the point at which many plants begin to experience water stress (Allen et al. 1998, 163, Table 22).

In the present study, supplemental irrigation was applied whenever substrate volumetric water content fell below a fixed threshold of 8% (Chapter 3). For the substrates used here, this threshold falls near the mid-point of the available water range. At that point, about half of the plant-available water has been used. This corresponds to a management allowable depletion of roughly 0.50 (Allen et al. 1998, 163, Table 22). The 8% trigger therefore aligns with the soil-water framework described above.

These relationships take on particular importance in engineered green roof media, which are formulated to remain lightweight while retaining sufficient plant-available water, and whose physical properties therefore differ markedly from those of natural soils (Kazemi and Mohorko

2017). Because such media are typically coarse and highly porous, a substantial fraction of their pore space drains rapidly and contributes little to plant-available water, so that a medium's total porosity or its laboratory-measured retention may overstate the water actually available to plants under field conditions (Kazemi and Mohorko 2017; Getter and Rowe 2006). This distinction between laboratory-measured retention and the water a substrate supplies in place on a roof is central to the substrate comparison developed in the following section.

Substrate Type, Composition, and the Distinction Between Laboratory and In-Situ Water Retention

Along with depth, the composition of the growing medium is a primary control on green roof plant performance. Substrate physical properties determine water retention, aeration, drainage, nutrient availability, and the rooting environment (Kazemi and Mohorko 2017; Young et al. 2014). Green roof substrates are typically engineered, mineral-dominated mixes, designed to be lightweight while retaining sufficient plant-available water. Modest changes in their composition can substantially alter plant growth and survival. The relevant properties include particle size distribution, organic matter content, and mineral constituents (Young et al. 2014). Reviews of growing media across world climates emphasize that no single substrate formulation is universally optimal. The appropriate composition is context-specific and must be matched to the local climate, plant palette, and management regime (Kazemi and Mohorko 2017).

Field studies of substrate composition have produced varied and sometimes counterintuitive results. In a pilot study on a Mediterranean green roof, Marouli et al. (2022) found, contrary to expectation, no strong relationship between substrate depth or composition and plant growth. They suggested that plant community composition and interspecies interactions may exert a stronger influence on performance than the substrate parameters alone. Muratet et al. (2024), in a three-year study of extensive green roofs in Paris, identified substrate structure, thickness, and fine-particle content, together with management and maintenance, as among the principal drivers of plant diversity. Such findings indicate that substrate effects are frequently contingent on the interplay among medium, depth, vegetation, and management. These effects are not always large or consistent when isolated.

A distinction of central importance to the present study is often underemphasized in the broader literature: the difference between the water-retention capacity of a substrate as measured in the laboratory and the water content that the same substrate holds under field conditions on a roof (Szota et al. 2017; Conn et al. 2020). Laboratory measures such as maximum water-holding capacity characterize the upper limit of retention under controlled saturation. In-situ moisture, by contrast, reflects the dynamic balance of infiltration, drainage, evapotranspiration, and substrate structure as the medium behaves in place (Conn et al. 2020). These two measures need not agree, and they can even diverge in direction (Szota et al. 2017; Alam et al. 2025).

This point is documented directly for the substrates used in the present study. Drawing on laboratory analyses and in-situ monitoring on the same Kansas State University green roof, Alam et al. (2025) characterized two contrasting media. The first was a commercial, low-bulk-density medium with high total pore space and a high maximum water-retention capacity measured in the laboratory. The second was a denser, sandier, regionally sourced medium with a higher bulk density and lower laboratory retention. Despite the commercial medium's higher laboratory maximum, in-situ measurements at both the 10-cm and 20-cm depths showed that the denser, sandier medium held more water by volume under field conditions. This result was attributed to the compact profile retaining greater volumes of water in place, while the more porous medium drained more freely (Alam et al. 2025; Decker 2021).

Irrigation of Green Roofs

Irrigation is among the most influential and most studied factors governing green roof plant performance (VanWoert et al. 2005; Nagase and Dunnett 2010; Van Mechelen et al. 2015). Its importance is greatest in climates where summer rainfall is insufficient to sustain vegetation through periods of high evaporative demand (Schroll et al. 2011; Van Mechelen et al. 2015; Dvorak and Skabelund 2021). Literature spans a continuum from fully irrigated intensive systems to extensive systems designed to survive with rainfall alone. Much of the recent research seeks strategies that sustain acceptable vegetation performance while minimizing water input (Nektarios 2018; Van Mechelen et al. 2015). The selection of appropriate plants and substrates is widely recognized as a means of reducing irrigation requirements. Reviews of green roof irrigation emphasize that thoughtful matching of plant palette, substrate, and management can substantially lower the supplemental water a system needs (Van Mechelen et al. 2015).

A recurring theme in the irrigation literature is that plant responses to watering differ markedly among species and functional groups. Nagase and Dunnett (2010) examined drought tolerance across different vegetation types on extensive green roofs and the effects of watering and diversity. They found that succulents (including many *Sedum* species) can persist in shallow substrates for extended periods without rainfall, by virtue of their internal water storage (Nagase et al. 2010). This finding is directly relevant to the mixed prairie-grass, forb, and sedum communities of the present study site.

Studies of irrigation methods and efficiency have compared overhead, drip, and sub-irrigation approaches as to their effects on water use and plant health (Rowe et al. 2014). This work reflects the practical importance of delivering supplemental water efficiently, as well as deciding how much to apply (Rowe et al. 2014). Investigations in the Pacific Northwest and Mediterranean regions have similarly linked plant selection and irrigation regime to establishment and survival on extensive systems (Schroll et al. 2011). Other approaches base irrigation decisions on real-time substrate water status rather than on fixed schedules. Maintaining a moderately low substrate water potential and irrigating only when a defined threshold is crossed has been shown to reduce applied water by roughly two-thirds across the summer months without compromising plant physiological performance (Tomasella et al. 2022).

The question of whether extensive green roofs can be sustained with little or no irrigation has been examined in several continental and monsoonal climates. Zhang et al. (2021) explored the feasibility of unirrigated extensive green roofs in Beijing's temperate monsoonal climate. Stress-tolerant species, supported by adequate substrate depth and soil moisture, were the most successful, although the authors acknowledged the difficulty of maintaining vegetation without supplemental water during dry periods. For the tallgrass prairie ecoregion, where summer heat and episodic drought are pronounced, the prevailing view is that some supplemental irrigation is necessary to sustain green roof vegetation (Dvorak and Skabelund 2021; Skabelund et al. 2017; Shrestha 2019; Decker 2021). The central management challenge is to minimize that irrigation without allowing vegetation to cross the threshold into irreversible decline (Dvorak and Skabelund 2021). Under this minimal-input philosophy, water is applied only when sensor monitoring indicates that substrate moisture has fallen to critically low levels.

This approach has guided management of the Kansas State University Experimental Green Roof and as noted by Alam et al. (2025). The present study extends it into a controlled comparison of two irrigation frequencies. A further emphasis of the irrigation literature is the timing of water deficits relative to peak heat. The consequence of a prolonged dry interval depends not only on its total duration but on its coincidence with the period of maximum evaporative demand. This point is developed in the analysis of the present study's central mid-summer irrigation gap.

Vegetation, Plant Community, and Canopy Cover

Plants are the defining element of a green roof, and the selection and performance of vegetation is one of the most active areas of green roof research. Green roof literature addresses which plants succeed under the harsh conditions of green roofs, and how plant choice interacts with substrate, depth, and irrigation (MacIvor and Lundholm 2011; Nagase and Dunnett 2010; Snodgrass and Snodgrass 2006). Those harsh conditions include shallow substrates, high wind exposure, intense solar radiation, and episodic drought. The plants characteristic of extensive green roofs share a recognizable suite of traits. These include rapid establishment and reproduction; low, cushion-forming or mat-forming growth habits; shallow but widespread root systems; and, in succulents, water-storing leaves and stems (Li and Yeung 2014; MacIvor and Lundholm 2011; Snodgrass and Snodgrass 2006).

The use of native plants on green roofs has received particular attention (Dvorak and Volder 2010; Dvorak and Skabelund 2021; Sutton et al. 2012; MacIvor and Lundholm 2011). Native species adapted to local climate stresses can in principle survive with reduced maintenance, watering, and fertilization while supporting native fauna (Li and Yeung 2014).

Surveys of award-winning and built green roofs have found that native plants are used for a substantial proportion of projects (Cantor 2008; Peck 2008). Reviews of the topic conclude that native plants are often advantageous, but that plant selection should be guided by local environmental conditions and performance rather than by a strict native-only policy (Dvorak and Volder 2010; Butler et al. 2012; Leotta et al. 2023). Biodiversity, substrate quality, and vegetation structure are held to be equally important to overall performance (Dunnett 2006). In the tallgrass prairie ecoregion specifically, native prairie grasses and forbs are leading candidates for green roof vegetation because of their adaptation to the regional climate and their analogous occurrence on thin prairie soils (Sutton et al. 2012; Ksiazek-Mikenas et al. 2021). Their performance relative to the succulents conventionally used on extensive roofs is nonetheless climate- and management-dependent (Dvorak and Skabelund 2021; Sutton et al. 2012).

Trait-based syntheses of the global green roof flora support this habitat-template logic (Lundholm and Walker 2018; Todeschini and Fett-Neto 2025). In a review of several hundred studies, Todeschini and Fett-Neto (2025) identified archetypal green roof plants for each major climate zone. They found that temperate and continental climate species share a common suite of morphophysiological traits, which implies that species adapted to continental grasslands are well matched to continental green roofs. Empirical trials outside North America point in the same direction. Iwata et al. (2025), for example, evaluated six native grassland species on extensive green roofs. Most established successfully across contrasting substrates over a growing season, with substrate properties shaping early growth. That result was obtained, as in the present study, through image-based measurement of plant cover.

The growth form of the vegetation has direct consequences for the canopy cover on green roofs (Lundholm et al. 2010; MacIvor and Lundholm 2011), and canopy cover is the primary response variable of this study. Mat-forming succulents such as many *Sedum* species spread horizontally and tend to cover the substrate surface efficiently, presenting high apparent cover (VanWoert et al. 2005; Durhman et al. 2007). Upright, clumping bunchgrasses characteristic of prairie communities, by contrast, leave visible gaps of bare substrate between individual tufts (MacIvor and Lundholm 2011; Snodgrass and Snodgrass 2006). Evaluating the development of five sedum species on extensive green roofs, Pérez et al. (2020) mentioned the importance of studying coverage capacity, shape, structure, and growth strategy. Studying canopy cover on APD-EGR is complex because sedums and native grasses are mixed. That is why multiple methods were applied to understand canopy behavior. In addition, vegetation height was measured to investigate the relationships.

Canopy cover, also termed vegetative or green cover, is a widely used and practical indicator of green roof and ecosystem performance. It integrates the combined effects of plant establishment, growth, health, and survival into a single measurable quantity that can be tracked over time (Lönnqvist et al. 2021; MacIvor et al. 2013). Vegetation cover has been linked to several of the functions for which green roofs are valued, including stormwater runoff reduction and thermal regulation (Lundholm et al. 2010; MacIvor and Lundholm 2011; Bevilacqua et al. 2015). The extent and persistence of cover is therefore not merely an aesthetic measure but a proxy for ecological function (Bevilacqua et al. 2015; Dunnett et al. 2008). The literature nonetheless cautions that cover and other vegetation attributes such as diversity can be decoupled, responding to different drivers. Cover should thus be interpreted as one informative dimension of performance rather than a complete description of it (MacIvor et al. 2013).

Studies tracking vegetation development on green roofs over multiple years further show that cover is dynamic, varying seasonally and across years in response to weather, substrate, and management. This variability argues for high-frequency measurement to capture its temporal behavior (Bates et al. 2013; Lönnqvist et al. 2021). These considerations inform this study's emphasis on frequent, season-long monitoring of canopy cover as a principal measure of vegetation performance.

Thermal Performance and Urban Heat Island Mitigation

Among the most consistently documented benefits of green roofs is their contribution to thermal regulation, both at the scale of the individual building and at the scale of the urban environment (Berardi et al. 2014; Santamouris 2014; Bevilacqua et al. 2015). Green roofs shade the roof surface, increase evapotranspiration, and add insulating substrate mass. Through these mechanisms, they reduce heat flux through the roofing system and lower roof-surface and near-roof air temperatures relative to conventional roofing membranes, which can reach very high surface temperatures under direct summer solar radiation (Jim and Tsang 2011; Liu and Minor 2005; Xu et al. 2012). Studies of intensive green roofs have reported substantial reductions in surface temperature relative to conventional roofs. Karachaliou et al. (2016), for example, measured surface temperatures approximately fifteen kelvin (fifteen degrees Celsius) lower on a large-scale intensive green roof on an office building in Athens than on adjacent conventional roofing. Investigations of the biophysical properties and thermal performance of intensive systems have characterized the temperature profiles of air, canopy, substrate, and structural layers across seasons and depths. This work demonstrates the role of substrate mass and vegetation in moderating heat transfer (Jim and Tsang 2011).

The thermal benefit of green roofs is closely coupled to substrate moisture and vegetation cover (Bevilacqua et al. 2015). Evapotranspiration, the conversion of liquid water to vapor, absorbs latent heat and is a primary cooling mechanism (Cascone et al. 2019). Moister substrates and more vigorous vegetation generally provide greater evaporative cooling (Cascone et al. 2019; Bevilacqua et al. 2015). Thermal performance is therefore linked to the same moisture and cover dynamics that govern plant survival (Bevilacqua et al. 2015). Solcerova et al. (2017) show that the substrate baseline persists under drought while air-cooling collapses and establish that the evaporative component scales with moisture. Vaz Monteiro et al. (2017) highlighted that Plant canopy traits strongly affect cooling and insulation by roof substrates and found that succulent plants did not perform best, compared to broad-leaf plants, in providing significant summertime environmental cooling and substrate insulation. In this study, I tried to understand the thermal behavior of different substrate depths, types, and moisture patterns governed by irrigation frequency, and how these are related to canopy cover changes over the season.

At the Kansas State University APD-EGR, Alam et al. (2024) investigated the climate mitigation performance of the system within the Flint Hills Ecoregion, and earlier work on this roof documented its microclimatic behavior under the region's urban-rooftop heat conditions (Alam 2022). Most directly, Alam et al. (2026) assessed the seasonal thermal performance of this same Mid-Continental green roof under real-world conditions and identified moisture-driven thermodynamic effects on its insulating behavior. That study showed that substrate water content mediates the system's contribution to building energy performance. It ties thermal benefits explicitly to the same moisture dynamics that govern canopy cover.

The present study examines substrate temperature across all sixteen instrumented APD-EGR plots. It evaluates the extent to which urban heat island mitigation is sustained across treatments and across the range of canopy cover observed, including under the drought-stressed conditions of the less-irrigated plots.

Methods for Assessing Canopy Cover and Vegetation Health

Because canopy cover and vegetation health are central response variables in green roof research, the methods used to quantify them require specific attention. Various studies have used different methods to quantify canopy cover. This section discusses the evolution of canopy cover assessment methods, including the strengths and limitations of each.

Historically, vegetation cover has been assessed through ocular, or visual, estimation. An observer estimates the proportion of a plot occupied by vegetation, often by assigning cover to predefined classes. The canopy-coverage method of Daubenmire (1959) formalized this approach using a quadrat and a small number of cover classes. It remains one of the most widely used techniques for characterizing rangeland and grassland vegetation. Ocular estimation is rapid and non-destructive, and it is well suited to characterizing mixed-species vegetation by functional group (Ónodi et al. 2017; De Stefano et al. 2021). As it is easy and requires minimal tools, this method is adopted by many researchers (Bergstedt et al. 2009; De Stefano et al. 2021). However, Bergstedt et al. (2009) have discussed observer bias and stochastic variation in using this method. In addition, Morrison (2016) pointed out three types of errors in using this method. Studies of estimation error have documented substantial variability between observers and between estimated and actual cover (Hatton et al. 1986).

Image-based analysis offers a more repeatable alternative to ocular estimation. It classifies the pixels of a digital photograph as vegetation or non-vegetation according to their color properties. Canopeo, developed at Oklahoma State University by Patrignani and Ochsner (2015), is a representative and widely adopted tool of this kind. It analyzes images using the red-to-green and blue-to-green color ratios together with an excess-green index, classifying each pixel and returning the fractional green canopy cover of the image. In the original evaluation, Canopeo classified approximately ninety percent of pixels in agreement with manual reference classification, while processing images far more rapidly than earlier software. It has since been applied across agronomy, turfgrass science, forestry, and ecological research (Patrignani and Ochsner 2015). Its speed and objectivity make it well suited to the high-frequency, season-long cover monitoring required to capture the temporal dynamics of green roof vegetation, and it is the principal cover-measurement tool of the present study. Visual and photographic methods have also been used in green roof cover research specifically. Some studies rely on visual observation, and others on photography and image analysis, to convert vegetation cover into quantitative data (Lönnqvist et al. 2021).

Other image-analysis platforms offer capabilities that complement Canopeo, and the choice among them involves trade-offs in speed, automation, and the level of detail recovered. Working on an extensive green roof, Cao and MacIvor (2024) compared manual segmentation against two ImageJ/Fiji tools. One is a color-threshold method conceptually similar to Canopeo. The other is a Trainable Weka Segmentation classifier, which must be trained by labeling pixels. Both were applied to digital RGB and thermal imagery (Cao and MacIvor 2024).

One distinction matters for the present study. Canopeo returns only the total fraction of green canopy and does not differentiate among species. Trainable, multi-class segmentation tools can in principle be taught to estimate the cover of individual species (Técher 2022), although at the cost of substantially greater labor in labeling and training. This tradeoff informs the measurement strategy adopted in this APD-EGR study.

Automated, high-frequency total-cover monitoring with Canopeo is paired with a separate ocular vegetation survey to resolve species and functional-group composition, rather than relying on a single tool to do both. These trade-offs have been encountered directly on the present study's roof. Decker (2021) measured the overhead percent cover of each APD-EGR green roof plot or cell in ImageJ, following a hue-saturation-brightness threshold protocol in which the thresholded image renders vegetation in black against a white background before the covered area is measured. Shrestha (2019) measured species-level cover on the same roof using a combination of Adobe Photoshop and ImageJ, separating individual plant footprints in Photoshop before measuring their cover in ImageJ, and recommended that subsequent work rely on ImageJ alone for plant-mix-level rather than species-level analysis. Both approaches produced usable estimates but were labor-intensive. A further limitation of threshold-based classification is that it identifies green pixels and thus tends to not identify or under-detect foliage with reddish, orange, or brown hues, such as the drought-stressed and senescing vegetation documented on this roof (Allyssa Decker, Dickinson College, personal communication, 2025).

More recently, remote sensing using unmanned aircraft systems has emerged as a means of assessing vegetation cover and health at the plot and roof scale. UAS platforms can acquire imagery at very high spatial resolution and at flexible intervals. They bridge the gap between labor-intensive ground surveys and coarser satellite or aerial imagery. On green roofs, color-infrared (multispectral) and thermal sensing has been applied to characterize vegetation condition, including on the Kansas State University Memorial Stadium green roofs (Van der Merwe et al. 2017).

Beyond visible-band imagery, multispectral sensors enable the calculation of vegetation indices, of which the Normalized Difference Vegetation Index (NDVI) is the most widely used.

NDVI is computed from the contrast between near-infrared and red reflectance, defined as the difference between the near-infrared and red bands divided by their sum (Rouse et al. 1974; Tucker 1979). It quantifies vegetation photosynthetic vigor, a dimension of plant performance distinct from the fractional green cover captured by visible-band image analysis (Tucker 1979; Pettorelli et al. 2005). The two measures are related but complementary (Carlson and Ripley 1997). Studies across multiple crops have demonstrated strong, convertible relationships between NDVI and Canopeo-derived fractional green canopy cover, while also confirming that each capture somewhat different information about the canopy (Lykhovyd et al. 2022). The present study combines high frequency near green roof surface image analysis with periodic high-resolution UAS RGB and multispectral imagery. Together, these yield four measures of canopy performance on the same plots: near surface iPhone photography analyzed with Canopeo, UAS imagery analyzed with Canopeo, UAS-derived NDVI, and human ocular observation. This combination allows canopy cover and vegetation vigor to be characterized across complementary scales and spectral domains. The integration of these four measures and the relationships among them are developed in Chapter 4.

Prior Research at the Kansas State University Experimental Green Roof

Kansas State University maintains several demonstration and experimental green roofs and has sustained an active research program within the Flint Hills Ecoregion. That program addresses monitoring, plant performance, soil-plant-water relations, biodiversity, and carbon sequestration. This accumulated work provides the immediate foundation for the present study. The present study is conducted on the same experimental green roof as several of these preceding investigations and adopts consistent site characterizations, substrate designations, and plant-community descriptions.

Early monitoring efforts on the university's two sloped Memorial Stadium Green Roofs documented vegetation change alongside temperature, soil moisture, and precipitation. This work established protocols and baselines for long-term observation (Skabelund et al. 2017). Subsequent survey work on the same sloped roofs catalogued the dominant vegetation. It recorded more than one hundred thirty unique species over two growing seasons, a large proportion of them volunteer and native or possibly native species, and it documented differences in weedy-species presence between the two roofs (Skabelund et al. 2022). The monitoring program has been accompanied by methodological work on the measurement of green roof abiotic inputs and outputs, including substrate moisture, temperature, and runoff, which underpins consistent long-term observation (Skabelund et al. 2015). The performance of the stadium roofs has also been documented through the Landscape Architecture Foundation's Case Study Investigation program (Skabelund and Alam 2020).

K-State research focused on the Experimental Green Roof (APD-EGR) between 2018 and 2025 provides a continuous record of vegetation, substrate, and moisture behavior on this green roof, against which the present canopy cover findings can be interpreted. The EGR's 4-inch bed was the subject of Shrestha's (2019) thesis work, which assessed the first-year (2018) survival, growth, and physiological performance of seven graminoid species across two substrate types. Of particular importance is the study by Liu et al. (2019), which evaluated the growth of prairie plants and sedums in different substrates on this experimental green roof in the Mid-Continental United States. This research assessed plant cover, survival, and growth across substrate types during establishment. It connects substrate composition directly to vegetation performance on the same roof and with the same general substrate set used here, and it included among its authors the soil-plant-water specialist (Dr. M. Kirkham) who serves as a committee member on the present study.

Decker (2021) examined soil-plant-water relations on the EGR's 4-inch and 8-inch beds, contributing to the site-specific understanding of substrate moisture behavior on which the present study relies. Examining EGR establishment-phase plant-water-substrate dynamics, Decker et al. (2022) tracked native plant growth on the same extensive beds over a four-year period (2018-2021). That study provides a longitudinal record of vegetation development on this roof that is directly relevant to the season-long cover dynamics examined here.

Perhaps the most directly relevant EGR research work is the sequence of studies by Alam and colleagues. Alam (2022) reported earlier data analysis from the experimental green roof, including observations relevant to its urban-rooftop microclimate and in-situ substrate moisture behavior. Alam et al. (2024) investigated the climate mitigation performance of the APD-EGR green roof system within the Flint Hills Ecoregion. Alam et al. (2026) assessed the EGR's seasonal thermal performance and the moisture-driven thermodynamics of its building-energy behavior under real-world conditions. Most comprehensively, Alam et al. (2025), in a two-year study, examined the carbon sequestration capacity of the APD-EGR. That study compared two distinct substrate depths, ~10 cm and ~20 cm; two contrasting substrate types; and three plant mixes (an all-sedum mix, a sedum-and-native-grass mix, and a native-grass-and-forb mix) arranged in a factorial design.

Alam et al. (2025) reported several findings that help frame the present work. It documented the physical properties of the two substrates and the in-situ moisture relationship, in which the denser, sandier medium held more water by volume in the field despite the more porous medium’s higher laboratory retention. This study found that the more porous, lower-bulk-density Rooflite substrate stored more carbon per unit volume than the sandier, denser BuildEx substrate. It found that vegetation composition, particularly the presence of native grassesplayed a critical role in modulating belowground carbon and microbial activity. And it found that shallower 10-cm beds planted with native grass species supported high root density and microbial biomass and could rival or exceed deeper beds in carbon storage. From these results, Alam et al. (2025) concluded that, for green roof applications in continental climates such as Manhattan, Kansas, shallower profiles planted with regionally appropriate native grasses may provide climate benefits comparable to or greater than those of deeper profiles.

These findings directly inform the hypotheses, questions, and interpretation of data for the present study, which extends this line of inquiry to aboveground canopy cover under contrasting irrigation regimes.

Synthesis and Research Gap

The literature reviewed in this chapter establishes several findings that, taken together, define the gap and issues that this thesis addresses. Green roofs deliver a well-documented suite of ecosystem services, including stormwater management, thermal regulation, and biodiversity support. They are conventionally classified by substrate depth into extensive, semi-intensive, and intensive types, whose performance and cost differ accordingly. Yet the great majority of green roof research has been conducted in temperate maritime, Mediterranean, and humid subtropical climates. The Continental interior of the U.S. Great Plains is underrepresented, despite the strong climate-dependence of green roof performance. That interior is characterized by severe summer heat, episodic drought, and large seasonal temperature fluctuations.

Within this broad gap, several more specific issues remain unresolved. Substrate depth is known to influence plant performance. How much depth is required to sustain canopy cover under minimal irrigation in a Continental climate, and whether intermediate semi-intensive depths suffice, has not been adequately answered. Substrate type also influences plant and system performance, but its effect is contingent. It is further complicated by the demonstrated divergence between laboratory water-retention capacity and in-situ water availability, a divergence specifically documented for the substrates used at the present study site. Irrigation is a dominant determinant of vegetation performance in hot, dry climates. Yet the literature emphasizes minimizing supplemental water through appropriate plant and substrate selection.

This leaves two important questions open: 1) How does canopy cover respond to two different irrigation frequencies? 2) How does the timing of soil/substrate moisture deficits relative to peak summer heat influence vegetation and plant cover on this mature prairie-like green roof?

Plant community and growth form shape both vegetation performance and the canopy cover that a roof presents, particularly when cover is measured from above (Lundholm et al. 2010; MacIvor and Lundholm 2011; Pérez et al. 2020). The relationship between functional-group composition and measured cover therefore warrants examination. Finally, canopy cover and vegetation health can be assessed through complementary near surface photography and UAS supported aerial imagery. Their integration on a single green roof, across a growing season, is important.

A related and often underappreciated gap concerns the measurement of canopy cover itself. As noted in earlier, quantifying green roof cover reliably has proven difficult for many researchers, and different tools had been applied to the APD-EGR without a fully satisfactory resolution. The accurate but highly labor-intensive image-analysis workflows used previously on the APD-EGR (Shrestha 2019; Decker 2021) are not sustainable for high-frequency monitoring of many plots across a full growing season. Canopeo offers a much faster alternative that makes such season-long monitoring feasible, and it is adopted as the primary cover tool in the present study for this reason. Canopeo was developed for agronomic research by Patrignani and Ochsner (2015), and one of its developers, Dr. Andres Patrignani, is now an associate professor in the Department of Agronomy at Kansas State University and a member of this thesis committee. Applying a tool created for agronomy to a mature prairie-like green roof expands its potential usefulness. It allows the performance of an established agronomic tool to be evaluated in a green roof context, and helps identify green-roof-specific refinements, such as improved detection of non-green foliage, that will likely strengthen future cover measurement.

Beyond adopting a faster tool, the present study brings several cover-assessment methods into direct comparison for the same plots. Canopy cover is derived from four independent approaches: 1) near surface iPhone photography analyzed with Canopeo, 2) UAS imagery analyzed with Canopeo, 3) UAS-derived NDVI, and 4) human ocular observation. The NDVI comparison spans all seventy-two experimental plots of the roof, within which the sixteen (16) sensor-instrumented plots (the primary focus of this thesis) are a subset. To the author's knowledge, no previous green roof study has compared this many canopy cover assessment methods on a single roof. This cross-method evaluation, discussed in Chapter 4, is a distinctive contribution of the present work. This research responds to the measurement challenges identified above by establishing not only how far near surface and aerial measures agree, but also where and why they diverge.

Prior research on the Kansas State University experimental green roof has established the site's substrate properties, in-situ moisture relationships, evolving plant mixes and vegetative communities, and belowground carbon dynamics, most comprehensively through the work of Alam et al. (2025). Several of the specific directions the present study pursues were, moreover, explicitly identified as future-research needs by the site's own investigators. Shrestha (2019) and Decker (2021) both recommended limiting irrigation on this roof to test the drought tolerance and resilience of the established planting, a test their establishment-phase, regularly irrigated studies could not provide. Decker (2021) also called for cover assessment at the species or community level rather than at the mix level, for the use of a small unmanned aerial system as a cover-measurement tool, and for soil-moisture monitoring over longer intervals than the short post-rainfall windows previously analyzed. Most recently, Alam et al. (2026), whose seasonal thermal analysis of this modeled green roof deliberately held vegetation constant, identified the absence of a canopy-cover and plant-community dimension as a limitation and called for future work that incorporates canopy density and plant mix alongside substrate and depth. The present study is positioned as a direct, context-specific response to these recommendations. What has not been examined on this roof is the aboveground canopy cover response of its mature extensive and intensive vegetation to systematic, contrasting irrigation frequencies in relation to the two EGR substrate types and three depths across a full growing season.

Informed by the green roof depth, substrate, irrigation, vegetation, and measurement literature reviewed above, this study evaluates how substrate depth, substrate type, and irrigation frequency influence the canopy cover performance of an established, in-situ green roof using two different supplemental irrigation frequencies within the Flint Hills Ecoregion of the U.S. Great Plains, while accounting for the pre-existing east–west difference in plant community descriptively rather than as an experimental factor. The experimental design and methods through which these questions are investigated are described in Chapter 3.

Chapter 3 - Research Setting and Methods

Overview of the Methodological Approach

This chapter describes the experimental site, the green roof system under investigation, the experimental design, and the field and laboratory methods used to evaluate the canopy cover performance of extensive and intensive green roofs under minimal supplemental irrigation during the 2025 growing season. The study was conducted on the established experimental green roof (EGR) on the rooftop of Seaton-Regnier Hall at Kansas State University (KSU) in Manhattan, Kansas, the same green roof used by Alam et al. (2025) for their investigation of green roof carbon sequestration in the U.S. Great Plains. Because the present thesis study and the Alam et al. (2025) study share the same site, substrates, and construction history, the EGR and substrate descriptions below draw substantially on that paper to provide context for this thesis.

The investigation for this thesis combined four complementary data streams collected over a single growing season: 1) continuous in-situ measurement of substrate volumetric water content (VWC) and substrate temperature between late June and early November 2025 using buried Teros 12 sensors; 2) high-frequency near surface measurement of fractional green canopy cover using digital (iPhone) photography analyzed with the Canopeo application; 3) periodic unmanned aircraft system (UAS) imagery used to derive both canopy cover and the Normalized Difference Vegetation Index (NDVI); and 4) an expert-guided vegetation survey of plant functional-group composition, supplemented by end-of-season measurement of dominant-grass canopy height.

A controlled supplemental-irrigation protocol imposed two distinct irrigation treatments on the instrumented plots, and an on-site weather station provided the meteorological context for interpreting plant and substrate responses. Each of these components is described in turn below, followed by a description of the data-processing and statistical-analysis procedures.

Research Site

Location and Site Description

The study was conducted on the College of Architecture, Planning and Design Experimental Green Roof (APD-EGR), located on the rooftop of Seaton-Regnier Hall at Kansas State University in Manhattan (Figure 3.1), Kansas, USA (39°11′23.0″N, 96°34′54.4″W; Alam et al., 2025). The green roof sits above the second floor, approximately 30 feet (about 9 m) above the surrounding landscape. The APD-EGR comprises 72 experimental plots, each measuring approximately 1 m × 1 m, arranged across three substrate-depth categories: 24 extensive plots at a nominal 4-inch (~10 cm) depth, 24 semi-intensive plots at a nominal 6-inch (~15 cm) depth, and 24 intensive plots at a nominal 8-inch (~20 cm) depth. The three depth categories form three contiguous beds of 24 joined plots each. All three depth categories have been present since construction in 2017-2018. As is common for in-situ green roof research, the nominal substrate depths represent target values; Alam et al. (2025) reported that actual substrate depth on this green roof ranged from approximately 7 to 12 cm in the 10-cm beds and 17 to 23 cm in the 20-cm beds.

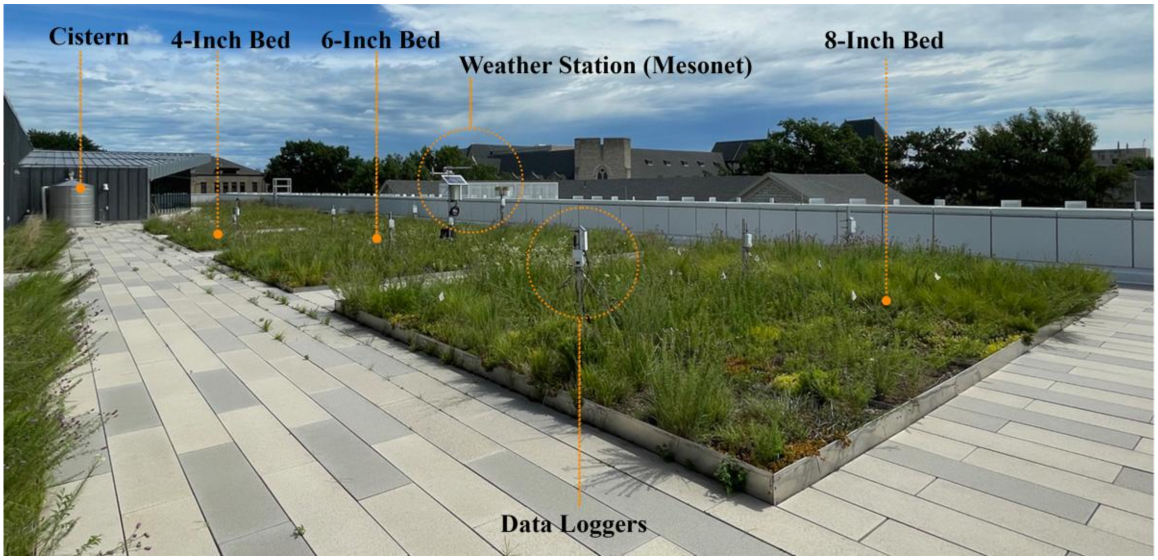

Figure 3.1. View of the APD-EGR from the south-west corner of the roof.
Shows the location of the 8-inch, 6-inch, and 4-inch green roof beds along with the cistern that stores stormwater running off the Ekdahl roof (Lee Skabelund, 30 June 2025).

It is important to mention that the APD-EGR is a real, in-situ green roof installed on an occupied building, which is different from a portable, modular, or test-tray experimental apparatus. Metal divider plates separate the approximately 1 m × 1 m cells (or plots), but from roughly 10 to 15 feet the divisions are not visible (for example, in the figure above) where nearly full vegetative cover is present. Each plot (24 per bed) supports its own plant dynamics and species diversity. As noted by Alam et al. (2025), this in-situ character is a methodological strength since data collected came from an operating green roof rather than on a controlled modular platform. As such, the findings apply directly to real-world green roof practice. The limitation of studying a real green roof is that, without having control over many variables, it is challenging to determine the impact of any specific variable. It is challenging to determine the impact of any particular variable. The strength, on the other hand, is that the findings apply directly to real-world green roofs. This trade-off between ecological realism and experimental control is acknowledged throughout the interpretation of results.

Climate and Ecoregion

The APD-EGR is situated within the Flint Hills Ecoregion of the U.S. Great Plains, a region characterized by tallgrass prairie vegetation and thin ridgeline soils that are broadly analogous to engineered green roof substrates (Alam et al., 2025; Liu et al., 2019). The site experiences a humid continental climate (Köppen-Geiger classification) with hot summers and cold winters. The region receives an average annual precipitation of approximately 904.75 mm; July is the warmest month, with a mean maximum temperature of 33.4°C, and January is the coldest, with a mean minimum temperature of −7.5°C (Alam et al., 2025). These conditions, marked by high summer heat, episodic drought, and pronounced temperature swings, make the region a demanding and underrepresented setting for green roof research, and they motivated the present study's focus on canopy cover performance under minimal supplemental irrigation.

Green Roof Construction and Vegetation Establishment

The vegetation on the APD-EGR was initially established as live plugs planted in September to October 2017, with replacement of dead or poorly performing plants in June 2018 to ensure consistent establishment across all plots. By the 2025 growing season, the vegetation had been established for approximately eight years and was therefore fully mature. The canopy cover and vegetation health responses reported here reflect the behavior of a mature, well-established green roof system rather than the establishment dynamics of a newly planted roof, and the findings should be interpreted accordingly.

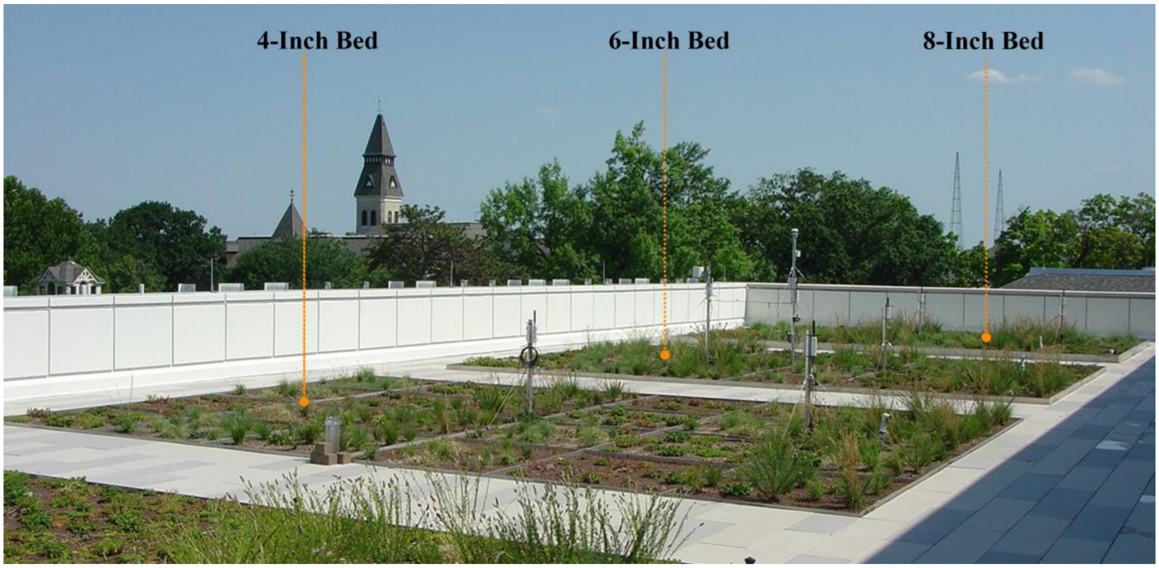

Figure 3.2. APD-EGR 2018 photo.
A 7 July 2018 photo of APD-EGR showing comparatively less vegetation and more bare soil during its establishment years (Lee Skabelund).

Substrate Materials

Two contrasting substrate types are present on the green roof, hereafter referred to as BuildEx and Rooflite (see Figure 3.3). Their physical properties were characterized at installation by Decker (2021), whose values were tabulated by Alam et al. (2025), and analyzed again for the present study in 2025 via two independent K-State Soils Lab analyses. Physical and hydraulic properties, comprising particle density, bulk density, field capacity, and permanent wilting point, were measured by K-State's Department of Agronomy Soils Lab staff. Particle-size distribution, organic matter, and chemical properties were determined on composite samples collected from the beds in May 2025. Except where noted, the values of substrate properties reported below are those measured in 2025. These 2025 substrate property values were used to configure the sixteen (16) Teros 12 soil moisture sensors, installed in June 2025.

Rooflite: Less dense, more porous

BuildEx: Greater density, less porous

Figure 3.3. Closer view of Rooflite and BuildEx substrates.
Photos by author (2025).

BuildEx (Kansas BuildEx)

BuildEx is a regionally sourced, dense, sandy substrate that was left over from implementation of the East Memorial Stadium Green Roof in 2016. The 2025 particle-size analysis returned a sand content of 88.2% of the material finer than 2 mm, with 7.0% silt and 4.8% clay, and a coarse fraction larger than 2 mm amounting to 21.4% of the total sample mass. Expressed on a whole-sample basis for comparison with the installation-era data, this corresponds to a sand content of approximately 69.3%, closely matching the 67.6% reported by Decker (2021). Organic matter, determined by loss on ignition, averaged 2.05%, and the substrate was mildly alkaline, with a mean pH of 7.97 and an electrical conductivity of 0.63

dS/m. BuildEx is the denser of the two media, with a measured dry bulk density of 1.24 g/cm^3 and a particle density of 2.01 g/cm^3, giving a total porosity of approximately 38% (Table 3.4).

Rooflite (rooflite extensive 800)

Rooflite is a commercial green roof substrate often used on extensive green roofs. Its distinguishing physical characteristic is a large coarse fraction, with material larger than two (2) mm accounting for 43.9% of the total sample mass in the 2025 K-State Soils Lab analysis, approximately twice the coarse fraction of BuildEx. Within the material finer than two (2) mm, sand accounted for 85.5%, silt for 10.0%, and clay for 4.5%, which on a whole-sample basis corresponds to a sand content of approximately 47.8%, comparable to the 52.4% reported by Decker (2021). Rooflite contained more organic matter than BuildEx, at 2.67% by loss on ignition, with a mean pH of 7.93 and an electrical conductivity of 0.64 dS/m. It is the lighter and more porous medium, with a measured dry bulk density of 0.84 g/cm^3 and a particle density of 1.83 g/cm^3, giving a total porosity of approximately 54% (Table 3.4). In the installation-phase laboratory testing of substrates (analyzed in 2018), Rooflite exhibited a higher maximum water-retention capacity than BuildEx, at 35.0% versus 29.5%, determined under ASTM E2399 (Decker 2021; ASTM International 2019).

Research Plot Selection and setting up the site

Figure 3-4 shows the positioning of 16 selected plots for this research among the 72 total plots (24 each for extensive, semi-intensive, and intensive). Among the sixteen selected plots, eight are extensive (shallow), and eight are intensive (deeper). One combined soil moisture and temperature sensor was installed in each of these sixteen plots.

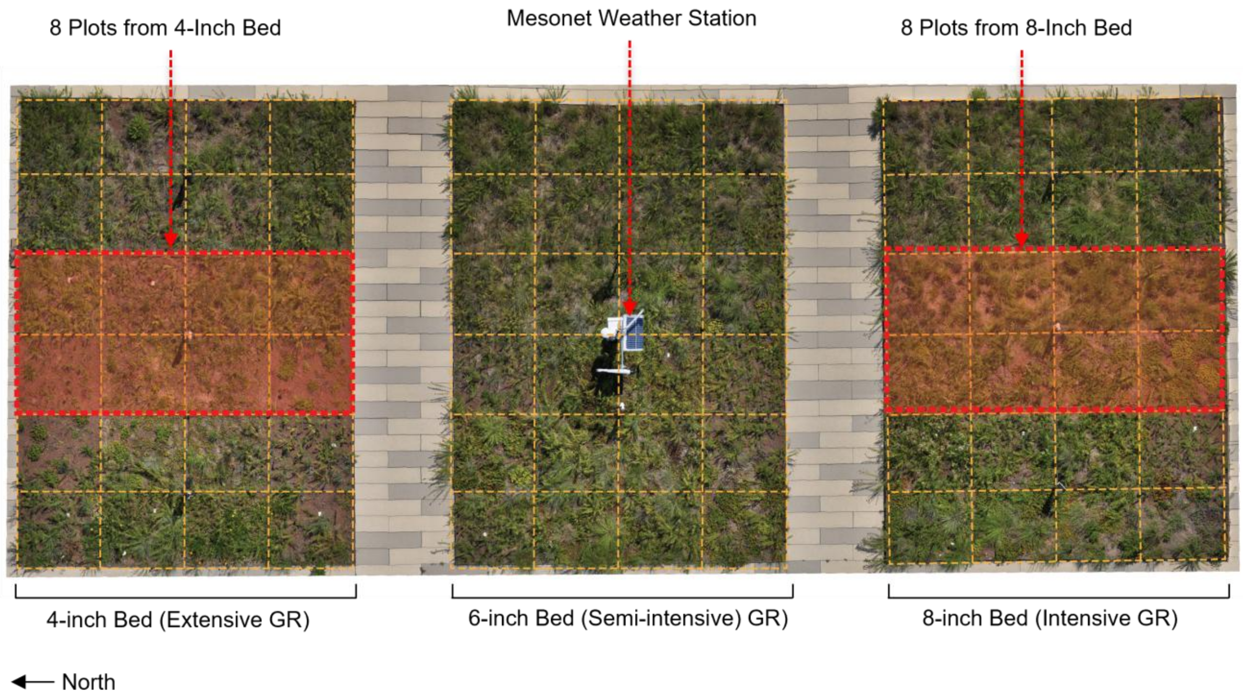

Figure 3.4. The selected plots for the experiment and soil moisture and temperature sensor installation.

Aerial view taken from a drone shows the location of the 4-inch, 6-inch, and 8-inch beds. The 16 study plots are shown in red within the 4-inch and 8-inch beds. Diagram by author using Kaden Spencer's July 9, 2025 UAS image as a base.

Figure 3-5 shows a simplified diagram that indicates the numbering system of the sixteen selected plots that was used throughout this research. This diagram also shows the positioning of BuildEx (gray plots) and Rooflite (non-gray plots) substrate mixes. The plots marked with blue dashed lines were assigned to receive more irrigation than the unmarked plots. The sensors from each of the sixteen plots were connected to four dataloggers and uploaded hourly soil moisture and temperature data, which were monitored remotely using the ZENTRA Cloud platform. Irrigation decisions were triggered based on this subsoil volumetric water content data. The east side plots (shown in green) were dominated by native grass, and the west side plots (shown in orange) were sedum- and forb-dominant at the time of this study. The establishment phase plant communities are shown in Figure 3-5.

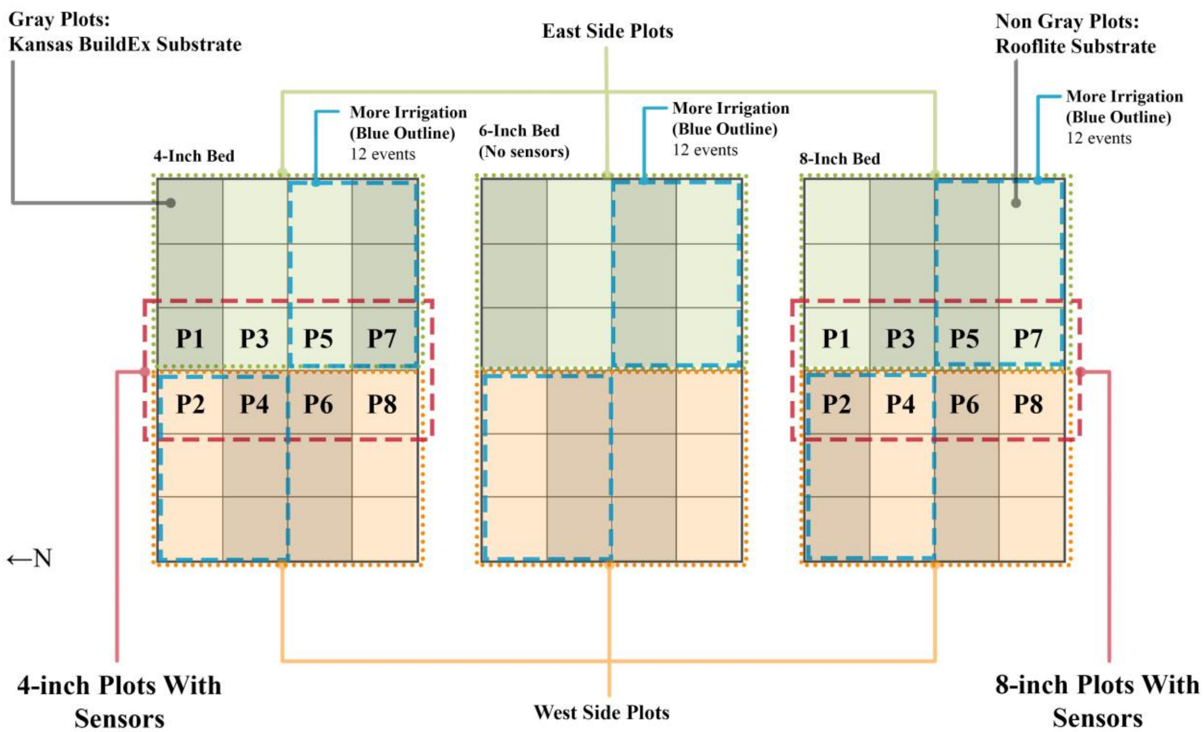

Figure 3.5. Plot numbering for the research, irrigation treatment selection, and composition of BuildEx and Rooflite substrates.

The red dotted area shows the selected experimental plots where sensors were installed. The blue dotted area shows the plots assigned for more supplemental irrigation. The gray plots represent Kansas BuildEx while the non-gray plots represent Rooflite substrate. Diagram by author (2026).

Analysis of Substrate Physical Properties

At a thesis committee meeting held before the sensors were installed, the previously reported bulk-density values for the two substrates were questioned by the committee member specializing in soil physics, who recommended that the substrates be re-sampled and analyzed and that substrate-specific sensor calibrations be developed rather than relying on the factory default conversion (Andres Patrignani, personal communication, 2025). Both recommendations were adopted, and together they shaped the instrumentation methodology for this thesis.

Undisturbed core samples were collected from the 8-inch and 4-inch beds in May 2025 and analyzed for particle density, bulk density, field capacity, and permanent wilting point. Resulting values are reported in Table 3-4. The re-determined dry bulk densities are 0.84 g/cm³ for Rooflite and 1.24 g/cm³ for BuildEx, compared with 0.98 and 1.47 g/cm³ in the earlier record.

The two sets of values are not measurements of the same quantity. The earlier figures originate from Decker (2021), who submitted samples drawn from the substrate supply used at installation but never placed on the roof. In 2018, a commercial testing laboratory analyzed these pre-installation substrates, where dry bulk density was determined under ASTM E2399, a standard test method that establishes the maximum media density of green roof media for the purpose of dead-load estimation (ASTM International, 2019). Alam et al. (2025) noted those laboratory values. A maximum density obtained under a standardized packing procedure is not expected to equal the bulk density of the same medium as it lies in a roof bed. Decker (2021) noted that samples taken from the APD-EGR in 2019 gave bulk densities different from those reported by the laboratory in 2018. The 2025 values, by contrast, were measured on undisturbed cores extracted directly from the beds by Lee Skabelund and Muhaiminul Islam in May 2025. They are in-situ-based field values, which soil moisture sensor calibrations require.

For this thesis, the 2025 values are used. They were entered into ZENTRA Cloud as the additional media parameters accompanying the substrate-specific calibration equations, and the entire 2025 soil-moisture record analyzed in Chapter 4 therefore rests upon them. The earlier values are retained in this section for continuity with the published record of the APD-EGR.

The In-Situ versus Laboratory Substrate Moisture Paradox

A key feature of these two substrates, central to the interpretation of the present study, is the apparent contradiction between laboratory and field moisture behavior. In the laboratory, Rooflite was the medium that held more moisture. It exhibited the higher maximum water-retention capacity in the installation-phase substrate testing (Decker 2021), and the 2025 core measurements reproduce the same contrast independently, with Rooflite holding more water at field capacity than BuildEx (0.150 against 0.130 m^3/m^3) and providing roughly one-third more plant-available water per unit volume (Table 3.4).

From substrate samples from the EGR plots, the relationship reverses. Decker (2021) found that BuildEx had the greater water-holding capacity at every substrate depth examined, and the continuous sensor record collected for the present study shows the same ordering, with BuildEx plots averaging a higher seasonal mean volumetric water content than Rooflite plots (as discussed in Chapter 4). The reversal is attributable to the contrasting physical structure of the two media. The dense, sandy profile of BuildEx retains greater volumes of water under actual rooftop conditions, whereas Rooflite, with a coarse fraction more than twice as large and a correspondingly lower bulk density, drains more freely once free water has moved through the shallow profile. A laboratory determination of retention on a packed sample and the behavior of a shallow, freely draining roof bed are therefore not interchangeable. This site-specific moisture paradox was treated as an established condition in the present study. 2025 soil moisture data are interpreted in relation to the in-situ behavior of the two media rather than laboratory retention values.

Plant Communities

Two distinct plant (vegetation) communities are present on the APD-EGR, corresponding to its east-west spatial organization. The east plots are dominated by native prairie grasses and forbs, corresponding to the Mix C plants, which includes *Carex brevior*, *Dalea purpurea*, *Koeleria pyramidata*, *Packera obovata* (only a few of these plants were present within the three EGR beds in 2025), *Schizachyrium scoparium* (the dominant grass on the EGR beds in 2025, especially on the east side), *Bouteloua curtipendula*, and *Sporobolus heterolepis* (only a few of these plants were present on each quadrant of the EGR in 2025). Sedum species are also present on the east side but are mostly shaded by native grasses and forbs. The west plots contain a mixed prairie-and-sedum community, with Mix A, Mix B, and Mix C (including the three native grasses mentioned above), along with *Carex brevior*, *Dalea purpurea*, the eight *Sedum* species planted in Fall 2017, and more than a half dozen native forbs planted by Lee Skabelund from seed in early June 2023 on selected west side plots (including *Asclepias tuberosa*, *Asclepias verticillata*, *Dalea candida*, and *Symphyotrichum ericoides*, the four most abundant new forbs observed during the summer of 2025). The species composition of each plot (16 plots of this experiment) was confirmed against two field surveys during the 2025 vegetation survey in June and December. If a species was present in any one of the surveys, it was considered present throughout the season.

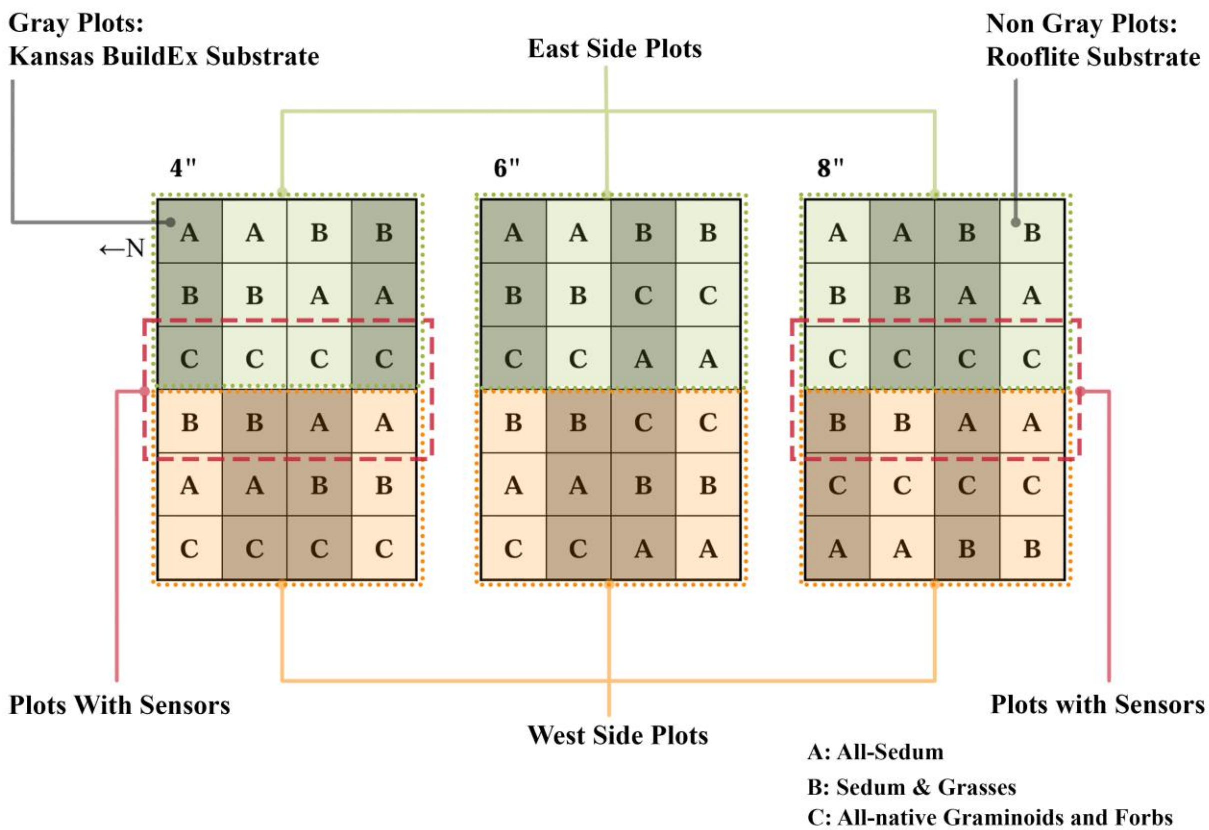

Figure 3.6. Earlier and present plant community composition.

East and west side plots shaded in green and orange, and the selected 16 plots for this study are outlined in red, where the soil moisture and temperature sensors were buried. Initially, there were three plant communities (A: All-Sedum, B: Sedum and Native Grasses, and C: All Native Graminoids and Forbs) and 15 distinct plant species introduced. The gray shades represent the Rooflite substrate, and the non-gray boxes represent the BuildEx substrate. In 2022, the west side plots were not irrigated. This caused a drop in native grasses in the west section (shown in orange). As a result, during the present study, the east side plots (shown in green) were dominated by native grasses with a few sedum species present. The west plots have sedums, native forbs, and native grasses. In 2025, the west side had much fewer native grasses than the east side. Diagram by author (2026).

Presently, the east-west plant-community division arose due to irrigation differences in 2022 when the 36 west-side plots received no supplemental irrigation. As such, the plant community types were not randomly assigned as part of the present experiment. The plant community is discussed descriptively rather than being treated as a fourth variable due to the limited number of replicates (only two per bed depth).

Experimental Design

Statistical Design and Rationale

The 16 instrumented plots were analyzed as a balanced 2^3 factorial treatment structure combining three two-level primary treatment factors (substrate depth: 4-inch vs 8-inch, substrate type: BuildEx vs Rooflite, and irrigation frequency: more vs less; see Table 3.1). As this is a mature green roof, constructed in 2017-18, the substrate depths and substrate types could not be randomly assigned to the plots. The middle 8 plots from 4-inch and 8-inch beds were selected to have similar environmental variables, mainly the evening shade cast by the building west of the beds, and to avoid edge effects (the edge plots on the east and west sides have more vegetation due to access to additional moisture below the pavers). Irrigation frequency was assigned in a way to have an equal number of BuildEx and Rooflite plots to get more irrigation and less irrigation on each 4-inch, 6-inch, and 8-inch bed. Also, the more irrigation plots and less irrigation plots were grouped alternatively in a way that 18 east plots and 18 west plots get more irrigation on every three beds. The same strategy was followed to select the less irrigated plots. From a management perspective, similar irrigation plots were grouped to facilitate easy irrigation with a hosepipe. The study is therefore observational (quasi-experimental) with respect to depth, substrate, and community, and the data were analyzed with a fixed-effects factorial linear model (factorial ANOVA) rather than as a randomized experiment. This yields eight unique treatment combinations with two replicates per combination (n = 2 per plot) and eight error degrees of freedom.

The contrasting east versus west plant community, which resulted from previous irrigation management (no supplemental irrigation on the west-side plots in 2022), was accounted for descriptively rather than as an experimental factor in this study. The decision to treat the plant community as a pre-existing, observed difference, rather than as a fourth experimental factor, was made for three reasons. (i) The effect of the plant community is not the primary interest of this study; however, the east–west plant-community split is a pre-existing condition that cannot be avoided. (ii) Including plant community as a fourth factor would reduce replication to a single unit per combination ($n = 1$), leaving zero error degrees of freedom and rendering the analysis of variance impossible. (iii) Treating the east and west sides as two pre-existing groups preserves the ability to describe and discuss community effects qualitatively throughout the thesis while retaining a statistically tractable 2^3 design.

Table 3.1. Layout of the eight depth, substrate, and irrigation treatment combinations across the east and west sides of the roof.
Each side contains one instance of every combination, so the treatment structure is balanced across the two sides. The east-west grouping reflects a pre-existing difference in plant community (East, native grass-forb; West, prairie–sedum) established at planting in 2017-2018, not a randomized block assignment; it is described in this study rather than analyzed as an experimental factor.

Treatment combination (depth · substrate · irrigation)	East block	West block
4″ (~10 cm) · BuildEx · Less	4″ P1	4″ P6
4″ (~10 cm) · BuildEx · More	4″ P7	4″ P4
4″ (~10 cm) · Rooflite · Less	4″ P3	4″ P8
4″ (~10 cm) · Rooflite · More	4″ P5	4″ P2
8″ (~20 cm) · BuildEx · Less	8″ P3	8″ P6
8″ (~20 cm) · BuildEx · More	8″ P5	8″ P2
8″ (~20 cm) · Rooflite · Less	8″ P1	8″ P8
8″ (~20 cm) · Rooflite · More	8″ P7	8″ P4

Note. Plot labels follow the sequence used throughout data collection (4″ P1-P8, 8″ P1-P8). The east–west grouping is a pre-existing feature of the roof (planted 2017-2018) rather than a randomized block assignment.

Primary Treatment Factors

The three primary treatment factors and their attributes were as follows:

(i) **Substrate depth:** the 4-inch (~10 cm) extensive beds and 8-inch (~20 cm) intensive beds.

(ii) **Substrate type:** BuildEx and Rooflite growing media.

(iii) **Irrigation frequency:** a more-irrigated treatment (12 supplemental events, totaling approximately 78 gallons per plot over the season) and a less-irrigated treatment (4 events, totaling approximately 26 gallons per plot over the season), yielding an approximate 3:1 ratio of applied water between the two treatments.

Plot Selection Rationale

Of the 72 plots on the APD-EGR green roof, 16 were selected for full sensor instrumentation and inclusion in the primary experiment: eight 4-inch (~10 cm) extensive plots and eight 8-inch (~20 cm) intensive plots in the middle (east-west) of each of these two EGR beds. The 24 semi-intensive 6-inch (~15 cm) plots were intentionally excluded from the instrumented experiment to maximize the substrate-depth contrast between the two extreme depths (~10 cm and ~20 cm) and to allow the available sensor and logging resources to be concentrated on a fully replicated two-depth design. The semi-intensive plots were retained in the broader UAS-derived NDVI analysis, which included all 72 plots and thus permitted a separate, supplementary understanding of the 6-inch depth category.

Plot Registry

Figure 3.5 shows the plot numbering assignments for the 4-inch and 8-inch beds for the selected plots of this study, where the soil moisture and temperature sensors were buried. This plot numbering assignment was used consistently throughout the study. Table 3.2 presents the substrate depth, type, irrigation frequency, plant community, and EDR Plot Number. EGR Plot Number is a numbering system to address all 72 plots of the EGR, used in previous research at this site. As this study focused on only 16 plots among them, P1 to P8 numbering was assigned to 4-inch and 8-inch beds to simplify the tracking of the plots.

Table 3.2. **Treatment assignments for the 16 sensor-instrumented plots.**
Plot labels (4″ P1-P8 and 8″ P1-P8) follow this sequence. "EGR Plot #" refers to the plot's position number within its depth bed on the full 72-plot green roof. East plots were dominated by the native grass-and-forb community (with some sedums). West plots were composed of a mixed prairie-and-sedum community (with abundant native forbs).

Plot	Depth	Substrate	Irrigation	Plant community	EGR Plot #
4″ P1	4″ (~10 cm)	BuildEx	Less irrigated	E (grass/forb)	Plot 3
4″ P2	4″ (~10 cm)	Rooflite	More irrigated	W (prairie/sedum)	Plot 4
4″ P3	4″ (~10 cm)	Rooflite	Less irrigated	E (grass/forb)	Plot 10
4″ P4	4″ (~10 cm)	BuildEx	More irrigated	W (prairie/sedum)	Plot 9
4″ P5	4″ (~10 cm)	Rooflite	More irrigated	E (grass/forb)	Plot 15
4″ P6	4″ (~10 cm)	BuildEx	Less irrigated	W (prairie/sedum)	Plot 16
4″ P7	4″ (~10 cm)	BuildEx	More irrigated	E (grass/forb)	Plot 22
4″ P8	4″ (~10 cm)	Rooflite	Less irrigated	W (prairie/sedum)	Plot 21
8″ P1	8″ (~20 cm)	Rooflite	Less irrigated	E (grass/forb)	Plot 3
8″ P2	8″ (~20 cm)	BuildEx	More irrigated	W (prairie/sedum)	Plot 4
8″ P3	8″ (~20 cm)	BuildEx	Less irrigated	E (grass/forb)	Plot 10
8″ P4	8″ (~20 cm)	Rooflite	More irrigated	W (prairie/sedum)	Plot 9
8″ P5	8″ (~20 cm)	BuildEx	More irrigated	E (grass/forb)	Plot 15
8″ P6	8″ (~20 cm)	BuildEx	Less irrigated	W (prairie/sedum)	Plot 16

Plot	Depth	Substrate	Irrigation	Plant community	EGR Plot #
8″ P7	8″ (~20 cm)	Rooflite	More irrigated	E (grass/forb)	Plot 22
8″ P8	8″ (~20 cm)	Rooflite	Less irrigated	W (prairie/sedum)	Plot 21

Near-Surface Canopy Cover Measurement (Canopeo)

Fractional green canopy cover is the primary response variable for this thesis. It was measured near the surface of the 16 selected green roof plots (eight in each of the two depths, 4-inch and 8-inch) using the Canopeo application (Patrignani and Ochsner, 2015) applied to all overhead iPhone photos taken by the author between late June and early November 2025, for a total of 56 days. Canopeo classifies each pixel of a digital image as green canopy or non-canopy based on red-to-green and blue-to-green color ratios and an excess-green index, returning the percentage of the image classified as actively green vegetation.

On each measurement day, a single overhead (nadir) photograph of each of the 16 instrumented plots was captured from a ladder positioned above the plot, using an iPhone 11 Pro Max or iPhone 12 Pro held parallel to the plot surface so that each image framed a full 1 m × 1 m area for each of the 16 plots. While taking the photos, the camera was approximately 157 cm to 165 cm (62 to 65 inches) above the green roof plots. A quality-control step was applied at the moment of capture: each photograph was cropped immediately, before moving to the next plot, to confirm that the image was a flat, undistorted, two-dimensional overhead view. Any distorted image was deleted on the spot, and the photograph was retaken until a satisfactory overhead crop was obtained. The 16 cropped images (one per plot, P1-P16) were uploaded to OneDrive each day after capturing. To minimize variation in illumination, photographs were taken in the evening, when the building cast uniform shade across the green roof, avoiding the direct sunlight and hard shadows that can bias color-threshold classification. Plots were photographed in a fixed sequence on each date, the eight 4-inch plots (P1 through P8) followed by the eight 8-inch plots (P9 through P16), to maintain consistent plot identification. Figure 3.7 shows how the photos were taken using a ladder.

Figure 3.7. Taking a photo with an iPhone using a ladder.

For the inner plots, two pedestals of the ladder were placed on the aluminum divider to minimize disturbance on the roof and to get closer to the center. (KSU Photographer Jeff Moore, 2025)

Image analysis was performed later using the Canopeo Desktop application, rather than the Canopeo mobile application, which provided a consistent processing environment for the full image set. Each cropped image was analyzed to yield a single fractional green cover value per plot per date. The entire set of images was analyzed in a single processing campaign using one installation of the Canopeo Desktop application, and the classification parameters supplied as that version's defaults were retained without modification. The parameters were the image size of original photos, a color-ratio threshold of 0.97, noise reduction enabled, a blended-overlay opacity of 35, and a neon mask color. For each image, the application generated a results table together with a blended overlay image and a boolean mask. Processing every image on every date under one software version and one unmodified parameter set ensured that the seasonal record rests on a single, reproducible classification rule. Figure 3.8 shows the window of the Canopeo desktop app with the default values that were used for analyzing all photos.

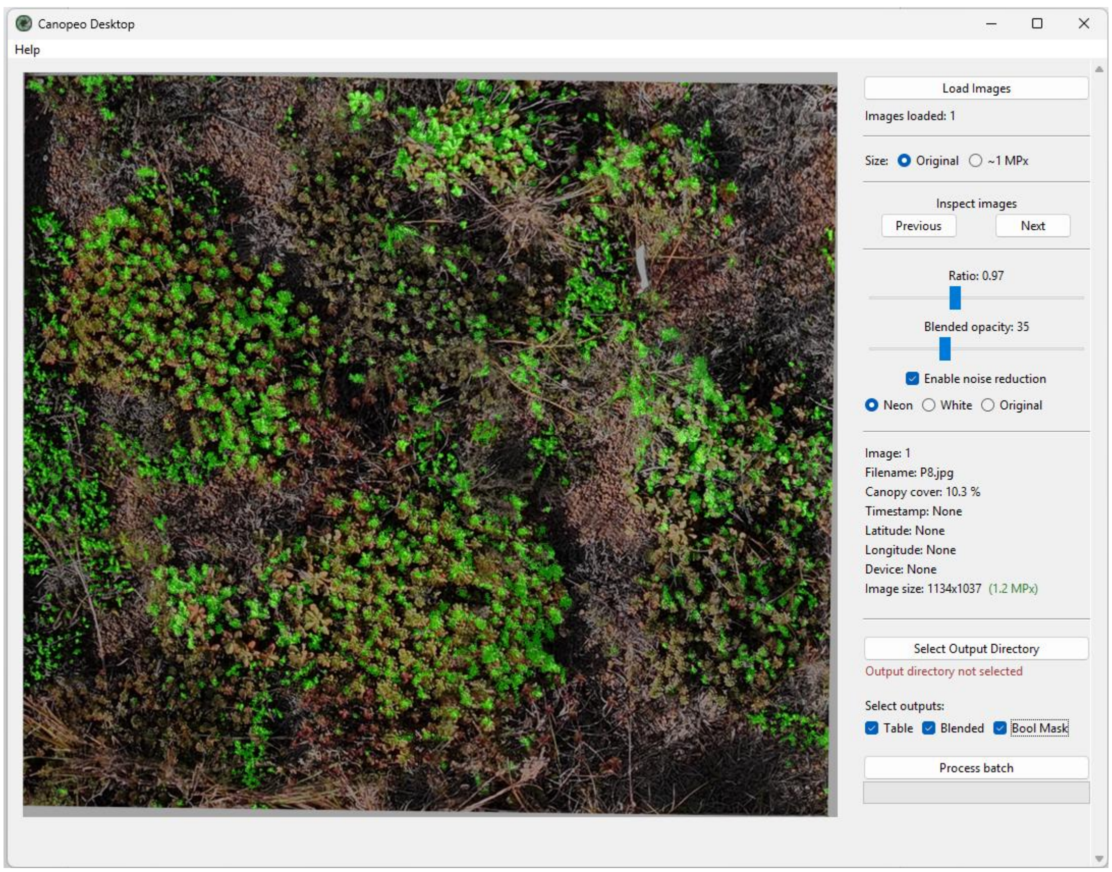

Figure 3.8. Canopeo window showing the default settings and values used for analyzing the overhead iPhone images and the drone images.

The settings and two values shown in this image were used for analyzing all images of this study while using Canopeo. Author (2026).

The classification threshold governs how much cured, straw-colored tissue is counted as green, and the choice of parameters therefore affects absolute cover values materially, most of all late in the season when the warm-season grasses senesce. Absolute canopy cover values are consequently comparable across studies only where the same software version and the same classification parameters have been applied, whereas the relative differences among treatments are considerably more robust to that choice.

Canopy cover was thus measured on 56 dates across the growing season, spanning June 30 to November 5, 2025. This high measurement frequency, particularly dense during the July to August peak-stress period, was designed to capture the temporal dynamics of canopy response to the supplemental-irrigation treatments and to the prevailing weather conditions.

Soil Moisture and Temperature Monitoring

Sensor and Logger Configuration

Substrate volumetric water content and substrate temperature were monitored continuously in all 16 instrumented plots using METER Group TEROS 12 sensors. One TEROS 12 sensor was installed in each plot, buried approximately 2 inches (~5 cm) below the substrate surface. Each sensor reported volumetric water content (m^3/m^3), substrate temperature (°C), and bulk electrical conductivity (mS/cm). Substrate-specific calibration equations were applied to the moisture readings, with the Rooflite equation assigned to sensors installed in Rooflite plots and the BuildEx equation assigned to sensors in BuildEx plots (Table 3.4), so that reported water content reflected the differing dielectric behavior of the two media.

The 16 sensors were distributed across four METER Group ZL6 cellular data loggers, with four TEROS 12 sensors connected to each logger and grouped by bed and side of the roof:

one logger served the east 4-inch plots, one the west 4-inch plots, one the east 8-inch plots, and one the west 8-inch plots. All loggers recorded on an hourly measurement interval (3,600 s) and transmitted data to the METER Group ZENTRA Cloud service for near-real-time monitoring, which also supported monitoring when to irrigate. Sensors were installed, and logging commenced on June 18, 2025, and the continuous record used in this thesis extends through the end of the 2025 growing season. Logged data were exported from ZENTRA Cloud for organization, processing, and analysis.

Logger-to-Plot Port Mapping

Table 3-3 shows which plots relate to which datalogger. Each data logger connects to four sensors from four different plots, showing how the four data loggers cover the sixteen plots. Figure 3.9 shows how the TEROS 12 sensors were connected to the data loggers, with four sensors wired to each logger and east- and west-side sensors kept on separate east- and west-side loggers.

Table 3.3. Mapping of data-logger ports to instrumented plots. Logger identifiers are METER Group ZL6 device names. Port assignments were verified against logger port labels and the corrected green-roof layout.

Logger	Bed	Port	Plot	Substrate / irrig.	Sensor label
z6-03500	East 4″	1	4″ P7	BuildEx / More	East-4in-22-K
z6-03500	East 4″	2	4″ P5	Rooflite / More	East-4in-15-R
z6-03500	East 4″	3	4″ P3	Rooflite / Less	East-4in-10-R-stressed
z6-03500	East 4″	4	4″ P1	BuildEx / Less	East-4in-3-K-stressed
z6-07870	West 4″	1	4″ P8	Rooflite / Less	West-4in-21-R-stressed
z6-07870	West 4″	2	4″ P6	BuildEx / Less	West-4in-16-K-stressed
z6-07870	West 4″	3	4″ P4	BuildEx / More	West-4in-9-K
z6-07870	West 4″	4	4″ P2	Rooflite / More	West-4in-4-R
z6-03504	East 8″	1	8″ P7	Rooflite / More	East-8in-22-R
z6-03504	East 8″	2	8″ P5	BuildEx / More	East-8in-15-K
z6-03504	East 8″	3	8″ P3	BuildEx / Less	East-8in-10-K-stressed
z6-03504	East 8″	4	8″ P1	Rooflite / Less	East-8in-3-R-stressed
z6-03501	West 8″	1	8″ P8	Rooflite / Less	West-8in-21-R-stressed
z6-03501	West 8″	2	8″ P6	BuildEx / Less	West-8in-16-K-stressed
z6-03501	West 8″	3	8″ P4	Rooflite / More	West-8in-9-R
z6-03501	West 8″	4	8″ P2	BuildEx / More	West-8in-4-K

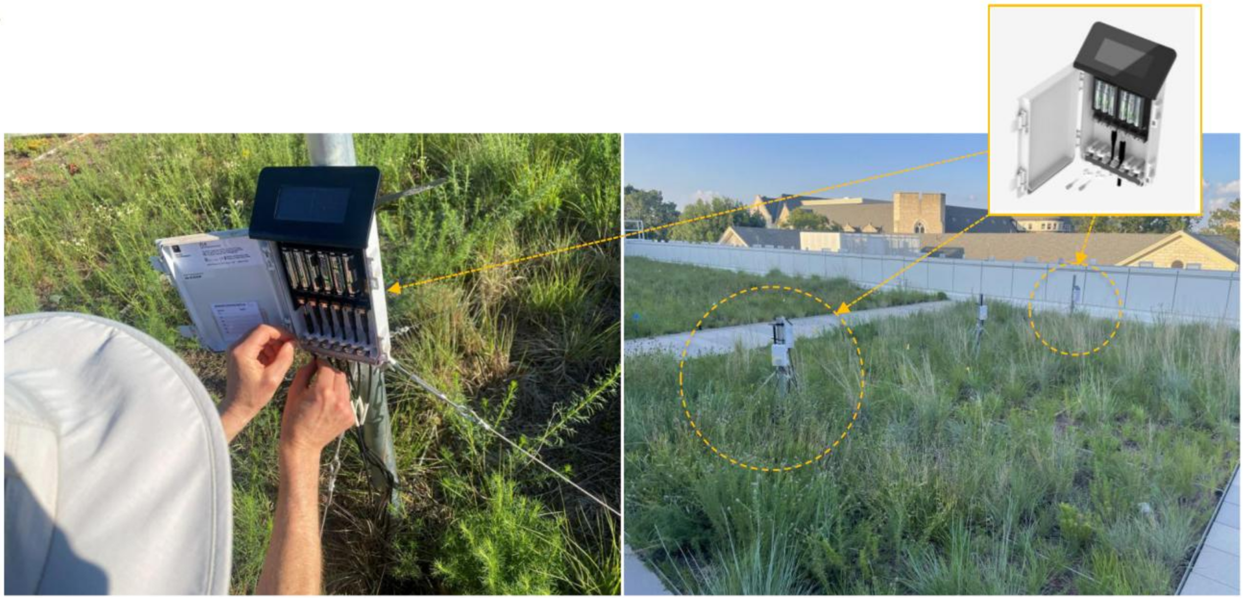

Figure 3.9: Connecting sensors with data loggers.

Each data logger connects to four TEROS 12 sensors. Sensors from east side plots are connected to east side data loggers, and sensors from the west side plots are connected to west side data loggers. Author (2026).

Substrate-Specific Sensor Calibration

Figure 3.10 shows the main steps of sensor preparation and deployment, from collecting substrate samples on the APD-EGR, through substrate-specific calibration of the TEROS 12 sensors in the soil-water laboratory, to installing the sensors in the plots. TEROS 12 sensors infer volumetric water content from the dielectric permittivity of the surrounding medium, and the factory-supplied conversion, designated the “Mineral” calibration, is derived from mineral agricultural soils. Engineered green roof substrates differ substantially from such soils in bulk density, pore structure, and mineral-organic composition, so the default conversion cannot be assumed to be accurate for them. All previous soil-moisture monitoring and research on the APD-EGR, including the studies that established the site’s moisture record, relied on this factory Mineral calibration, and Decker (2021) explicitly reported difficulty in developing substrate-specific calibrations for the two media. Deriving and applying substrate-specific calibration equations for BuildEx and Rooflite was therefore undertaken as a prerequisite of the present study, and it constitutes a methodological advance for the APD-EGR.

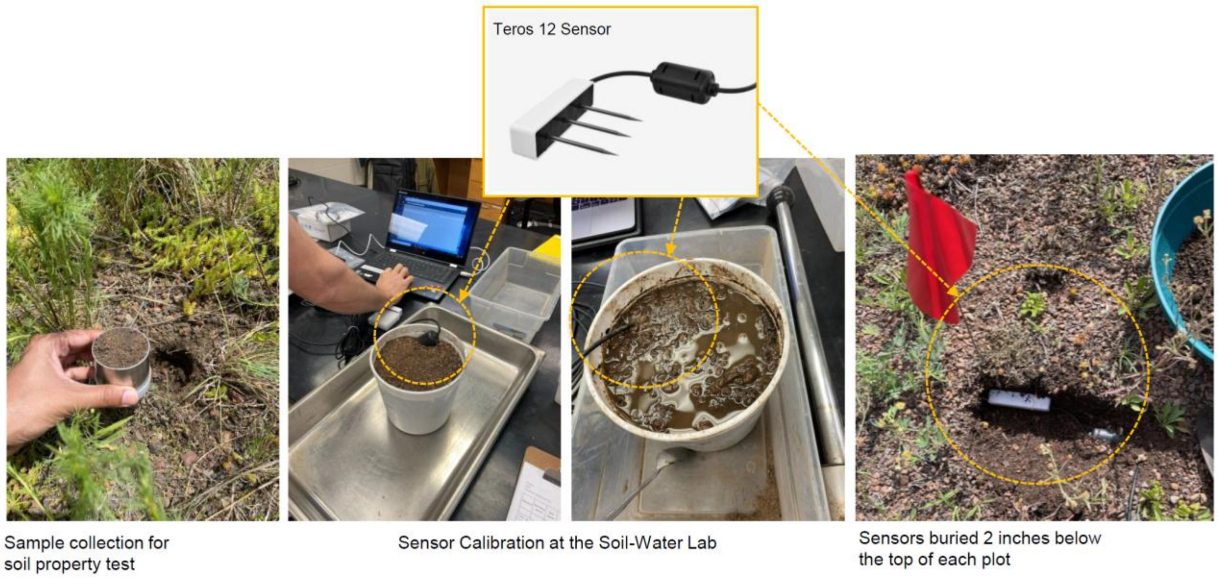

Figure 3.10. Substrate sample collection from APD-EGR, sensor calibration in the soil-water lab, and installation of sensors in the plots.
Red flags were used to mark the sensor locations in the eight extensive plots, and white flags were used to mark the sensor locations in the eight intensive plots. Author (2025).

Calibration was performed in K-State's Soil-Water Laboratory of the Department of Agronomy on May 27, 2025. For each substrate, material was packed into a container of known volume (1,852 cm^3), and an oven-dry reference mass was established. Water was then added in successive increments, and after each increment, the container was reweighed, and the sensor's raw output, expressed in millivolts, was recorded once the reading had stabilized. Volumetric water content at each step was computed as the mass of water present, taken as the difference between the wet mass and the oven-dry mass, divided by the known substrate volume, assuming a water density of 1 g/cm^3. The resulting series spanned conditions from near oven-dry to near saturation. Figure 3.11 shows the saturation step that preceded the water-holding-capacity measurements. Three replicate samples of each substrate were fully wetted and then allowed to drain, so that the retained water content could be determined for Rooflite (left-hand cylinders) and BuildEx (right-hand cylinders). Running three replicates per substrate provided a measure of within-substrate variability in retention.

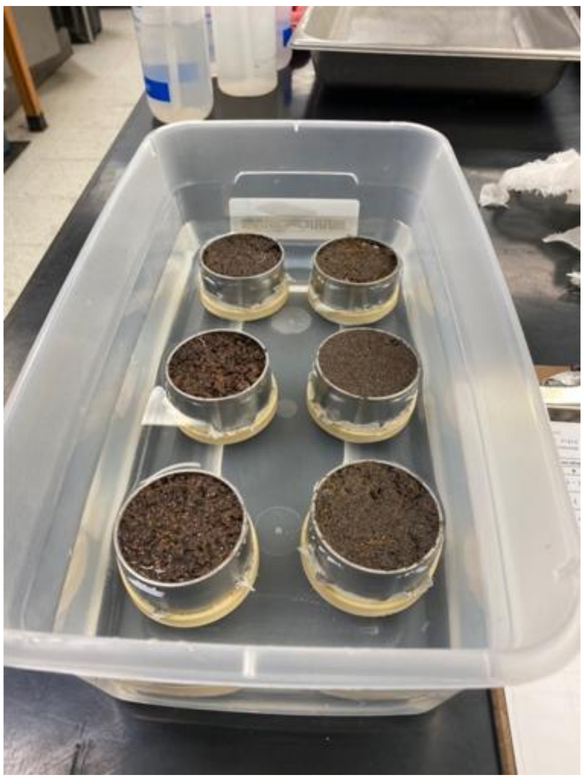

Figure 3.11. Saturation of soil samples before determination of water holding capacity. Three samples were collected from each substrate type. Cylinders on the left contain Rooflite and the right-side cylinders contain BuildEx substrates. Author (2025).

For BuildEx, twelve TEROS 12 observations were obtained across a raw range of 1,957 to 2,590 mV and a water-content range of 0.000 to 0.338 m^3/m^3. For Rooflite, eleven observations were obtained across a raw range of 1,930 to 2,764 mV and a water-content range of 0.000 to 0.377 m^3/m^3. Parallel calibration series were also collected for the older-generation

METER 5TM sensors, a few of which remained installed on the roof from the earlier instrumentation described by Decker (2021).

Only TEROS 12 sensors were used in the sixteen (16) instrumented plots analyzed in this thesis. TEROS 12 was selected because it is the current-generation replacement for the legacy 5TM and 5TE sensors, because it reports bulk electrical conductivity in addition to the water content and temperature returned by the 5TM, and because it allowed the 16 plots to be instrumented uniformly with new sensors of known condition, whereas the surviving 5TM units on the roof were of varying age and only some remained functional. The bulk electrical conductivity records were retained as part of the logged dataset but were not analyzed for this thesis, which focused on changes in substrate water content and temperature.

Volumetric water content was regressed on raw sensor output using polynomial models. A third-order polynomial was required to describe the BuildEx response, whereas a second-order polynomial was sufficient for Rooflite, and higher-order terms produced no meaningful improvement for that medium. The curves were first fitted using spreadsheet trendline functions, but the coefficients returned in that form carried too few significant figures to be usable. Because the predictor is raw sensor output in the range of roughly two thousand millivolts, the higher-order coefficients are extremely small in magnitude and rounding them to a single significant figure propagates into physically impossible water contents when the polynomial is evaluated. Entering those coefficients into ZENTRA Cloud produced implausible values and erratic time-series plots. The curves were therefore refitted at full numerical precision using Python, and the corrected coefficients were supplied by the committee member supervising the soil-water measurements (Andres Patrignani, personal communication, July 15, 2025). The final equations are reported in Table 3.3, and they explain 94.8 percent of the variance in the BuildEx calibration series and 99.6 percent of the variance in the Rooflite series.

Table 3.4 presents the calibration equations derived for each substrate type, which relate the raw TEROS 12 output (x, in mV) to volumetric water content (θ, in m^3/m^3). Separate equations were fitted for Rooflite and BuildEx, because the two substrates differ in composition and bulk density and therefore return different sensor readings at the same true water content. These equations were applied to the Zentra Cloud platform. All raw logger data of the volumetric water content values reported in Chapter 4 were influenced by these equations.

Table 3.4. **Substrate-specific calibration equations relating TEROS 12 raw sensor output (x, in mV) to volumetric water content (θ, in m^3/m^3).**

Substrate	Calibration equation	R^2
BuildEx	$\theta = -39.34620275 + 0.05185726x - (2.27550613 \times 10^{-5})x^2 + (3.33651882 \times 10^{-9})x^3$	0.948
Rooflite	$\theta = -2.16239357 + 0.00160120x - (2.47285241 \times 10^{-7})x^2$	0.996

The equations were entered into ZENTRA Cloud as custom calibrations, assigned sensor by sensor according to the substrate of the plot in which each sensor was installed, so that BuildEx plots were processed with the BuildEx equation and Rooflite plots with the Rooflite equation. Because the Rooflite model is second order, its third-order coefficient was set explicitly to zero. The custom calibration was accompanied by the substrate physical parameters mentioned in Table 3.5, which ZENTRA Cloud requires for additional media parameters. The equations are valid within the calibrated raw range, approximately 1,960 to 2,700 mV, and predictions outside that range are extrapolations.

The custom calibration was activated on July 16, 2025, after which ZENTRA Cloud reprocessed the entire logged record, including data collected between the start of logging on June 18, 2025, and the date of activation. The retroactive reprocessing was confirmed during setup by alternating between the Mineral and custom calibrations and observing that the historical series updated accordingly, and it is evident in the exported data, where the signature of the custom equations is present throughout the record. The complete 2025 dataset analyzed in this thesis therefore rests on the substrate-specific calibration rather than on the factory default.

Substituting the substrate-specific equations for the Mineral default systematically lowered the reported water contents. Across the eight sensor ports compared at the time of implementation, seven returned lower values under the custom calibration, by between 1.5 and 7.8 percentage points of volumetric water content, while one returned a value 1.0 percentage point higher. The divergence was greatest at the dry end of the range, which is the condition of greatest interest in a minimal-irrigation experiment, and this pattern indicates that the factory calibration had been overstating the water available to plants in these substrates. A consequence of the polynomial form is that both equations return small negative values when raw output falls below the calibrated range, below approximately 1,959 mV for BuildEx and 1,920 mV for Rooflite. A small number of readings in the driest shallow, less-irrigated plots fell into this region and were returned as slightly negative water content. These values were set to zero prior to analysis, as described in Chapter 4, and they should be understood as indicating that the substrate had dried below the range represented in the calibration series rather than as physically meaningful measurements.

Substrate Physical and Hydraulic Properties

Table 3.5 summarizes the physical and hydraulic properties of the Rooflite and BuildEx substrates, measured from undisturbed 100 cm^3 cores. Plant-available water capacity (PAWC), the difference between field capacity and permanent wilting point, defines the range of water the plants can draw on, and the irrigation threshold used in this study corresponds to 50 percent depletion of that range (May 2025). These measured values provide the physical basis for the 8 percent volumetric water content trigger applied during the 2025 season. The custom calibration in ZENTRA Cloud requires supporting physical parameters for each medium, and these were determined in the same laboratory campaign. Undisturbed core samples were extracted with 100 cm^3 rings from a representative 4-inch (~10 cm) Rooflite plot and a representative 4-inch (~10 cm) BuildEx plot, with three replicate rings per substrate. The rings were saturated and then drained to a matric potential of 10 kPa to establish field capacity, and subsequently oven-dried to determine bulk density. Particle density was determined for each medium, and the permanent wilting point was obtained by interpolating measured water-potential and gravimetric-water-content pairs to a matric potential of 1.5 MPa. The resulting values for each susbstrate are summarized in Table 3.5.

Table 3.5. Measured physical and hydraulic properties of the two substrates, determined from undisturbed 100 cm^3 core samples.

Plant-available water capacity (PAWC) is the difference between field capacity and permanent wilting point. The irrigation threshold corresponds to 50% depletion of PAWC (May 2025).

Property	Rooflite	BuildEx	Units
Particle density	1.83	2.01	g/cm^3
Bulk density	0.84	1.24	g/cm^3
Field capacity (10 kPa)	0.150	0.130	m^3/m^3
Permanent wilting point (1.5 MPa)	0.016	0.029	m^3/m^3
Plant-available water capacity	0.134	0.100	m^3/m^3
Irrigation threshold (50% PAWC depletion)	0.083	0.080	m^3/m^3

Bulk-density and particle-density values were entered into ZENTRA Cloud as rounded quantities at 0.84 and 1.83 g/cm^3 for Rooflite and 1.24 and 2.01 g/cm^3 for BuildEx. These values provide the physical basis for the irrigation decision rule. Depleting half of the plant-available water capacity corresponds to a volumetric water content of 0.083 m^3/m^3 in Rooflite and 0.080 m^3/m^3 in BuildEx. Because these two thresholds are nearly identical, a single operational trigger of 8 percent volumetric water content was adopted for both substrates, which simplified monitoring through ZENTRA Cloud without materially departing from the substrate-specific values. The measured properties also quantify the contrast between the two media, in that Rooflite combines a lower bulk density with a higher field capacity and consequently holds roughly one-third more plant-available water per unit volume than BuildEx under laboratory drainage conditions.

Supplemental Irrigation Protocol

Minimal-irrigation equipment and methods

Supplemental irrigation on the APD-EGR has been managed since 2021 under a deliberate minimal-maintenance strategy, in which water has been applied only when sensor readings indicate very low substrate moisture, consistent with the low-input management philosophy described by Alam et al. (2025). The 2025 growing season extended this practice into a controlled comparison between two irrigation frequencies imposed on the instrumented plots, designed to test the effect of two supplemental irrigation frequencies on canopy cover under the demanding summer conditions of the tallgrass prairie ecoregion as experienced on the main K-State campus in Manhattan, Kansas. Figure 3.12 shows the on-site cistern that captured stormwater from the roof of the Ekdahl lecture room. Using this harvested stormwater for irrigation was a priority, consistent with the study's minimal-input, low-resource approach to green roof management. On the occasions when the cistern did not hold enough water to irrigate all the required plots, potable water was used to complete the event.

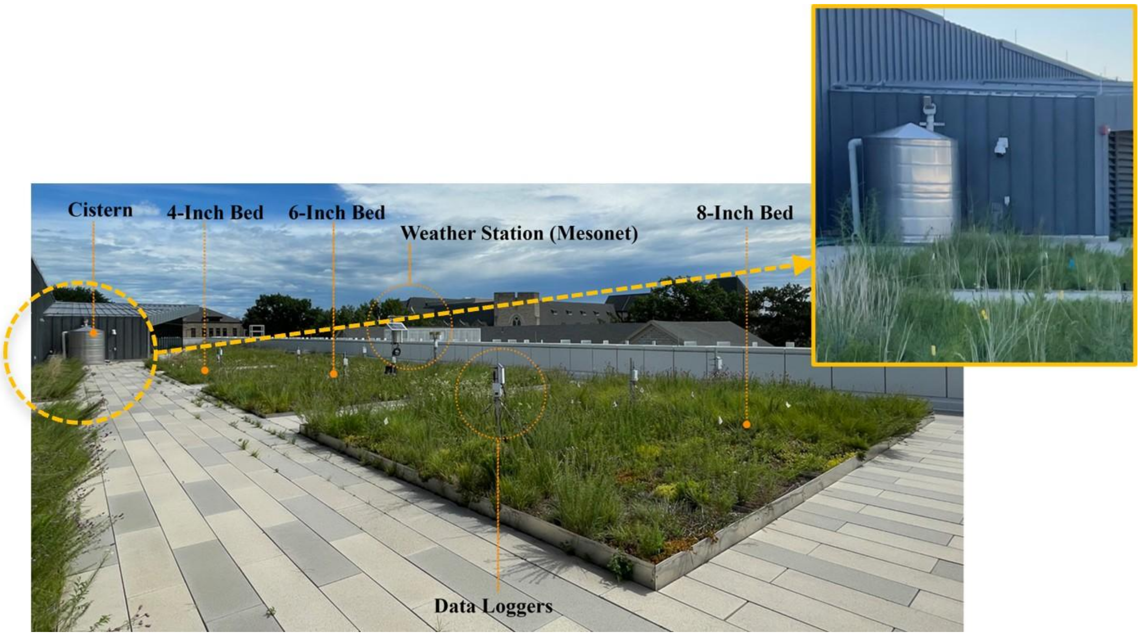

Figure 3.12. Cistern storing stormwater from the roof of the Ekdahl lecture room.
Using stormwater for irrigation was a priority. When there was not enough water in the cistern to water all required plots, potable water was used. Photos taken by Lee Skabelund in 2025; diagram by author (2026).

Whenever available, the stormwater stored in the cistern was used for irrigation. However, during dry spells, there was not enough stormwater in the cistern. Potable water was used in those cases. A garden hose (shown in Figure 3-13) was used to irrigate plots one by one. Each plot received one minute of irrigation. The pump transfers approximately 6.5 gallons of water (equivalent to one inch) in one minute. A bucket marked with two gallons of water was used to measure the estimated amount of water being used each day before irrigation.

Figure 3.13. Irrigating each plot for one minute manually using a garden hose.
The goal was to uniformly irrigate an entire plot in one minute to make it easy to consistently irrigate either half (36) or all (72) the APD-EGR plots. Photo by author (2025).

Irrigation Decision Rule

The timing of irrigation events was governed by a substrate-moisture trigger monitored through ZENTRA Cloud. An irrigation event was initiated when four of the monitored more-irrigated 4-inch plots fell below a volumetric water content of 8%, provided that the probability of rainfall over the following 24 hours was below 50%. The 4-inch extensive plots were used as the trigger because their shallow profile typically reaches critically low moisture sooner than the deeper intensive beds, making them the most sensitive indicator of the onset of moisture stress on the green roof.

Event Types and Volumes

Two event types were used. "All-plots" events applied water to all 72 plots on the APD-EGR, including both irrigation treatments, and therefore provided supplemental water to both the more-irrigated and less-irrigated plots. "More-only" events applied water to the more-irrigated plots alone (36 of the 72 plots in the three EGR beds) and skipped the less-irrigated group.

Following the irrigation trigger protocol, the first time the VWC of the four less-irrigated 4-inch plots dropped below 8%, only the more irrigated plots (36) were irrigated. If the dry period continued and the VWC of the four more-irrigated 4-inch plots dropped below 8% again, all 72 plots were irrigated. In case a rain event happened after less-irrigated plot irrigation, adding moisture to all plots, the cycle restarted, and when the sensors went below 8%, only the 36 less-irrigated plots were irrigated. At each irrigation event, approximately 6.5 gal/plot was applied (about 60 seconds of flow at roughly 10 seconds/gallon; equivalent to approximately 25 mm or one inch of rainfall) using water drawn from the on-site cistern. Over the full season, the more-irrigated treatment received twelve "more-only" irrigation events (~78 gallons/plot), and the less-irrigated treatment received four "all-plots" irrigation events (~26 gallons/plot), an approximate 3:1 ratio.

Figure 3.14 shows the spatial layout of the irrigation treatments across the three APD-EGR beds. The 36 more-irrigated plots, twelve in each bed, are marked in blue, and the eight instrumented study plots that fall within this more-irrigated group, four in the 4-inch bed and four in the 8-inch bed, are highlighted in red; the unmarked plots are the less-irrigated plots. Figure 3.15 shows the route followed when irrigating only the more-irrigated plots. The path was planned to move the hose efficiently between plots, beginning at the point marked with the white dot. Figure 3.16 shows the route followed when irrigating all plots, which delivered water to both the more-irrigated and less-irrigated plots in a single pass.

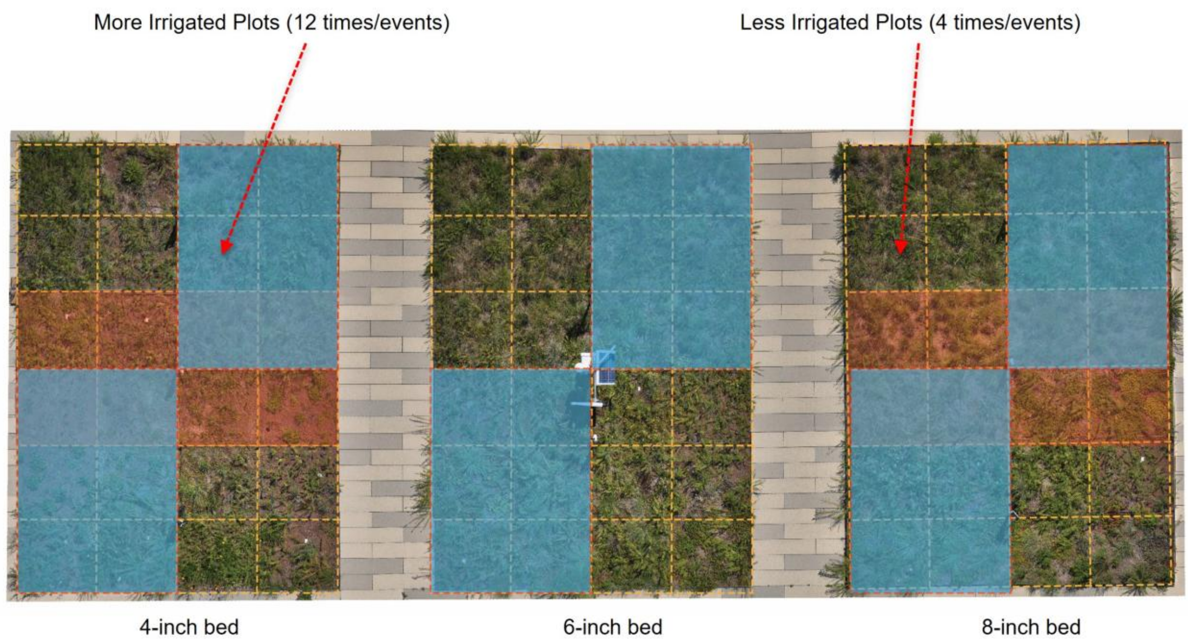

Figure 3.14. Aerial image of the 36 more irrigated plots (12 plots in each APD-EGR bed) marked in blue.

Study plots are shaded in red, showing four more irrigated plots in the 4-inch bed and four more irrigated plots in the 8-inch beds. The plots that are not marked in blue are the less irrigated plots. (Images 3.14, 3.15 & 3.16 prepared by author using Kaden Spencer's July 9, 2025 UAS image as a base.)

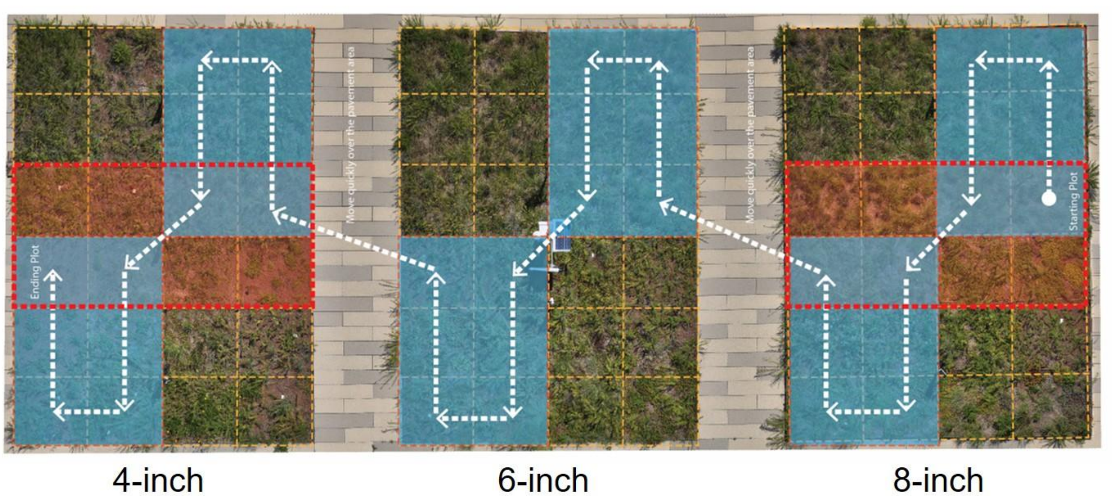

Figure 3.15. Irrigation path for more irrigated plots.

This path was followed to move with the hose efficiently while irrigating. The starting point is marked with the white dot.

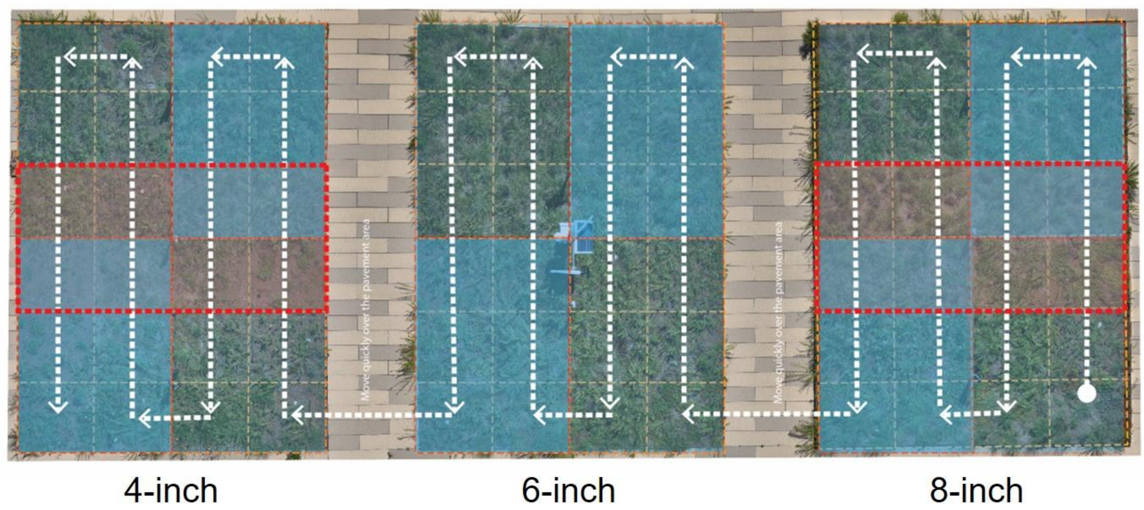

Figure 3.16. Irrigation path for irrigating all plots.
This pattern irrigated both the more irrigated and less irrigated plots.

Samples of the irrigation water were submitted to the Kansas State University Soil Testing Laboratory in May 2025 to confirm that the applied water introduced no confounding chemical effect. Two samples were drawn on May 19, 2025, one from the cistern that supplied supplemental irrigation and one from the spigot. Both were near neutral, at pH 6.99 and 7.24 respectively, and both were very dilute. Electrical conductivity was 0.03 mS/cm in the cistern sample and 0.04 mS/cm in the spigot sample, and total dissolved solids were 17.8 and 31.2 mg/L. Nutrient concentrations were correspondingly low, with total nitrogen at 0.55 and 0.76 ppm and total phosphorus at or below 0.06 ppm. Zinc was present at 1.58 ppm in the cistern water and 2.31 ppm at the spigot. Concentrations were consistent with the galvanized components of the roof water collection system; zinc was not investigated further in this thesis. Whenever possible, the water applied to the plots was drawn from the cistern.

A third sample, collected from the cistern on April 21, 2022, was submitted in the same batch. It had been stored refrigerated in a single-use plastic bottle for more than three years before analysis, and it returned the highest values in the batch for zinc (4.83 ppm), total nitrogen (2.88 ppm), total dissolved solids (62.0 mg/L), and electrical conductivity (0.09 mS/cm). Because prolonged storage in a plastic container may alter water chemistry, this archived sample is not treated as representative of the water applied during the 2025 season and is reported here only for completeness.

Sodium was not determined, so the sodium adsorption ratio was not calculated, and sodicity was not formally assessed. Nevertheless, the very low electrical conductivity and total dissolved solids of the 2025 samples indicate a negligible salinity load.

Season Irrigation Log and the 39-Day Gap

Table 3.6 summarizes the supplemental irrigation events applied during the 2025 growing season. Each event is classified as either "All 72," which watered both treatment groups, or "More only," which watered the 36 more-irrigated plots alone. At approximately 6.5 gallons per plot per event (equivalent to about one inch of rain), the more-irrigated plots received twelve events and the less-irrigated plots four, producing the roughly three-to-one difference in applied water that defined the irrigation treatment. The extended interval between the less-irrigated events, most notably the 39-day gap from July 2 to August 10, is central to interpreting the canopy cover results in Chapter 4.

Table 3.6: Supplemental irrigation events during the APD-EGR 2025 growing season.

"All 72" events provided water to both treatment groups; "More only" events (36 plots) provided water to the more-irrigated treatments only. Cumulative totals are approximate, based on approximately 6.5 gallons (equivalent to 1 inch of rain) per plot per event.

#	Date	Event type	Plots watered	Cum. more (gal/plot)	Cum. less (gal/plot)
1	Jun 30	More only	36 (more-irrigated)	6.5	0
2	Jul 2	All 72	72 (both groups)	13.0	6.5
3	Jul 15	More only	36 (more-irrigated)	19.5	6.5
4	Jul 27	More only	36 (more-irrigated)	26.0	6.5
5	Aug 6	More only	36 (more-irrigated)	32.5	6.5
6	Aug 10	All 72	72 (both groups)	39.0	13.0
7	Aug 15	More only	36 (more-irrigated)	45.5	13.0
8	Aug 17	All 72	72 (both groups)	52.0	19.5
9	Aug 23	More only	36 (more-irrigated)	58.5	19.5
10	Aug 28	All 72	72 (both groups)	65.0	26.0
11	Sep 15	More only	36 (more-irrigated)	71.5	26.0
12	Oct 2	More only	36 (more-irrigated)	78.0	26.0

A notable feature of the 2025 irrigation regime was a 39-day interval, from July 2 to August 10, during which the less-irrigated plots received no supplemental water. This interval coincided with the peak summer heat of July and early August. Following the final "all-72" plots event on August 28, the less-irrigated plots again received no further supplemental irrigation for the remainder of the season and relied on rainfall alone. Because substantial rainfall fell during the July-to-August interval, this period is not treated as a rainless dry period; rather, it is examined in Chapter 4 as a test of how the less-irrigated plots, and the shallow substrates in particular, responded to reliance on rainfall alone under high evaporative demand.

Figure 3.17 combines the season's daily rainfall, maximum and minimum air temperature, and irrigation events from June 30 to November 5, 2025, with the 39-day irrigation gap (July 2 to August 10) shaded. Notably, about 41 percent of the season's rainfall fell during this gap, yet heat stayed high (mean daily maximum 33.1°C versus the seasonal 29.3°C, with the season's peak of 38.1°C on July 15 inside the gap).

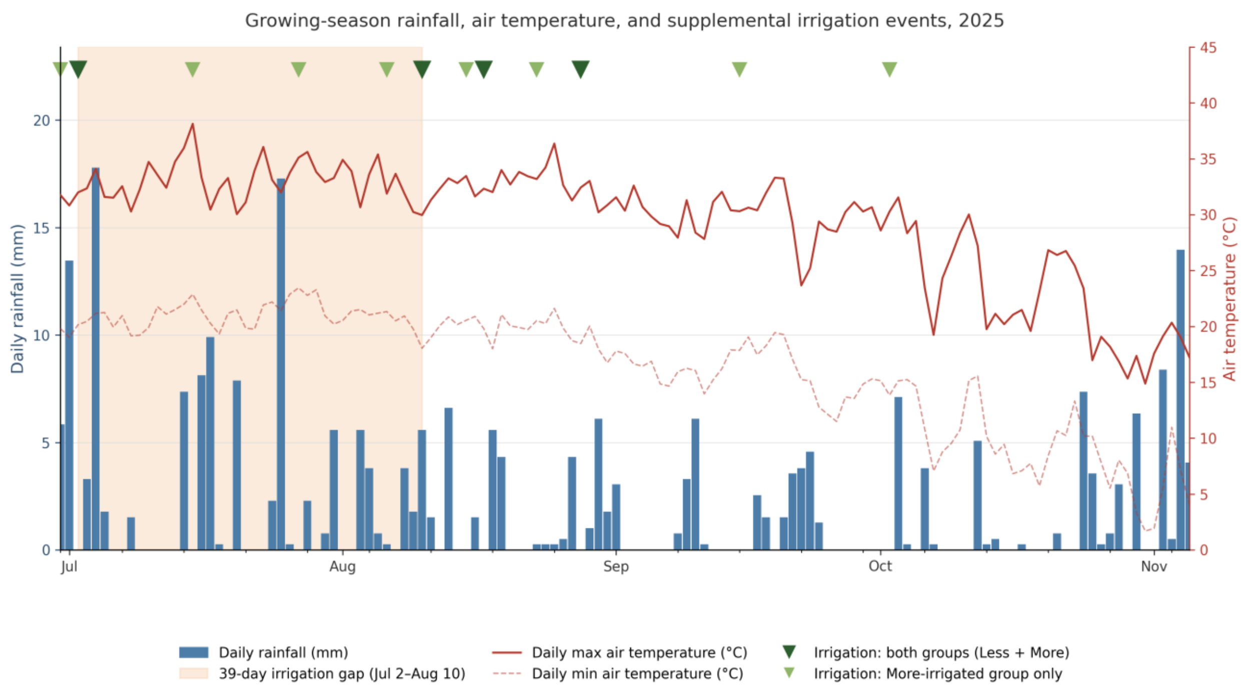

Figure 3.17. Daily air temperature, rainfall, and supplemental irrigation events on the APD-EGR from June 30 to November 5, 2025.

Blue bars show daily rainfall; the upper and lower lines show daily maximum and minimum air temperature; and irrigation events are marked for both treatment groups (more plus less) and for more-only events. The shaded area indicates the 39-day irrigation gap (July 2 to August 10) during which the less-irrigated plots received no supplemental irrigation. (Author using the Ekdahl weather station data, irrigation data).

Weather Data

Meteorological context for the growing season was obtained from the Ekdahl station of the Kansas Mesonet. The station consists of an on-site weather station mounted on the green roof at the center of the 6-inch semi-intensive bed, which lies between the 4-inch and 8-inch beds. Because the station sits within the experimental green roof rather than at a distant reference site, its record directly represents the rooftop microclimate experienced by the plots and requires no off-site adjustment. Figure 3.18 shows the on-site mesonet weather station, including its solar panel and tipping-bucket rain gauge, which supplied the air temperature and rainfall data used in this study.

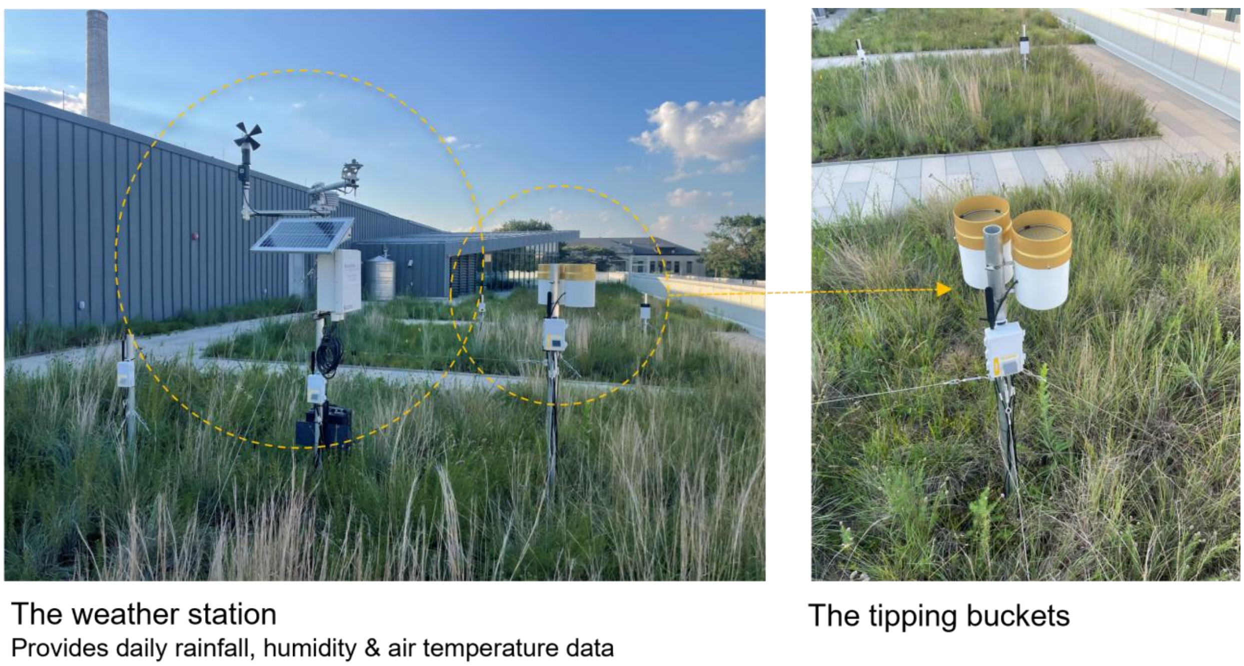

Figure 3.18. Mesonet weather station with solar panel and tipping buckets.
APD-EGR photos by author (2026).

Daily observations of maximum and minimum air temperature, relative humidity, precipitation, wind speed, and solar radiation were compiled for the growing season and used to characterize the temperature and rainfall regime against which the plant and substrate responses are interpreted. Precipitation was of particular importance for interpreting the soil moisture record, because rainfall was the sole water input to the less-irrigated plots during the extended intervals between supplemental irrigation events, and the timing and magnitude of individual rain events therefore bear directly on the moisture stress experienced by those plots. The weather record and its integration with canopy cover and soil moisture data are presented in Chapter 4.

Unmanned Aircraft System (UAS) Imagery

Image Acquisition and Orthomosaic Processing

Aerial imagery of the APD-EGR was acquired on four UAS flight dates during the 2025 growing season: July 9, August 9, September 19, and November 1. Three of these dates (July 9, August 9, and September 19) coincided exactly with ground-based Canopeo measurement days, allowing direct comparison between the aerial and ground-based cover metrics; the November 1 flight occurred four days before the final ground-based measurement on November 5. All UAS flights, image processing, and vegetation-index extraction related to UAS imagery were carried out by Kaden Spencer (Graduate Research Assistant, Department of Agronomy, Kansas State University), who served as drone pilot for the campaign.

Imagery was collected with a DJI Mavic 3 Multispectral (DJI Mavic 3 Enterprise Series) unmanned aircraft, which carries an integrated multispectral imaging system comprising a red-green-blue (RGB) camera together with discrete green, red, red-edge, and near-infrared (NIR) multispectral bands, as well as a top-mounted sunlight (downwelling irradiance) sensor. Radiometric calibration was performed before each flight using the aircraft's onboard sunlight sensor in combination with a Sentera radiometric calibration (reflectance) panel, ensuring that reflectance values were comparable across flight dates and illumination conditions. Flights were flown at approximately 25 ft (about 7.6 m) above ground level. All four flights were conducted during the mid-morning window between approximately 8:00 a.m. and 11:30 a.m., and flights were not undertaken on windy or overcast days, so that illumination and atmospheric conditions were kept as consistent as practicable across the four dates. Figure 3.19 shows drone pilot Kaden Spencer operating the UAS above the APD-EGR on July 9, 2025, during the first of the four UAS flights that provided the aerial imagery and NDVI data used in this study.

Figure 3.19. UAS pilot Kaden Spencer operating his UAS above the EGR July 9, 2025. Photo by Lee Skabelund (2025).

The individual images from each flight were stitched into a single calibrated orthomosaic in Pix4Dfields. The resulting orthomosaics had a ground sampling distance (GSD) of 0.25 cm/pixel (2.5 mm/pixel), a very fine spatial resolution that resolves individual plants and substrate gaps within each nominal 1 m × 1 m plot, and that is substantially finer than the 4.8 to 10 cm/pixel typical of agricultural-field UAS mapping. This high resolution is a methodological strength for plot-scale green roof analysis, where the relevant vegetation features are small.

UAS-Derived Canopy Cover

For the 16 instrumented plots, fractional green canopy cover was derived from the RGB orthomosaic of each flight to provide an aerial counterpart to the ground-based Canopeo measurements. Each orthomosaic was opened in Adobe Photoshop, and the image of each plot was manually cropped and saved within a structured date-by-depth-by-plot folder hierarchy. The cropped plot images were then processed in batch using the Canopeo Desktop application, and the resulting fractional cover values were compiled in a spreadsheet. Because the aerial imagery captures the full 1 m × 1 m plot from altitude, including bare-substrate gaps, the UAS-derived cover values are systematically lower than the corresponding near surface cover values derived from iPhone photos, captured at closer range and emphasizing the denser canopy interior.

UAS-Derived NDVI

In addition to RGB-based cover, the calibrated multispectral orthomosaics were used to derive the Normalized Difference Vegetation Index (NDVI) for all 72 plots on the green roof, including the 24 semi-intensive 6-inch (~15 cm) plots excluded from the instrumented experiment. Vegetation indices were computed within Pix4Dfields from the green, red, red-edge, and near-infrared bands, with NDVI defined as NDVI = (NIR − Red) / (NIR + Red). For each flight date, a polygon was delineated for every plot, and the mean NDVI within each plot polygon was extracted using QGIS; the corresponding per-plot mean reflectance values for the green, red, red-edge, and NIR bands were extracted in the same manner. The full 72-plot coverage of the NDVI dataset enabled a supplementary characterization of vegetation health across all three substrate-depth categories simultaneously, an analysis not possible from the 16 instrumented plots alone. The NDVI data and their analysis are presented in Chapter 4.

As noted previously, all flights were flown at approximately 25 ft (about 7.6 m) above ground level. All four flights were conducted during the late-morning window, between 10:12 a.m. and 11:10 a.m. local time, and each required approximately 20 to 26 minutes to complete (Kaden Spencer, Kansas State University Agronomy student, personal communication, 2026). Flights were not undertaken on windy or overcast days, so that illumination and atmospheric conditions were kept as consistent as practicable across the four dates.

Vegetation Survey Method

Plant community composition was assessed through expert-guided ocular estimation, a quadrat-based visual cover assessment method (Daubenmire, 1959; Hatton et al., 1986). Two surveys were conducted, one during the active-growth period and one during the post-senescence period. Plant species present within each approximately 1 m x 1 m plot were identified in the field by Lee R. Skabelund (green roof researcher and landscape architect) while the thesis author recorded species occurrence and together they estimated the percentage cover of four functional categories: native grasses, forbs, sedums, and non-vegetated surface. A species was considered present for the season if observed on at least one of the two survey dates.

The survey was conducted on two days (June 3, 2025 and December 9, 2025) for the two depths and plant communities (4-inch and 8-inch substrate depths, East and West plant communities). On each date the presence of every species was recorded for each plot, and percent cover was estimated by functional group. This allowed characterization of both community composition and persistence for both the early and late season in 2025. The per-plot species-presence records were later used to corroborate the plant identities underlying the grass-height measurements.

Plant Community and Functional-Group Survey

Percent cover was estimated by functional group, comprising grasses, forbs, sedum, and bare soil, for each plot, providing a functional-group characterization of each plot's vegetation to complement the quantitative canopy cover and NDVI measurements. The ocular estimation approach was selected because it allowed rapid, non-destructive characterization of mature, mixed-species green roof vegetation by functional group, consistent with established rangeland and grassland survey practice. Where vegetative cover for each EGR plot was recorded as a range, the midpoint was used.

End-of-Season Grass Canopy Height

At the close of the growing season, on November 19, 2025, the canopy height of the two dominant native warm-season grasses, little bluestem (*Schizachyrium scoparium)* and sideoats grama (*Bouteloua curtipendula)*, was measured in every plot to provide a vertical structural measure complementing the horizontal canopy cover record for the APD-EGR. In each plot, up to three representative individuals of each species were measured from the green roof substrate surface to the top of the plant, and the per-plot value used in analysis is the mean of the sampled individuals. Height was recorded to the top of the standing plant irrespective of whether the tissue was green or senesced. By November 19 the warm-season grasses had almost entirely cured to a straw-colored, non-green condition, a state reflected in the concurrent canopy cover record, in which mean green cover across the instrumented plots had declined to 4.6 percent by

November 5. The height measurement therefore describes the standing vertical structure of the canopy at the end of the season rather than the extent of photosynthetically active tissue, and it is interpreted in Chapter 4 alongside, rather than as a proxy for, the green cover record. Little bluestem occurred in all 16 plots and therefore supported the full factorial analysis of height, whereas sideoats grama occurred in fewer plots, predominantly the shallow 4-inch plots, and is reported descriptively. The height records were cross-checked against the species-presence data from the June and December surveys; a few discrepancies were identified, including one plot in which sideoats grama was recorded as present but not measured and an unidentified second "grama grass" entry co-occurring with sideoats grama in four plots. These gaps are noted where relevant in Chapter 4.

Data Processing and Statistical Analysis

The hourly soil moisture and temperature records were exported from ZENTRA Cloud and summarized at the plot level to seasonal mean, minimum, and maximum values for volumetric water content and substrate temperature. Because the irrigation-focused experiment was concerned with the onset of moisture stress rather than average conditions alone, minimum volumetric water content was retained as a distinct summary metric alongside the seasonal mean. Ground-based Canopeo cover values were compiled into a plot-by-date matrix spanning the season, and the seasonal trajectory of each plot was summarized both by its mean cover and, where appropriate, by the area under the cover curve (AUC) to integrate canopy performance over the full measurement period.

To characterize the plot-level response to the extended interval without supplemental irrigation, a stress-and-recovery analysis was performed for the less-irrigated plots. For each plot, three quantities were summarized: the minimum daily-mean VWC reached during the July

2 to August 10 interval, as an index of moisture stress exposure; the decline in canopy cover from its early-season peak to the peak-stress trough; and the subsequent recovery in cover during the September partial-recovery phase. The seasonal peak was defined as the maximum cover over the establishment window, the trough as the minimum cover during the peak-stress window, and the recovery as the gain from that trough to the highest cover attained in September. These plot-level summaries were used to identify which plots experienced moisture stress, which retained canopy cover through the stress period, and which recovered afterward.

The primary inferential analysis of canopy cover used a balanced 2^3 factorial treatment structure with substrate depth, substrate type, and irrigation frequency as the three crossed factors, with the two sides of the roof providing replication; the pre-existing east–west difference in plant community is described separately rather than entered as a factor. The analysis of variance therefore carried eight error degrees of freedom. Because of the limited replication inherent in a fully instrumented two-depth design ($n = 2$ per cell), the statistical power of the analysis was low, such that only very large treatment effects would reach conventional significance at the $\alpha = 0.05$ level. For this reason, effect sizes (partial eta-squared, η^2) are reported alongside significance tests, and non-significant results are interpreted as reflecting limited statistical power rather than the absence of a treatment effect. The normality assumption underlying the analysis of variance was assessed using the Shapiro-Wilk test. The end-of-season little bluestem height data were analyzed with the same 2^3 factorial analysis of variance and partial eta-squared effect-size approach used for canopy cover; sideoats grama, being present in too few plots for a balanced analysis, was summarized descriptively.

Relationships among the continuous variables were examined using correlation analysis. The relationship between substrate moisture and canopy cover was assessed by correlating plot-level volumetric water content metrics with canopy cover, and the relationship between the spectral and color-threshold measures of vegetation performance was assessed by correlating plot-level NDVI with UAS-derived Canopeo cover on the matched flight dates. The relationship between vertical and horizontal canopy structure was examined by correlating plot-level little bluestem height with seasonal canopy cover. Throughout, statistical significance was evaluated at $\alpha = 0.05$, and results are reported with their associated effect sizes and sample sizes to support transparent interpretation given the design's replication structure.

Using Claude AI for Research, Data Analysis, and Synthesis

The artificial intelligence platform Claude (Anthropic) was used to assist with statistical data analysis and synthesis. The Opus 4.8 model (high-effort setting) was used throughout the analysis, within a workspace created using the "Claude Projects" feature. Consensus, an AI-based scholarly literature search engine, was connected to the Claude platform through the Claude connectors feature to help identify and organize sources for the literature review.

Context and data files were uploaded to the project workspace so the model could reference them during analysis. These included the Canopeo green cover data, the 2021 to 2025 irrigation data, Kansas Mesonet weather data (MHK versus Ekdahl comparisons prepared by NRES students), volumetric water content and substrate temperature data from the data loggers, the APD-EGR plot layout with substrate depth, type, and irrigation treatment details, NDVI data from the four flights over all 72 plots, drone-derived green cover data for the sixteen 4-inch and 8-inch plots, and the 2025 APD-EGR plant survival data.

In addition, two dissertations and one thesis, by Allyssa Decker (PhD, 2021), M. M. Lekhon Alam (PhD, 2022), and Priyasha Shrestha (MLA, 2019), together with previously published articles on Kansas State University's green roofs, were provided to the model as reference material to contextualize the study.

Using the uploaded data, the model was prompted to fit the study's statistical models and generate the corresponding graphs. The primary analysis was a three-way factorial ANOVA relating seasonal canopy cover to substrate depth, substrate type, and irrigation frequency, developed through iterative prompt engineering. The results were regenerated multiple times using the same procedure to confirm that the process was replicable. A cross-check using conventional statistical platforms (for example R or Python) was not performed because of time constraints. Such a comparison would help further verify the results reported here.

Chapter 4 - Analysis and Findings

This chapter presents the analysis and findings from the 2025 growing season (June 30 to November 5) of the College of Architecture, Planning and Design Experimental Green Roof (APD-EGR) at Kansas State University. Data from five complementary measurement systems are integrated in this chapter: 1) overhead canopy cover analysis performed using the Canopeo Desktop application on photographs captured with iPhone 11 Pro Max and iPhone 12 Pro devices (56 measurement days), 2) continuous soil volumetric water content (VWC) monitoring via Teros 12 sensors installed in all 16 sensor-instrumented plots, 3) substrate temperature recordings from the same sensor network, 4) a detailed supplemental irrigation log, and 5) daily weather data from the Ekdahl on-site mesonet station. Together, these datasets allow a multidimensional interpretation of how substrate depth, substrate type, irrigation frequency, and plant community interacted to determine green roof canopy cover performance under the humid continental climate conditions within the Flint Hills (tallgrass prairie) Ecoregion.

Overview of the 2025 Growing Season

Figure 4.1 presents a timeline of the 2025 growing season characterized by four functionally distinct phases observable across all 16 plots regardless of treatment. The establishment phase (approximately July 1 through July 25) was marked by rising canopy cover as plants resumed active growth following a pre-season irrigation event on June 21 and the first growing-season event on June 30. The peak stress phase (approximately July 26 through August 28) coincided with the highest air temperatures of the season, with mean daily maximum air temperatures of 33.1°C in July and 32.7°C in August at the Ekdahl weather station and encompassed the 39-day irrigation gap for less-irrigated plots (July 2 through August 10), during which that treatment group received no supplemental water and relied on rainfall. The partial recovery phase (September through early October) followed the reinstatement of more regular irrigation events and associated moderate air temperatures. The senescence phase (October onward) produced universal cover collapse across all plots, consistent with normal winter dormancy of the prairie species assemblage and was considered separately from growing-season analysis. October 1 was adopted as the functional end-of-season endpoint for statistical comparisons.

Daily air temperature and precipitation for the growing season were recorded at the on-site Ekdahl Mesonet station (refer to Figure 3.17). Mean daily maximum air temperature was 33.1°C in July and 32.7°C in August, and the seasonal maximum of 38.1°C occurred on July 15, within the peak stress phase. Growing-season precipitation totaled 260 mm (10.24 inches) between June 30 and November 5, falling on 68 of the 129 days, or 53% of the season, so that rainfall was frequent but generally light; August alone recorded measurable precipitation on 20 of 31 days, while the longest continuous dry interval extended eight days from September 25 to October 2. This rainfall pattern is important for interpreting the substrate moisture results: frequent light rain partially offset the withheld supplemental irrigation in less-irrigated plots, which helps explain the relatively modest differences in mean VWC between irrigation groups, yet it was insufficient to prevent the shallow 4-inch substrates from reaching near-wilting-point moisture during the 39-day irrigation gap, because their limited storage could not retain enough of each small rainfall event.

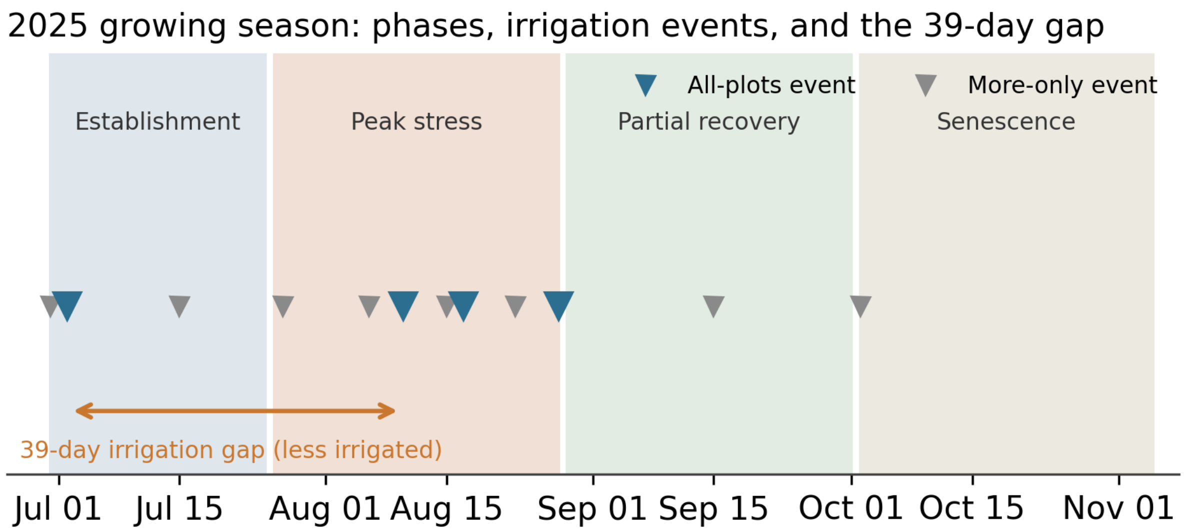

Figure 4.1. Timeline of the APD-EGR 2025 growing season.

The season had four functional phases: the twelve supplemental irrigation events (all-plots vs more-only), and the critical 39-day irrigation gap experienced by less-irrigated plots. (Diagram by author from the APD-EGR irrigation log and Ekdahl weather station data, 2025).

Canopy Cover Performance

Visual overview

The compilation of four drone photos shows how canopy cover changed over the season. Visual observation of these four images indicates the greenness in July dropped in August and recovered in September. However, due to seasonal change, overall greenness dropped in November. The difference between more-irrigated and less-irrigated plots is not strongly visible in July. In the August image, this difference is more clearly visible. Figure 4.2 shows UAS RGB images of the APD-EGR plots captured on the four flight dates in July, August, September, and November 2025, illustrating how canopy greenness changed across the growing season. The contrast between the more-irrigated and less-irrigated plots is most visible in the August image, taken during the peak-stress period near the end of the 39-day irrigation gap.

Figure 4.3 shows UAS-derived NDVI images of the APD-EGR plots on the four flight dates in July, August, September, and November 2025, mapping photosynthetic activity across the roof. As in the RGB imagery, the difference between the more-irrigated and less-irrigated plots is clearest in the August image, and the intensive (8-inch) and semi-intensive (6-inch) plots appear closely matched in retained greenness.

Figure 4.4 shows iPhone photographs of the 4-inch bed plots on twelve representative dates selected from the 56 measurement days, giving a visual overview of how canopy greenness changed across the season on each plot. All 56 days of photographs were used in the Canopeo analysis; the twelve shown here are a subset for illustration.

Figure 4.2. UAS RGB images of APD-EGR Plots in July, August, September, and November 2025 showing how greenness changed over the growing season.

The difference between more irrigated and less irrigated plots can be easily seen in the August image (images taken and prepared by Kaden Spencer, 2025).

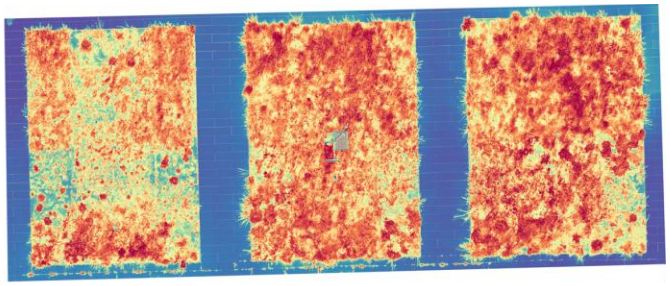

July 9

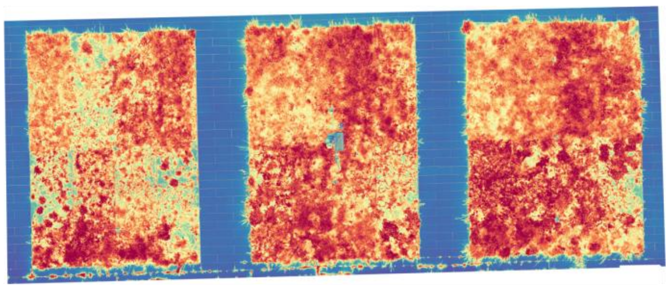

August 9

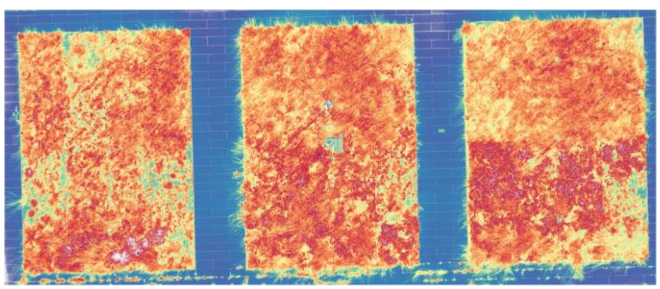

September 19

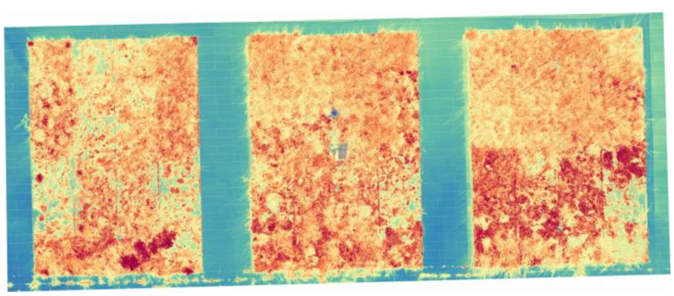

November 1

Figure 4.3: NDVI images of APD-EGR Plots in July, August, September, and November 2025.

Red colors indicate more photosynthetically active green materials. Here, the difference between more-irrigated and less-irrigated plots can be easily seen in the August image. Intensive and semi-intensive plots seem to be very close in retaining greenness (images taken and prepared by Kaden Spencer, 2025).

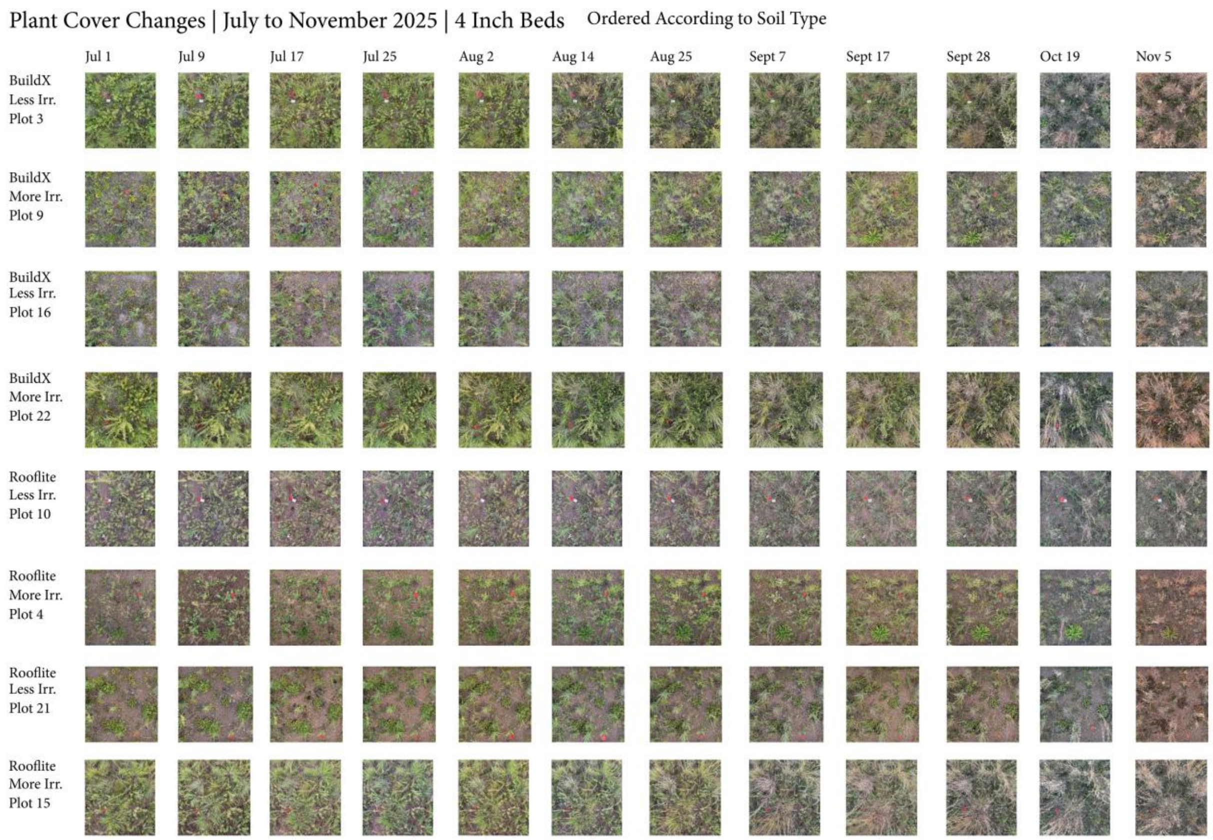

Figure 4.4. iPhone photos of APD-EGR 4-inch beds.

12 days were selected from 56 days to give an overview of how greenness changed on each of the sixteen experimental plots over the season (photos by the author from all 56 days were used for analysis).

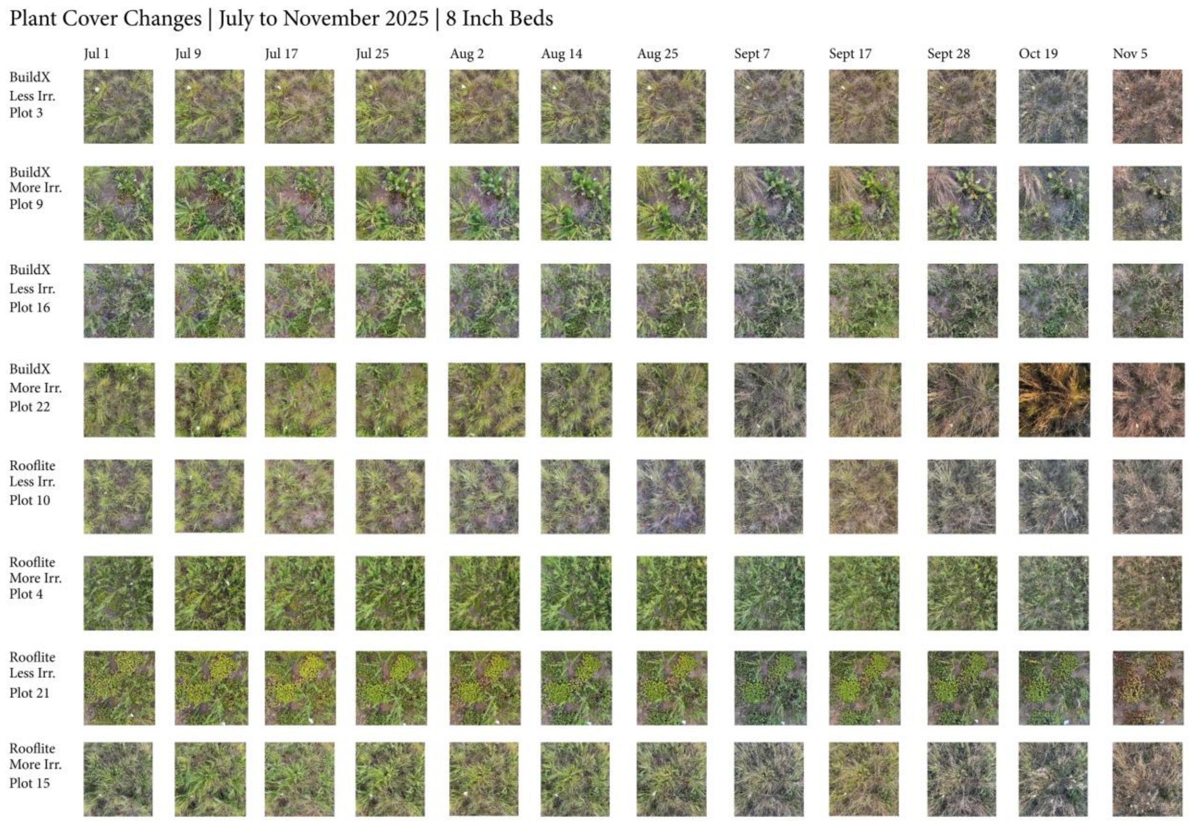

Figure 4.5: iPhone photos of APD-EGR 8-inch beds.

Overall greenness gradually declined with season. More-irrigated plots held more greenness than less-irrigated plots. However, overall stress seems to be lower than in the 4-inch bed plots. Less-irrigated plots in 8-inch beds seem to perform better than less-irrigated plots of the 4-inch bed (photos by author, 2025).

Summary Statistics by Plot

The green canopy cover analysis of the above iPhone photos extracted the greenness data through the Canopeo Application. This helps to quantify the performance of each experimental plot and figure out the highest and lowest performing plots.

Table 4.1 presents the five primary visibly green canopy cover response variables computed for each of the 16 plots: seasonal mean canopy cover, peak canopy cover, end-of-season canopy cover, area under the curve (AUC) related to cover-time, and seasonal decline.

Table 4.1. Summary statistics for visibly green canopy cover (%) across all 16 APD-EGR green roof plots during the 2025 growing season (June 30 to November 5).

Plot irrigation treatment assignments are shown with the plot numbering and datalogger port numbers. Green highlight indicates the highest-performing plot.

Plot	Depth	Substrate	Irrigation	Mean Cover	Peak Cover	End-Season	AUC	Decline
4″ P1	4″	BuildEx	Less	42.8%	73.2%	21.4%	2,359	51.8%
4″ P2	4″	Rooflite	More	22.4%	34.2%	16.2%	1,246	18.0%
4″ P3	4″	Rooflite	Less	17.8%	29.5%	15.5%	984	14.0%
4″ P4	4″	BuildEx	More	35.5%	48.7%	33.9%	1,964	14.8%
4″ P5	4″	Rooflite	More	32.7%	52.9%	16.2%	1,808	36.7%
4″ P6	4″	BuildEx	Less	23.7%	34.8%	21.4%	1,311	13.4%
4″ P7	4″	BuildEx	More	47.0%	65.1%	17.8%	2,601	47.3%
4″ P8	4″	Rooflite	Less	21.1%	33.3%	10.5%	1,170	22.8%
8″ P1	8″	Rooflite	Less	**15.9%**	35.1%	2.0%	876	33.1%
8″ P2	8″	BuildEx	More	**64.3%**	**77.9%**	**57.4%**	**3,564**	20.5%
8″ P3	8″	BuildEx	Less	20.7%	38.3%	8.0%	1,145	30.3%
8″ P4	8″	Rooflite	More	45.0%	61.4%	26.6%	2,488	34.8%
8″ P5	8″	BuildEx	More	43.7%	74.0%	15.8%	2,411	**58.2%**
8″ P6	8″	BuildEx	Less	43.8%	61.3%	36.8%	2,414	24.5%
8″ P7	8″	Rooflite	More	30.7%	54.8%	3.1%	1,693	51.7%
8″ P8	8″	Rooflite	Less	44.8%	57.7%	46.5%	2,478	**11.2%**

Seasonal mean visibly green canopy cover across all 16 plots ranged from 15.0% (8-inch Rooflite, less irrigated, Plot 8" P1) to 65.5% (8-inch Rooflite, more irrigated, Plot 8" P7), a range of 50.5 percentage points. The grand mean across all plots and measurement days was 38.4%. AUC ranged from 843 (8" P1) to 3,681 (8" P7), a 4.4-fold difference representing the widest cumulative performance gap in the experiment. Peak visibly green canopy cover ranged from 29.5% to 77.9%, with all plots reaching their individual maximum during July. End-of-season canopy cover ranged from 2.3% to 58.8%, reflecting substantial differences in late-season resilience among treatment combinations. The largest seasonal decline was recorded in Plot 8" P5 (52.5 percentage points), which achieved a high early-season peak (54.8%) before experiencing a rapid and largely irreversible visibly green cover decline during late August.

Seasonal Canopy Cover Trajectory

The full-season canopy cover trajectory for all 16 plots revealed a shared seasonal rhythm superimposed on large between-plot differences. Despite variation in treatment, all plots exhibited the four-phase pattern (establishment, peak stress, partial recovery, and senescence), differing primarily in the magnitude of stress-phase decline and the degree of subsequent recovery. The divergence between treatment groups was most pronounced during the August stress period (approximately August 1 through August 28), a window identified empirically from the canopy cover data rather than from the irrigation schedule. This window coincided with the season's most severe atmospheric and soil-moisture conditions. Mean daily maximum air temperature over August 1–28 was 32.8°C, well above the seasonal average of 29.3°C, and 19 of the 28 days reached at least 32.2°C (90°F), including the season's second-hottest day on August 25. At the same time, rainfall fell to 1.84 inches over the window, less than half the 4.25 inches that had fallen during the preceding July 2–August 10 irrigation gap, when frequent rain had made supplemental irrigation unnecessary. With rainfall diminished and evaporative demand high, volumetric water content in the less-irrigated plots declined to its seasonal lows during this period. The coincidence of peak air temperature, reduced rainfall, and minimum soil moisture identifies August 1–28 as the primary diagnostic period for treatment effects. The August window is identified throughout this chapter as the primary diagnostic period for treatment effects.

The spread between the highest and lowest visibly green cover readings on any given measurement day ranged from approximately 40 to 60 percentage points, demonstrating that treatment factors produced large, ecologically and practically meaningful differences in plant performance. Plots receiving more frequent irrigation (12 events, approximately 78 gallons per plot across the season) generally occupied the upper portion of the visibly green cover distribution, while less-irrigated plots (4 events, approximately 26 gallons per plot) generally occupied the lower portion. However, within each irrigation group, considerable plot-to-plot variability was observed, reflecting the influence of substrate depth, substrate type, and plant community on the expression of irrigation benefits. Figure 4.6 shows the seasonal trajectories of visibly green canopy cover averaged by treatment group across the 56 measurement days. The gap between the more-irrigated and less-irrigated groups widened through the peak-stress period (shaded), reaching its maximum in mid-August 2025, then narrowed as the less-irrigated plots recovered through September, before the two groups converged as the canopy senesced at the end of the season. Individual-plot trajectories are shown in Figure 4.7. The contrast between the strongest and weakest plots is shown directly in Figure 4.8, which tracks the two through the season as Canopeo-classified green cover. Even at peak season, the less-irrigated Rooflite East plot (8-inch P1) carried far less green canopy than the more-irrigated BuildEx West plot (8-inch P2), and its green area thinned to almost nothing by autumn, while the high performer retained a substantial green canopy well into the season.

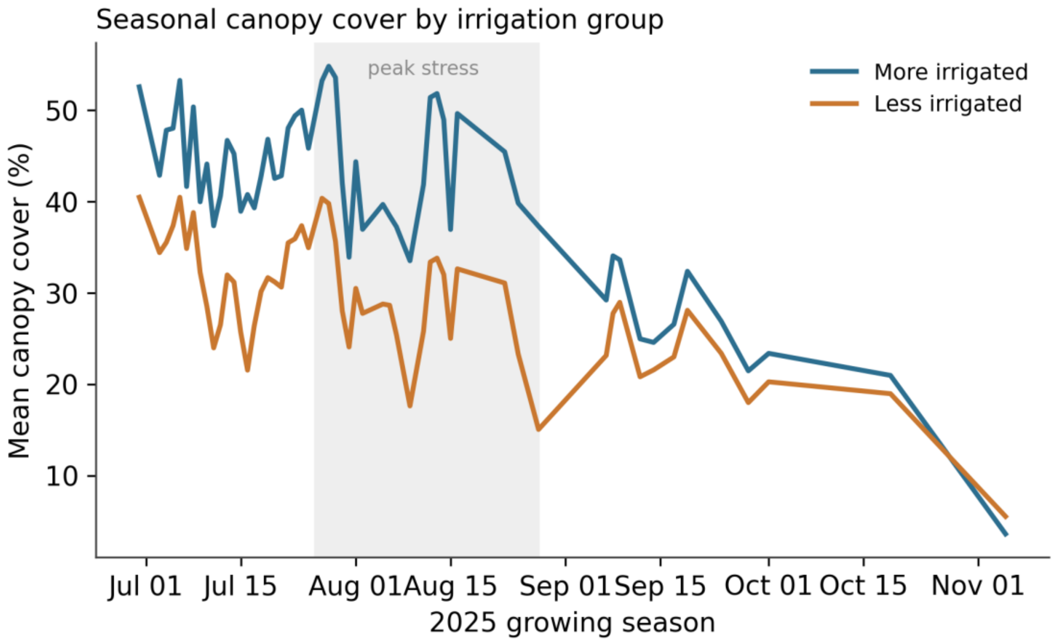

Figure 4.6. Seasonal visible green canopy cover trajectories averaged by treatment group across the 56 measurement days.

The divergence between more-irrigated and less-irrigated groups widened through the peak stress period (shaded), reaching its maximum in mid-August 2025. It narrowed thereafter as the less-irrigated plots recovered through September, and the two treatment groups converged as the canopy senesced at the close of the season. Individual-plot trajectories are shown in Figure 4.7. Author working with 2025 APD-EGR data (2026).

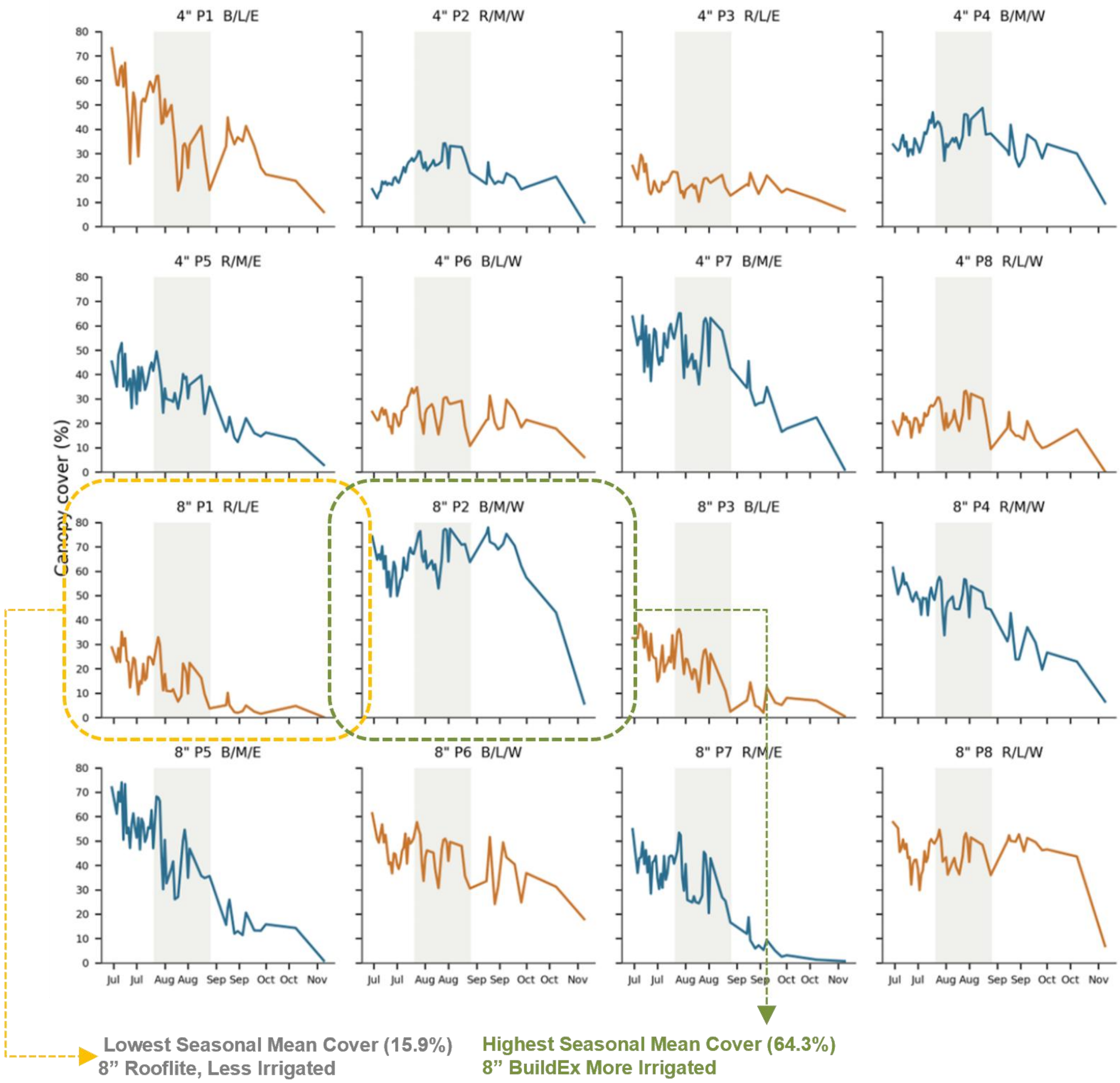

Figure 4.7. Individual visibly green canopy cover trajectories for all 16 experimental plots across the 2025 growing season.

Blue = more irrigated, orange = less irrigated; shaded band = peak stress period. Labels indicate plot identity and treatment as substrate, irrigation, and community (for example, B/M/E denotes BuildEx, more-irrigated, East). The disaggregated view resolves the timing of each plot's seasonal peak, the depth of the mid-season decline, and the degree of autumn persistence that the treatment-group means average out. Source: Author working with 2025 APD-EGR data (2026).

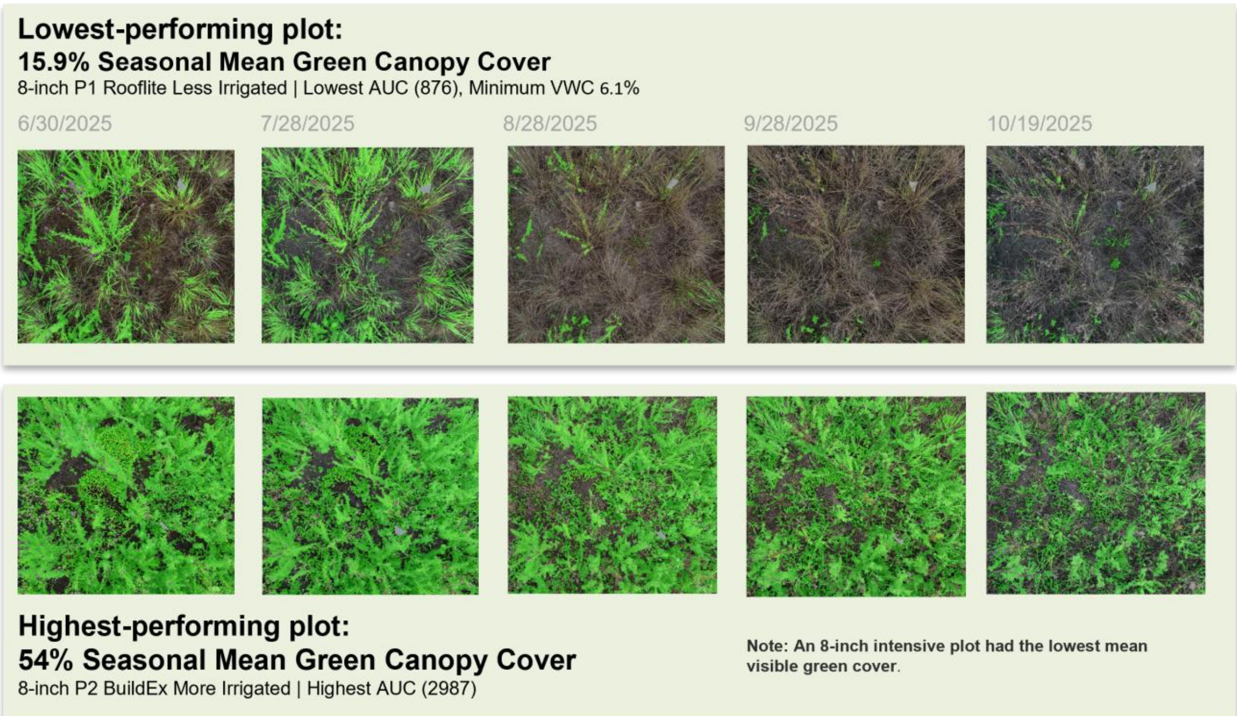

Figure 4.8. Canopeo-processed images of the lowest- and highest-performing plots on six dates (June 30 to October 19, 2025).

The green overlay marks the pixels classified as living green canopy, so the green area is the measured visibly green cover. Top row: 8-inch P1 (Rooflite, less-irrigated, East; 15.9 percent seasonal mean). Bottom row: 8-inch P2 (BuildEx, more-irrigated, West; 64.3 percent). Both are 8 inches deep, so the difference reflects substrate, irrigation, and community rather than depth. Photographs by author (2025). Analysis by author (2026).

Viewed plot by plot, several patterns emerge that the group averages obscure. First, the season peaked early: twelve of the sixteen plots reached their maximum visibly green canopy cover during the establishment phase in late June or July, before or at the onset of the 39-day irrigation gap, and only four peaked later. The gap did not merely slow canopy development; it capped the season close to its beginning, and no plot regained its early-season maximum in the months that followed. Second, the envelope of performance was wide. Seasonal mean cover spanned roughly fourfold, from 15.9% in the lowest plot (8-inch Rooflite less-irrigated, 8” P1) to 64.3% in the highest (8-inch BuildEx more-irrigated, 8” P2). The extremes corresponded to the extreme treatment combinations, the highest-performing plot combining the more productive substrate, the deeper profile, and more frequent irrigation, and the lowest combining the opposite of each, consistent with the substrate and irrigation main effects reported below. However, the treatment combination is unlikely to be the only influence. Because Canopeo classifies cover from green pixels, species-specific responses to stress, in which some plants change color rather than die back, may also shape these plot-level differences. Several species present on the roof shift color under stress, including *Dalea purpurea* (yellowing), *Sedum album* (reddening), and *Schizachyrium scoparium* (reddening to brown); a plot's particular species mix could therefore raise or lower its measured green cover independently of the substrate and irrigation treatments. Quantifying this species-level contribution was beyond the scope of the present study and is identified as a direction for future research.

Third, the treatment groups converged as the 2025 growing season ended. The irrigation advantage was largest at peak, when more-irrigated plots averaged 58.6% visibly green cover against 45.4% for less-irrigated plots, but it narrowed to only a few percentage points by the October 1 endpoint (23.4% versus 20.3%). More-irrigated plots in fact declined more in absolute terms over the season, on average 35.2 percentage points from peak to October 1 versus 25.1 percentage points for less-irrigated plots, because they had accumulated more cover to lose. By November nearly all plots had senesced toward bare-substrate values as the warm-season grasses went dormant and cured.

Fourth, substrate depth influenced autumn persistence more than it influenced peak visibly green cover. Eight-inch plots retained more cover at the October 1 endpoint than four-inch plots (24.5% versus 19.1%), and several less-irrigated eight-inch plots held substantial cover well into the autumn (36.8% in 8” P6 and 46.5% in 8” P8), behavior consistent with the deeper substrate functioning as a moisture reservoir that may have extended the functional growing season.

Finally, Figure 4.7 shows that individual plots varied in ways the treatment averages do not capture. A few plots behaved very differently from others in their group. For example, 8″ P8 (Rooflite, less-irrigated) held a high amount of visibly green cover even though it was one of the most water-limited combinations, while 8″ P7 (Rooflite, more-irrigated) fell below 5% despite frequent irrigation.

These exceptions suggest that factors beyond the three treatments influence plot performance. On an established, in-situ green roof, many such factors are present and difficult to control. One is the pre-existing difference in plant communities between the east and west sides. Others may include differences in root biomass, subsurface drainage, and the evening shade cast by the adjacent building on the west side. This study did not measure these factors, so their influence cannot be determined here.

The practical lesson is that the plots which behaved differently from their group warrant further research to identify which additional factors shaped their performance.

Main Effects of Substrate Depth, Substrate Type, and Irrigation Frequency

Table 4.2 presents the marginal means for seasonal visibly green canopy cover and the area under the curve (AUC) for each level of the three primary treatment factors, averaged across all other factors (n = 8 plots per level). AUC is important because it measures the total amount of visibly green cover a plot maintained *over the whole season* rather than on any single day, so it rewards plots that stayed green longest.

Table 4.2. Marginal means for seasonal visibly green canopy cover (%) and AUC by factor level (n = 8 plots per level).

Values represent the mean across all plots at each factor level. Irrigation frequency and substrate type (mix) produced the two largest marginal effects (~11 percentage points each), followed by substrate depth.

Factor	Level	Mean Cover	Mean AUC	Summer VWC
Substrate Depth	4-inch (extensive)	30.4%	1,680	13.0%
	8-inch (intensive)	38.6%	2,133	11.9%
Substrate Mix	BuildEx	40.2%	2,221	12.8%
	Rooflite	28.8%	1,593	12.1%
Irrigation Frequency	More irrigated	40.2%	2,222	13.5%
	Less irrigated	28.8%	1,592	11.4%

Two factors produced the largest and nearly identical marginal effects. Irrigation frequency raised seasonal visibly green cover from 28.8% in less-irrigated plots to 40.2% in more-irrigated plots, a difference of 11.3 percentage points, and the corresponding AUC difference (2,222 versus 1,592) indicates that the advantage was sustained across the season rather than concentrated at a single time point. Substrate mix produced an almost equal effect: BuildEx plots averaged 40.2% cover against 28.8% for Rooflite plots, a difference of 11.4 percentage points, with a parallel AUC gap (2,221 versus 1,593). Substrate mix and irrigation frequency were therefore the two leading influences on canopy cover; each associated with a difference of roughly 11 percentage points.

Substrate depth produced a smaller but consistent effect, with 8-inch plots averaging 38.6% seasonal visibly green cover against 30.4% for 4-inch plots, a difference of 8.3 percentage points, about three-quarters the magnitude of the irrigation and substrate effects. The direction of the substrate effect deserves emphasis because it revises an earlier reading of this experiment. Rather than being negligible, substrate mix emerged as a leading factor, with BuildEx outperforming Rooflite by 11.4 percentage points. This direction is consistent with the in-situ moisture behavior reported by Alam et al. (2025) for this site, in which BuildEx retained more water by volume in place than Rooflite. The mean VWC difference between irrigation groups was more modest than the visibly green cover difference (13.5% in more-irrigated versus 11.4% in less-irrigated plots), because rainfall partially compensated for withheld irrigation. However, it is the lowest moisture episodes rather than the seasonal mean that best explains canopy loss, with less-irrigated 4-inch plots reaching minimum VWC near 1.3% (0.013). Figure 4.9 shows the marginal mean seasonal visibly green canopy cover for each factor. Substrate type and irrigation frequency were the two largest and nearly equal effects (each about 11 percentage points, favoring BuildEx and more-irrigated plots), while substrate depth was smaller (about 8 percentage points, favoring the 8-inch plots).

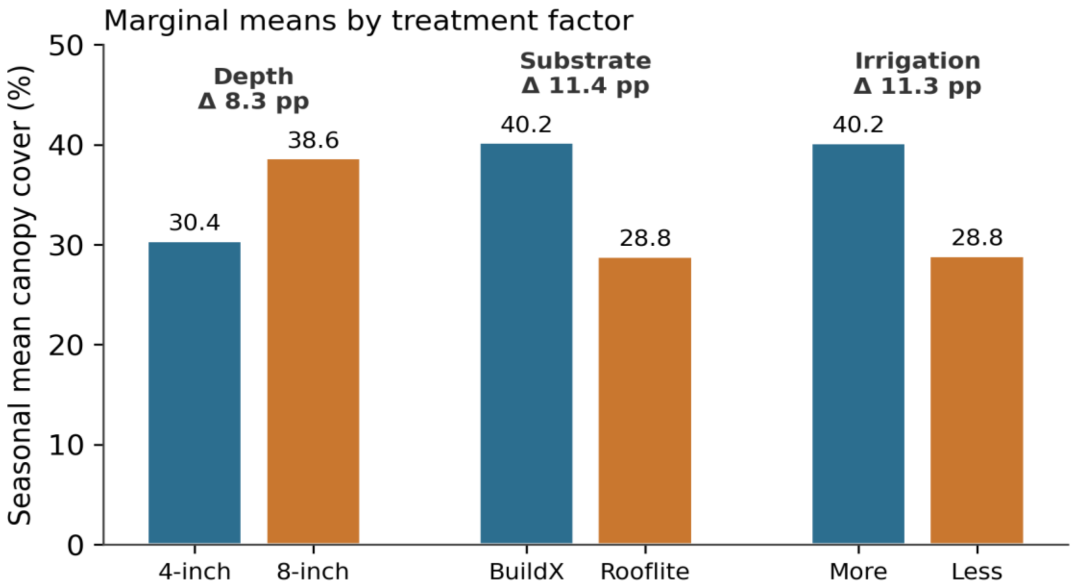

Figure 4.9. Marginal mean seasonal visibly green canopy cover by treatment factor. Substrate mix and irrigation frequency produced the two largest effects for the 16 APD-EGR plots, with BuildEx and more-irrigated plots each about 11 percentage points higher than their counterparts, while substrate depth produced a smaller effect of about 8 percentage points. Author using 2025 APD-EGR data (2026).

Treatment Cell Means and Interaction Patterns

Table 4.3 presents the mean seasonal cover, AUC, mean VWC, and minimum VWC for each of the eight treatment combinations (depth × substrate × irrigation), each represented by two plots (n = 2 per cell).

Table 4.3. Treatment cell means for seasonal canopy cover (%), AUC, mean VWC (%), and minimum VWC (%) for all eight treatment combinations (n = 2 per cell).
Green highlight indicates the highest-performing cell (8-inch BuildEx, more-irrigated).

Depth	Substrate	Irrigation	n	Cover	AUC	VWC Mean	VWC Min
4″	BuildEx	More	2	41.2%	2,283	13.1%	3.5%
4″	BuildEx	Less	2	33.3%	1,835	11.1%	0.8%
4″	Rooflite	More	2	27.6%	1,527	16.4%	5.8%
4″	Rooflite	Less	2	19.5%	1,077	11.5%	1.8%
8″	BuildEx	More	2	54.0%	2,987	14.7%	7.3%
8″	BuildEx	Less	2	32.3%	1,779	12.4%	6.4%
8″	Rooflite	More	2	37.9%	2,090	9.9%	5.5%
8″	Rooflite	Less	2	30.4%	1,677	10.8%	6.1%

The 8-inch BuildEx more-irrigated treatment cell produced the highest mean seasonal visibly green cover of all eight cells, at 54.0%, together with the highest AUC (2,987), demonstrating that the combination of deeper substrate, the more water-retentive BuildEx mix, and frequent supplemental irrigation maximized canopy cover under the tallgrass prairie ecoregion climate. The 4-inch Rooflite less-irrigated cell produced the lowest mean cover (19.5%) and the lowest AUC (1,077), pairing the shallowest profile, the less retentive substrate, and infrequent irrigation with one of the lowest minimum VWC values (1.8%).

The cell means show the three main effects acting consistently rather than through strong interactions. Within every depth and substrate combination, the more-irrigated cell exceeded its less-irrigated counterpart, and within every depth and irrigation combination, the BuildEx cell exceeded its Rooflite counterpart. The BuildEx advantage was present at both depths, for example 54.0% against 37.9% within the 8-inch more-irrigated pair and 41.2% against 27.6% within the 4-inch more-irrigated pair. No cell reversed the expected direction and no single cell behaved anomalously, so the earlier characterization of an underperforming 8-inch BuildEx more-irrigated cell does not hold once the plot data are correctly assigned.

The magnitude of the irrigation advantage varied somewhat across combinations, from about 8 percentage points within the 4-inch Rooflite plots (27.6% versus 19.5%) to about 22 percentage points within the 8-inch BuildEx plots (54.0% versus 32.3%), but its direction was uniform across all four depth-and-substrate combinations. Because more irrigation raised cover regardless of depth or substrate, the interactions among the three factors were weak, and the main effects (Figure 4.9) accounted for most of the treatment differences.

Figure 4.10 shows the substrate-by-irrigation relationship in mean seasonal visibly green canopy cover, plotted separately for each depth. BuildEx exceeded Rooflite at both irrigation levels and in both depths, with no crossover between the lines, indicating that the substrate advantage held regardless of irrigation frequency or depth. The separation was widest in the more-irrigated plots, whereas in the 8-inch less-irrigated plots the BuildEx and Rooflite values were close, though BuildEx still remained slightly higher. The highest cover occurred in the 8-inch BuildEx plots, which combined the more productive substrate with the deeper profile.

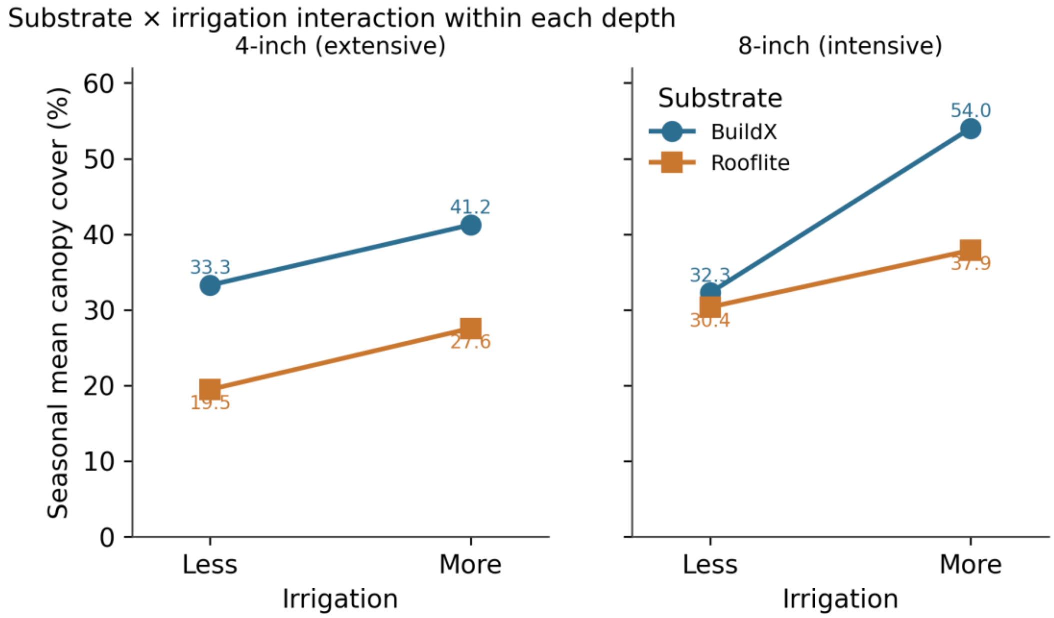

Figure 4.10. Substrate type by irrigation interaction in mean seasonal canopy cover, shown separately for each depth.

BuildEx (blue) exceeded Rooflite (orange) at both irrigation levels and both depths, with no crossover. The highest-performing combination was the 8-inch depth with more irrigation for the BuildEx plots on the APD-EGR. 2025 APD-EGR data analysis by the author (2026).

Soil Volumetric Water Content

Seasonal VWC Patterns by Depth and Irrigation

Soil volumetric water content was continuously monitored at hourly intervals throughout the growing season using Teros 12 sensors installed in all 16 experimental plots across four dataloggers (03500, z6-07870, z6-03501, and z6-03504). Hourly readings were averaged to daily means and then aligned to the 56 Canopeo measurement dates for integrated analysis. Negative sensor readings, which occurred sporadically in 4-inch less-irrigated plots during extreme drought periods (likely reflecting sensor calibration drift at very low moisture levels), were set to zero before analysis.

Table 4.4 summarizes the seasonal volumetric water content of the sixteen plots by substrate depth and irrigation level (amount). The values show that substrate depth governed moisture stability more than it governed average moisture: the 8-inch plots held mean VWC similar to, or slightly below, the 4-inch plots, but varied over a much narrower range, while the 4-inch plots swung between higher maxima and far lower minima.

Table 4.4. Seasonal volumetric water content (VWC, %) by substrate depth and irrigation level (amount).

All values are growing-season daily means; range = maximum minus minimum.

Depth	Irrigation	Mean VWC	Min VWC	Max VWC	Range (pp)
4-inch	More irrigated	14.8%	4.7%	24.4%	19.7
4-inch	Less irrigated	11.3%	1.3%	21.7%	20.4
8-inch	More irrigated	12.3%	6.4%	18.2%	11.8
8-inch	Less irrigated	11.6%	6.3%	19.5%	13.2

The most striking pattern in the VWC data was the difference in moisture volatility between 4-inch and 8-inch plots. The 4-inch plot groups exhibited a seasonal VWC range of 19.7 to 20.4 percentage points, compared to 11.8 to 13.2 percentage points in 8-inch plots, a difference of roughly 7 to 8 percentage points. This greater volatility in shallow substrates reflects their smaller total water storage volume: with less water to lose, 4-inch substrates reached critically low moisture more rapidly during dry periods and rebounded more sharply following irrigation or rainfall events.

The minimum VWC values are particularly significant in explaining the effect of substrate depth. Four-inch less-irrigated plots reached a mean minimum VWC of 1.3%, well below the 5 to 7% VWC range commonly cited as the wilting-point zone for green roof substrates, whereas 8-inch plots maintained mean minima of 6.3 to 6.4%, at the upper edge of that zone. This difference in minimum moisture, more than any difference in mean VWC, explains why 4-inch less-irrigated plots suffered the most severe and least reversible visibly green canopy reductions during the August stress period.

Figure 4.11 shows the seasonal range and mean of volumetric water content for each depth and irrigation group. It makes the buffering role of depth visible: the 4-inch plots swung down into the approximate wilting-point zone at their minima, whereas the 8-inch plots held distinctly higher minima. So the deeper substrate limited the severity of the driest episodes rather than raising average moisture.

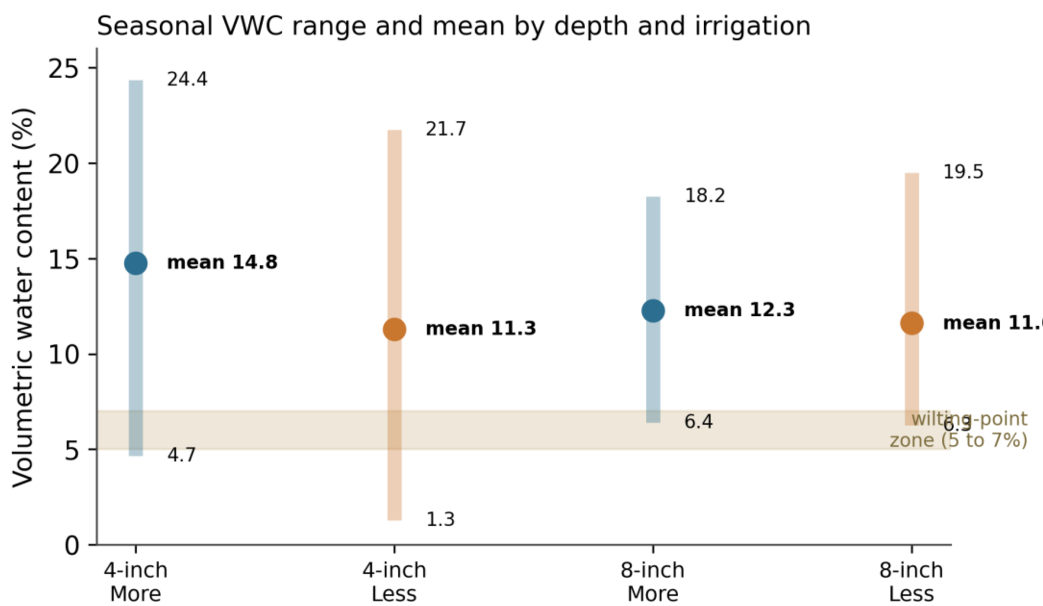

Figure 4.11: Seasonal volumetric water content range (minimum to maximum) and mean by depth and irrigation group.

Four-inch plots swung into the approximate wilting-point zone, whereas eight-inch plots maintained higher minima, illustrating substrate depth acting as a moisture buffer rather than a moisture source. 2025 APD-EGR data analysis by the author (2026).

The Irrigation Trigger Threshold and VWC Response

Supplemental irrigation decisions throughout the 2025 growing season were made using a threshold-based protocol linked to real-time VWC data monitored via the Zentra Cloud platform. Irrigation of all 72 plots was triggered when the VWC of at least four of the eight monitored 4-inch plots dropped below 8% VWC, provided that the 24-hour forecast showed less than 50% probability of rainfall. The 8% VWC threshold was selected to trigger intervention before plots approached the estimated or expected permanent wilting point, providing a moisture safety margin for the plant communities.

Analysis of the Teros 12 soil moisture data relative to the 8% threshold revealed that 4-inch less-irrigated plots repeatedly fell below this threshold during the season, with individual plots reaching daily mean VWC readings as low as 0.1%. In contrast, 8-inch plots in both irrigation groups maintained VWC above the 8% threshold for a greater proportion of the season, consistent with their larger total moisture storage volume. The VWC data confirmed that the irrigation protocol was ecologically appropriate: on the days immediately preceding each all-plots irrigation event, the monitored 4-inch more-irrigated plots were consistently at or below the 8% trigger level, validating the responsiveness of the monitoring-based management approach.

Substrate Temperature Behavior

Temperature Response to Depth and Irrigation

Substrate temperature was recorded at hourly intervals by the Teros 12 sensors, providing paired moisture and temperature data for each of the 16 experimental plots throughout the growing season. Table 4.5 summarizes substrate temperature by depth and irrigation level. Both deeper substrate and more frequent irrigation lowered substrate temperature: within each depth, the more-irrigated plots ran cooler than the less-irrigated plots, and the highest absolute maximum occurred in the shallow, less-irrigated plots, where low moisture and high heat coincided.

Table 4.5. Substrate temperature (°C) by depth and irrigation level.

Summer mean = mean of July-August daily temperatures. Orange highlight = highest absolute maximum temperature.

Depth	Irrigation	Season Mean (°C)	Summer Mean (°C)	Absolute Max (°C)
4-inch	More irrigated	24.1	29.1	35.8
4-inch	Less irrigated	24.9	30.3	38.4
8-inch	More irrigated	23.6	28.3	33.2
8-inch	Less irrigated	24.1	29.1	34.8

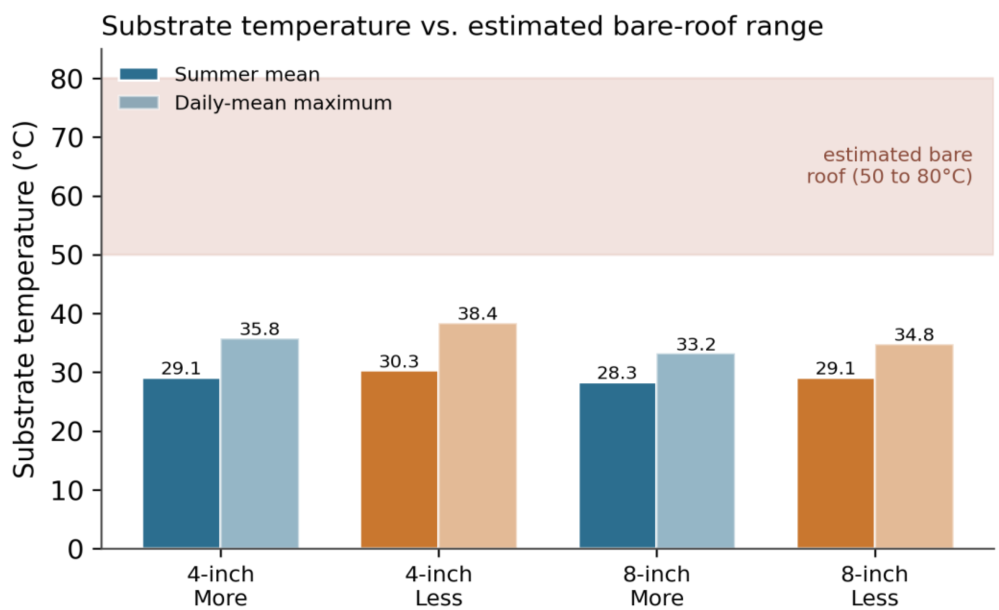

Figure 4.12: Summer mean and daily-mean maximum substrate temperature by treatment group.

Temperatures are shown against the estimated bare-roof surface temperature range (50 to 80°C). All treatments delivered substantial urban heat island mitigation regardless of canopy performance. 2025 APD-EGR data analysis by the author (2026).

Substrate temperature responded to both treatments that governed moisture. Eight-inch plots maintained summer mean temperatures 0.8 to 1.2°C lower than 4-inch plots within comparable irrigation groups, reflecting the greater thermal mass of the deeper substrate, and more-irrigated plots maintained summer means about 0.8 to 1.2°C lower than less-irrigated plots within the same depth class, consistent with evaporative cooling as latent heat is absorbed during evapotranspiration from moist substrate. Substrate temperature was therefore not independent of the moisture treatments but moved with them: the plots that were driest were also the warmest.

Coincidence of Heat and Moisture Stress

The most thermally extreme plots were the 4-inch less-irrigated plots, which reached the highest absolute substrate temperatures in the experiment (daily mean maximum 38.4°C) while simultaneously falling to the lowest moisture levels (minimum VWC near 1.3%). Because the driest plots were also the warmest, heat and moisture stress coincided in the same plots during the same August window rather than acting separately. This coincidence is the most likely explanation for the disproportionate canopy cover decline observed in these plots during August: high substrate temperatures raised evaporative demand at precisely the time when substrate water was least available to meet it. The two influences cannot be statistically separated in this dataset, because temperature and moisture are inherently confounded on this roof, moist plots are cooler by virtue of the same water that relieves drought stress, so they are best interpreted together as a compounding stress rather than as independent effects.

Supplemental Irrigation Events and Water Input

Irrigation Event Log and Protocol

Twelve supplemental irrigation events occurred during the 2025 growing season (June 30 through October 2), all using water from the on-site cistern system (Table 4.6). Events were classified into two types based on the number of plots watered: all-plots events (n = 4), in which both more-irrigated and less-irrigated plots received supplemental water, and more-irrigated-only events (n = 8), in which only the more-irrigated plots received water. Each irrigation event applied approximately 6.5 gallons per plot using a 60-second application per plot at approximately 10 seconds per gallon. This is equivalent to approximately 1 inch (0.25 mm) of irrigation per plot. Irrigation decisions were made in the early evening following confirmation that the VWC trigger condition had been met.

Table 4.6: Supplemental irrigation events during the 2025 growing season.
Green highlight = all-plots events in which less-irrigated plots also received water.

#	Date	Event type	Plots watered	Gal/plot	Notes
1	Jun 30	More only	36	~6.5	First GS event; forecast >90°F
2	Jul 02	All 72	72	~6.5	VWC trigger; all plots watered
3	Jul 15	More only	36	~6.5	13-day gap; less-irr. at 39-day gap start
4	Jul 27	More only	36	~6.5	12-day gap; peak summer heat
5	Aug 06	More only	36	~6.5	10-day gap; Aug stress period begins
6	Aug 10	All 72	72	~6.5	39-DAY GAP BROKEN for less-irr.
7	Aug 15	More only	36	~6.5	5-day gap; peak stress continues
8	Aug 17	All 72	72	~6.5	2-day gap; intensive intervention
9	Aug 23	More only	36	~6.5	6-day gap
10	Aug 28	All 72	72	~6.5	Last ALL event; less-irr. receives no more water
11	Sep 15	More only	36	~6.5	18-day gap; less-irr. rain-only from here
12	Oct 02	More only	36	~6.5	17-day gap; pre-senescence event

Over the full growing season, the more-irrigated plots received approximately 78 gallons (295 mm or 11.6 inches) of supplemental water per plot during 12 irrigation events, compared to approximately 26 gallons (98 mm or 3.9 in) per plot across 4 irrigation events for less-irrigated plots, a 3:1 ratio. The less-irrigated plots received water exclusively on the four all-plots events (July 2, August 10, August 17, and August 28). The intended alternating irrigation protocol (all-plots, then more-only, then all-plots, then more-only) had an exception if there was any rain event or at least a 50% chance of rain within 24 hours.

Figure 4.13 plots cumulative supplemental irrigation per plot by treatment group. The flat plateau in the less-irrigated series through the shaded 39-day gap (July 2 to August 10) marks the period when those plots received no supplemental water.

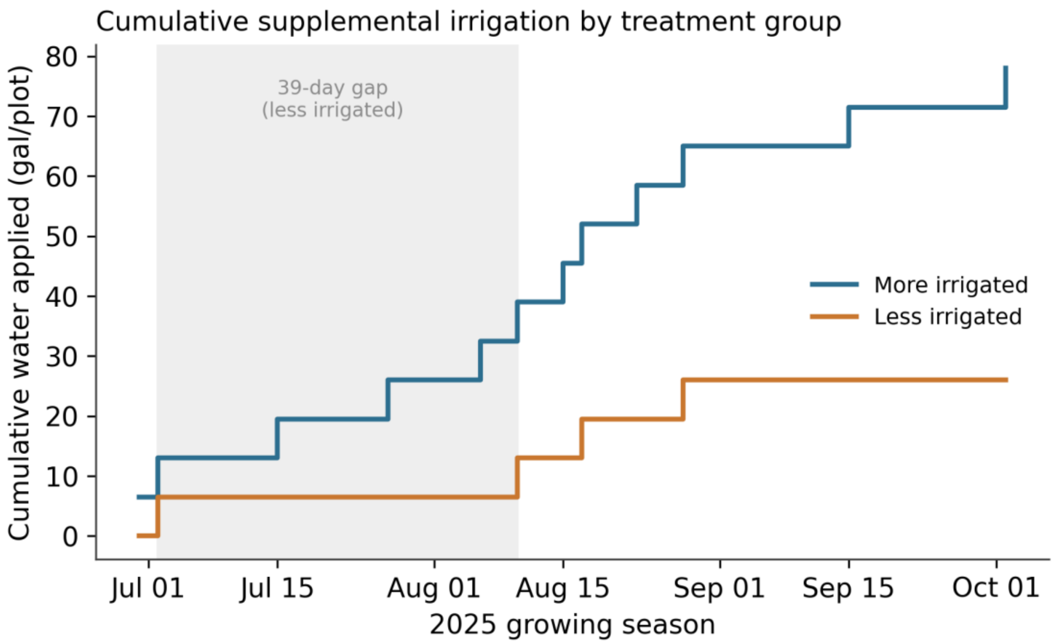

Figure 4.13. Cumulative supplemental irrigation applied per plot by treatment group across the season. The 39-day gap (shaded) is visible as a plateau in the less-irrigated series. Irrigation data recorded by Lee Skabelund (2021-2025). Analyzed by author (2025).

The 39-Day Irrigation Gap in the Context of Rainfall

The combination of VWC and weather forecast resulted in longer gaps of irrigation in less-irrigated plots. The longest period without supplemental irrigation for less-irrigated plots extended from July 2 through August 10, 2025, a gap of 39 consecutive days that coincided with the peak summer heat. During the gap, the Ekdahl (APD-EGR) weather station recorded 108 mm (4.25 inches) of rain across 22 of the 40 days, roughly 42% of the entire growing season total, and the longest genuinely rainless stretch within the window was only five days. In water-supply terms, the less-irrigated plots were not deprived: the rain that fell on them during the gap, about 108 L per square meter, was comparable to the total supplemental irrigation the more-irrigated plots received over the same period. The gap was therefore a gap in the irrigation log rather than a gap in water input.

Despite this rainfall, the sensor data show that real and severe moisture stress did occur, but only in shallow plots. The 4-inch less-irrigated plots dried to VWC minima between 0 and 3.3% at several points during the gap, well below the 5 to 7% wilting-point zone, whereas the 8-inch less-irrigated plots never fell below about 5.5%. The day-by-day record explains the difference: moisture in the shallow plots traced a sawtooth, in which each rain event recharged the substrate only briefly before four to five days of high evapotranspiration drew it back down to critical levels. It is hypothosized that the limiting factor was not the amount of rain but the shallow substrate's inability to store it, as rain that would sustain plants in a deeper profile likely passed through the shallow media faster than the plants could use it or was uptaken by plant roots.

The 39-day gap is best understood, then, not as the singular drought event of the season but as one clear illustration of a season-long vulnerability, namely that shallow extensive substrates cannot buffer a frequent-light-rain regime under high summer evaporative demand, and that supplemental irrigation matters chiefly as a hedge against this storage limitation rather than as a substitute for absent rainfall. Consistent with this reading, the low-moisture episodes in the 4-inch less-irrigated plots were not confined to the gap. Sub-7% VWC readings recurred across the season, including a sustained dry-down in late August after irrigation had resumed, when one plot again fell to 2.5% VWC. Low-moisture readings were most concentrated during the 39-day gap itself, but they were not unique to it, reinforcing that the shallow substrates' storage limitation was a season-long vulnerability rather than a one-time event.

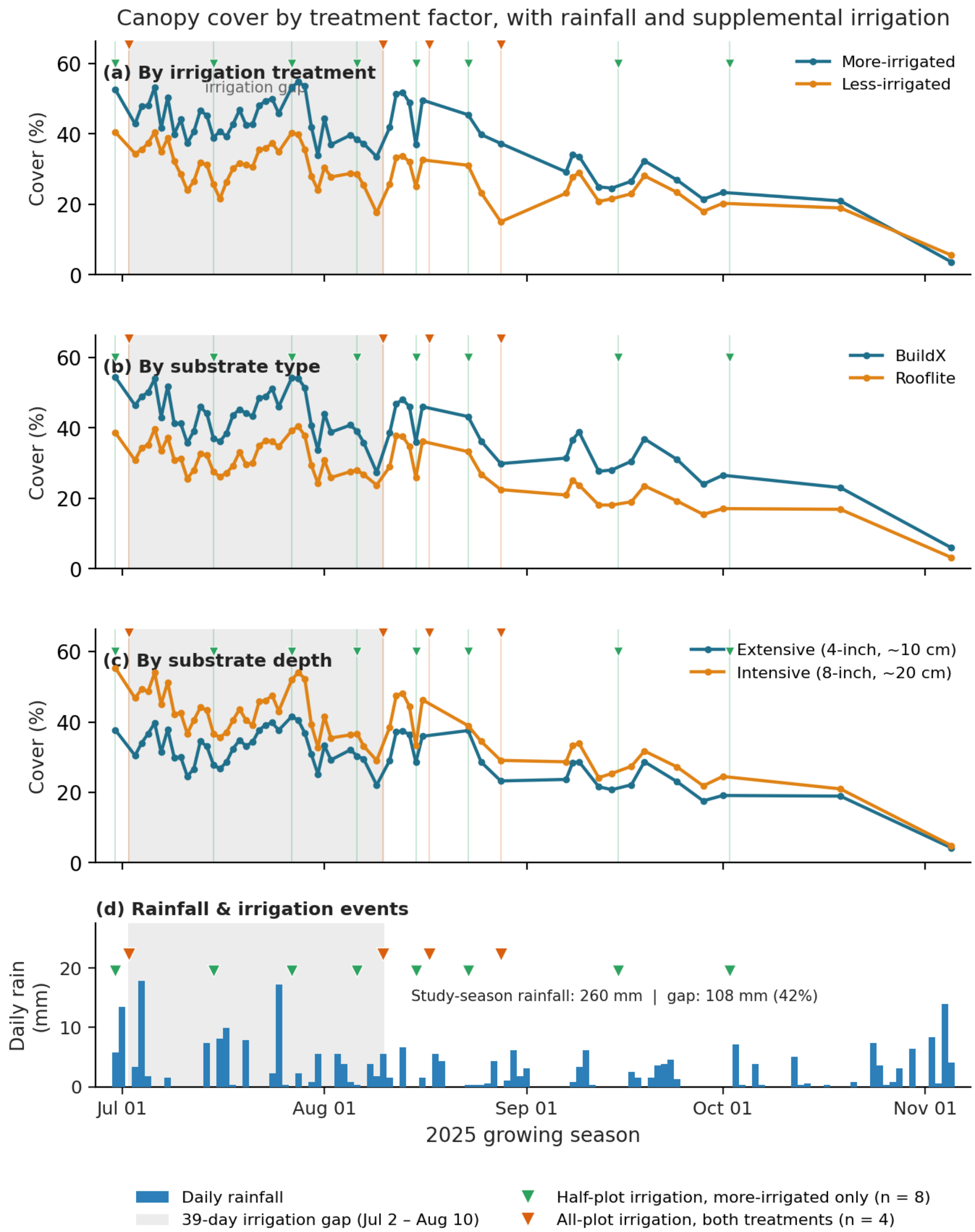

Figure 4.14. Seasonal visibly green canopy cover by irrigation frequency, substrate type, and substrate depth, with daily rainfall shown for reference.

Treatment differences developed during the mid-season stress period and persisted despite recurring rainfall. 2025 APD-EGR data analysis by the author (2026).

Figure 4.15 plots seasonal volumetric water content by treatment factor with daily rainfall for reference, showing that the less-irrigated and 4-inch plots drew down to their seasonal lows through the gap and the August stress window, while the 8-inch and more-irrigated plots held higher, steadier moisture.

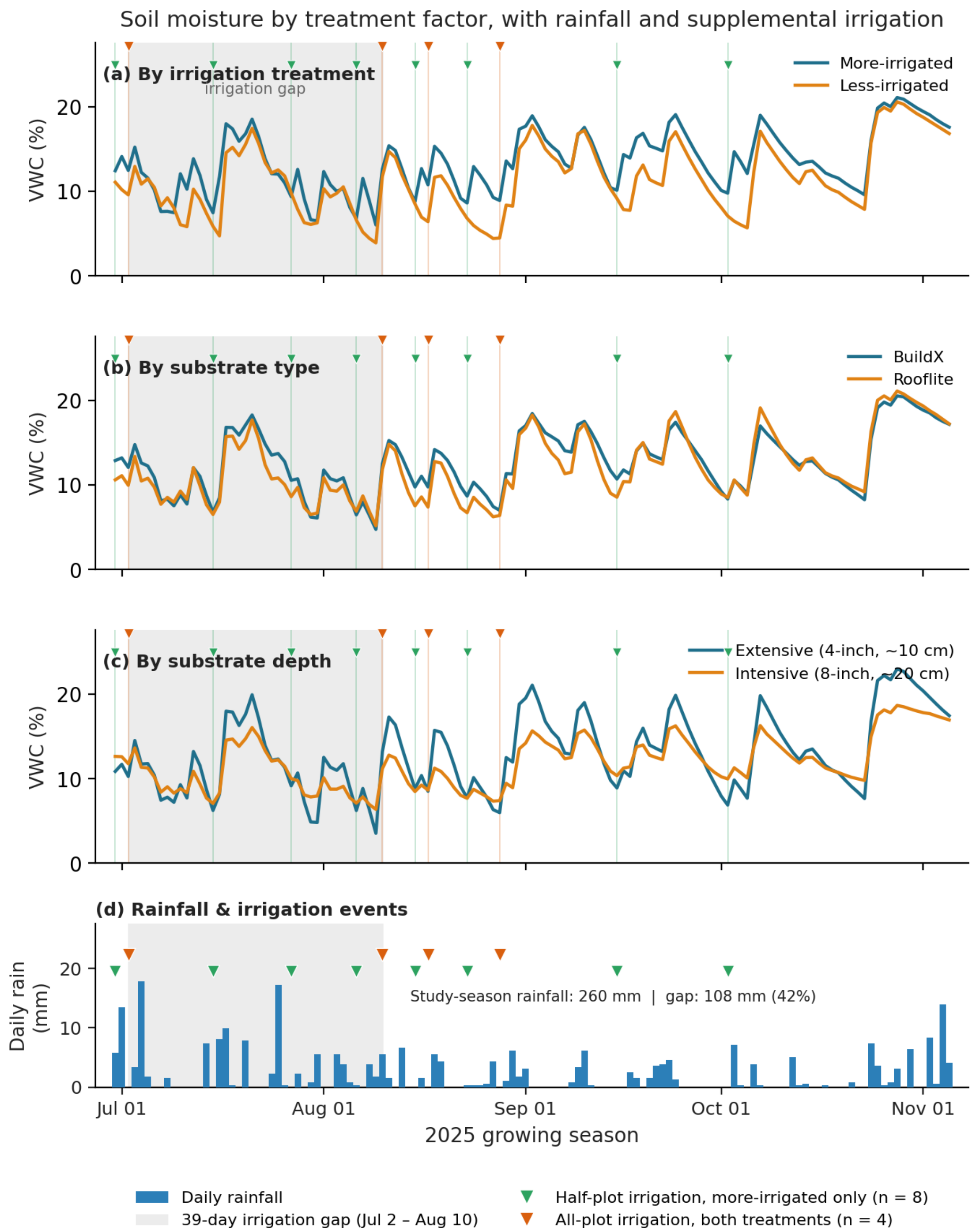

Figure 4.15. Seasonal volumetric water content by irrigation frequency, substrate type, and substrate depth, with daily rainfall shown for reference.

Moisture rose with rain events and drew down between them; the less-irrigated and 4-inch plots fell to their seasonal lows through the gap and the August stress window, while the 8-inch and more-irrigated plots held steadier. 2025 APD-EGR data analysis by the author (2026).

After August 28, less-irrigated plots received no further supplemental irrigation for the remainder of the growing season, a period of 35 or more days through the functional end of the growing season (October 1). During September, less-irrigated plots relied entirely on natural rainfall, which provided 13 rain event days but also included two 5-day dry spells and overall lower total precipitation than August. The combination of reduced irrigation, persistent dry spells, and gradually declining temperatures that limited plant recovery capacity continued the divergence between more-irrigated and less-irrigated plots through the end of the growing season.

Plot-Level Stress Response: Which Plots Struggled, Adapted, and Recovered

Because the gap exposed the less-irrigated plots to genuine transient stress, their individual responses provide an informative test of green roof resilience. Table 4.7 summarizes, for each of the eight less-irrigated plots, the minimum VWC reached during the gap, the decline in canopy cover from its seasonal peak to the seasonal minimum, and the degree of recovery during the September partial-recovery phase.

Table 4.7. Plot-level stress and recovery for the eight less-irrigated plots.

The Gap VWC minimum is the lowest daily mean between July 2 to August 10, 2025; the decline is the loss of visibly green cover from seasonal peak (peak cover) to the seasonal minimum (min. cover); recovery is the gain in cover during the September partial-recovery phase.

Plot	Depth	Substrate	Community	Gap VWC min	Peak cover	Min. cover	Decline	Sept recovery
4″ P1	4″	BuildEx	East	0.0%	73.2%	14.8%	80%	+30.0
4″ P3	4″	Rooflite	East	0.0%	29.5%	10.2%	65%	+11.9
4″ P6	4″	BuildEx	West	1.1%	34.8%	10.7%	69%	+20.6
4″ P8	4″	Rooflite	West	3.3%	30.6%	9.4%	69%	+15.2
8″ P1	8″	Rooflite	East	6.1%	35.1%	3.7%	89%	+6.4
8″ P3	8″	BuildEx	East	6.9%	38.3%	2.4%	94%	+12.0
8″ P6	8″	BuildEx	West	5.5%	61.3%	30.5%	50%	+21.1
8″ P8	8″	Rooflite	West	5.9%	57.7%	36.0%	38%	+16.7

Two clear patterns emerge, and they operate differently. First, genuine moisture stress was confined to shallow plots. All four 4-inch less-irrigated plots dried to damaging minima between 0 and 3.3% VWC, while all four 8-inch less-irrigated plots remained above 5.5%

throughout the 39-day irrigation gap. This pattern suggests that the greater substrate volume of the 8-inch plots buffered moisture even in the complete absence of supplemental irrigation, consistent with the depth-as-buffer mechanism and observed here under the most demanding conditions of the season.

Second, and more unexpectedly, the loss of visibly green canopy cover through the 39-day stress period did not follow the moisture stress. It followed the plant community as shown in Figure 4.9. Figure 4.16 plots peak-to-trough decline in visibly green canopy cover for the eight less-irrigated plots against their minimum volumetric water content during the 39-day gap, grouped by plant community. The West plots, whose mixed prairie and sedum communities includes several drought-tolerant Sedum species, retained far more visibly green cover than the grass-dominant East plots: the two 8-inch West plots lost only 38% (8” P8) and 50% (8” P6) of their visibly green peak cover and still held 30 to 36% absolute cover at the trough, whereas the East plots lost between 65% and 94%. The most telling comparison is between the two 8-inch East plots and their West counterparts. Plots 8” P1 and 8” P3 lost 89% and 94% of their cover despite never experiencing moisture stress, their VWC having remained above 6% throughout the gap. Their near-total loss of visibly green cover was therefore not caused by drought, but by the browning of warm-season grasses under heat. The sedum component, which is present in both communities but was more visible on the West side in 2025 where fewer tall grasses shaded it, remained green through the same conditions. Community composition, specifically the balance between browning warm-season grasses and visible drought-tolerant sedum, rather than water status, governed which plots remained visually vegetated through the peak-stress period.

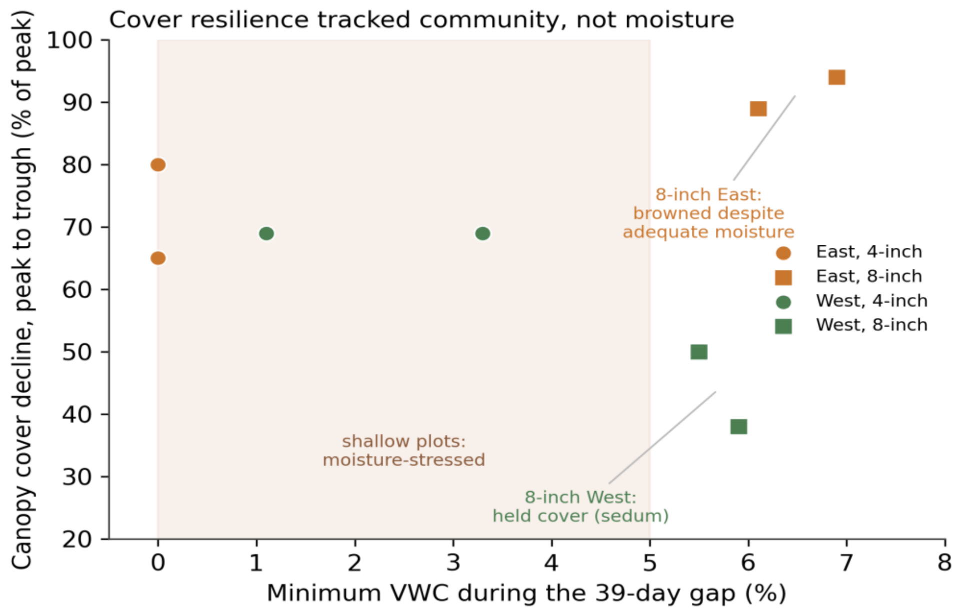

Figure 4.16. Canopy cover decline versus minimum VWC, by plant community.

Visibly green canopy cover declined from seasonal peak to peak-stress trough for the eight less-irrigated plots, plotted against the minimum VWC each plot reached during the 39-day gap and grouped by plant community. Cover decline was not explained by moisture status: the grass-dominant 8-inch East plots (upper right) lost most of their visibly green cover despite adequate moisture, while the sedum-bearing 8-inch West plots (lower right) retained cover at similar moisture levels. The shaded band marks the severe moisture-stress zone occupied by the shallow 4-inch plots. Community composition, rather than water status, governed cover resilience through the stress period. 2025 APD-EGR data analysis by the author (2026).

Third, recovery was broad. Almost every less-irrigated plot regained cover during September, and some of the most severely stressed did so most strongly: plot 4″ P1, which fell to near-zero VWC and to 15% cover, rebounded 30 percentage points, and the resilient 8-inch West plots each added a further 9 to 28 points. Only 8″ P1 recovered weakly, regaining about 6 percentage points. That a mature, eight-year planting could regreen so widely after a severe transient stress is an encouraging signal for green roof management.

Integrated Synthesis: Relative Influence of Treatment Factors

The integrated analysis of canopy cover, soil VWC, substrate temperature, irrigation history, and site weather data allows a ranked assessment of the relative influence of each treatment factor on canopy cover performance during the 2025 growing season. Three principal findings emerge from this synthesis.

First, moisture supply governed visibly green canopy cover, and it did so through two management levers of comparable importance: irrigation frequency and substrate mix. Irrigation produced a marginal effect of 11.3 percentage points and substrate mix a nearly identical 11.4 percentage points, each roughly one-third larger than the 8.3 percentage point effect of substrate depth. The irrigation advantage operated through two simultaneous mechanisms, direct plant water supply that kept VWC away from wilting-point levels, and evaporative cooling that held substrate temperatures about 0.8 to 1.2°C lower in more-irrigated plots. The combined effect of moisture sufficiency and thermal moderation was a cover advantage that widened through the August stress period and was not fully recovered by less-irrigated plots for the remainder of the season.

Second, substrate depth functioned as a moisture buffer rather than a moisture source. Eight-inch plots maintained substantially lower VWC volatility (seasonal range 11.8 to 13.2 percentage points) than 4-inch plots (19.7 to 20.4 percentage points), and their minimum VWC values were far higher (6.3 to 6.4% versus 1.3 to 4.7%). This buffering made 8-inch plots more resistant to the extreme low-moisture episodes that cause irreversible damage, even under the same irrigation frequency as 4-inch plots. Depth could not fully substitute for irrigation, however: 8-inch less-irrigated plots still declined during the 39-day gap, and their mean seasonal cover (31.4%) remained about 14.6 percentage points below that of 8-inch more-irrigated plots (46.0%).

Third, and in contrast to an earlier reading of this experiment, substrate mix was not neutral but one of the two leading factors. BuildEx plots averaged 11.4 percentage points more cover than Rooflite plots across depths and irrigation levels. This direction aligns with the in-situ moisture relationship documented at this site, in which BuildEx held the greater water-holding capacity in place at every substrate depth examined (Decker 2021), even though Rooflite showed higher maximum water retention in laboratory tests. Our own 2025 Teros 12 data are directionally consistent, with BuildEx plots averaging marginally higher mean VWC (12.8%) than Rooflite plots (12.1%). The substrate advantage appeared modest in the moisture record because the VWC-triggered irrigation protocol narrowed moisture differences between the two mixes, yet it was expressed clearly in canopy cover, which suggests that the water made available by BuildEx at the root-substrate interface translated into measurably greater vegetation performance over the season.

Fourth, the reassessment of the 39-day irrigation gap reframes how these factors combined during the season's most stressful period. The gap was not a drought because ample rain fell, but it exposed the inability of the shallow substrates to retain that rain, and the plot-level analysis showed that survival through the resulting stress was governed less by water status than by plant community. The sedum-bearing West plots held cover through the peak-stress period while the grass-dominant East plots browned, some of them despite adequate moisture. Substrate depth and irrigation frequency set the moisture environment, but community composition determined which plots remained visually vegetated under stress, and the broad recovery of the mature planting in September indicated substantial resilience to transient extremes. The practical implication is that substrate storage capacity and species selection are as important as irrigation scheduling for sustaining canopy cover on minimally irrigated roofs in this climate.

Statistical Analysis Findings

ANOVA Results: Seasonal Mean Canopy Cover

The Shapiro-Wilk test confirmed that model residuals were normally distributed ($W = 0.938$, $p = 0.329$), supporting the normality assumption of the ANOVA. No effect reached statistical significance at the conventional $\alpha = 0.05$ threshold. Substrate mix and irrigation frequency showed the strongest trends and the largest effect sizes, followed by substrate depth.

Substrate mix explained the largest share of variance in seasonal mean canopy cover ($eta^2 = 0.186$, $p = 0.113$), with irrigation frequency almost identical ($eta^2 = 0.185$, $p = 0.114$). Substrate depth was a secondary effect ($eta^2 = 0.098$, $p = 0.233$). All two-way and three-way interactions were negligible, each explaining less than 2% of variance (depth × substrate $eta^2 = 0.008$, depth × irrigation 0.016, substrate × irrigation 0.018, and the three-way term 0.019). The near-absence of interaction, and particularly the small depth × substrate term, indicates that the three factors acted additively and independently rather than through the crossover pattern suggested by an earlier analysis of this dataset. The residual (error) term accounted for roughly 47% of total variance ($eta^2 = 0.471$), reflecting the substantial plot-to-plot heterogeneity of the mature 2017 planting.

The absence of formal significance is attributable primarily to the limited power of the design (error $df = 8$), which requires very large effects, on the order of 30 percentage points, to reach significance at $\alpha = 0.05$. All observed treatment differences fall below that threshold. The results are therefore best interpreted as directional evidence whose magnitude and consistency across response variables (mean cover, AUC, and VWC minimum) indicate practical importance despite the absence of formal significance, a limitation consistent with published green roof experiments of comparable replication and discussed further in Chapter 5.

ANOVA Results: Area Under the Cover-Time Curve (AUC)

Figure 4.17 shows the effect sizes (partial eta-squared) from the three-way ANOVA on seasonal mean canopy cover. ANOVA on AUC produced results consistent with the seasonal mean cover analysis. Substrate mix and irrigation frequency again showed the strongest trends and nearly identical effect sizes (substrate $eta^2 = 0.186$, $p = 0.113$; irrigation $eta^2 = 0.187$, $p = 0.113$), followed by substrate depth ($eta^2 = 0.097$, $p = 0.236$). All interaction terms were again negligible, each with eta^2 below 0.02, including the depth × substrate term ($eta^2 = 0.008$). No effect reached significance at $\alpha = 0.05$. The close agreement between the mean-cover and AUC analyses, in both the ranking and the magnitude of effects, reinforces confidence in the directional conclusions.

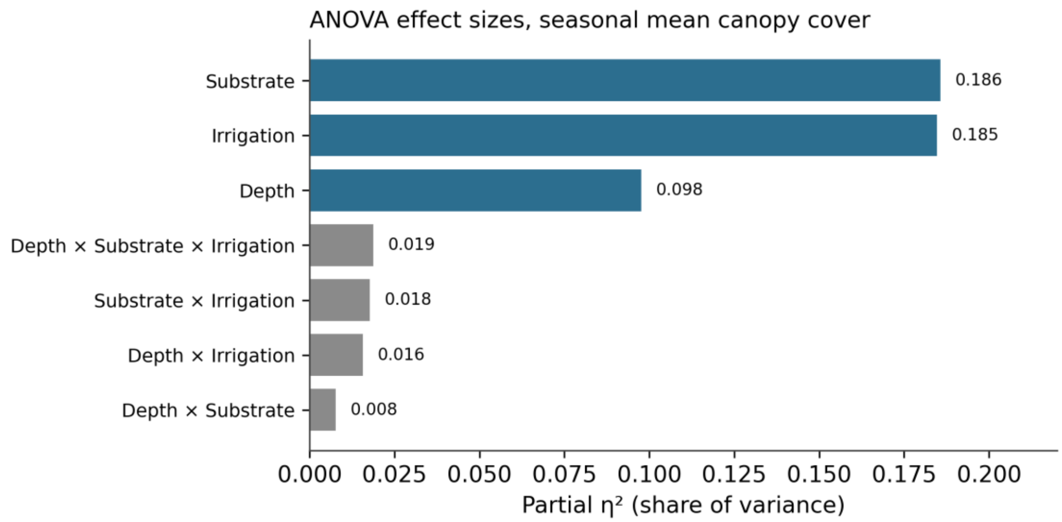

Figure 4.17. Effect sizes (partial eta-squared) from the three-way factorial ANOVA on seasonal mean canopy cover.

Substrate mix and irrigation frequency accounted for the largest shares of explained variance (eta-squared about 0.19 each), followed by substrate depth (0.10); all two- and three-way interactions were negligible (eta-squared below 0.02). 2025 APD-EGR data analysis by the author (2026).

Drone-Based Canopy Cover Analysis

Drone Canopy Cover Results and Comparison with iPhone Data

Drone-derived visibly green canopy cover values followed the same four-phase seasonal pattern observed in the iPhone dataset, and 8-inch intensive plots maintained higher mean cover than 4-inch extensive plots across all four flight dates. Three of the four drone flight dates (July 9, August 9, and September 19) coincided exactly with iPhone Canopeo measurement days, enabling direct comparison. Figure 4.18 compares the two ground- and air-based measures of green canopy cover across the four flight dates. Drone-derived cover values were systematically lower than iPhone values on these matched dates, by mean differences of approximately 9 to 13 percentage points. This offset is expected and reflects the different spatial perspective of the two methods rather than measurement error: the iPhone photographs, captured from approximately

1.5 to 2 m above the plot, emphasize the denser upper canopy zone, whereas the UAS imagery captures the entire plot surface from a true nadir aerial perspective, including plot edges and bare substrate gaps between plant clumps. The magnitude of the offset increased with canopy density across the matched observations ($r = 0.478$, $p < 0.001$), which is consistent with this interpretation, because a denser canopy leaves proportionally more inter-clump substrate for the aerial view to average into the plot value. Despite the systematic offset, the two datasets agreed closely in relative plot rankings and treatment-group patterns, with Spearman rank correlations between the two methods of 0.909, 0.944, and 0.929 on the three matched dates, confirming that they capture the same underlying gradient of vegetation performance. The two methods are therefore best understood as complementary: the iPhone dataset provides high-frequency near-surface canopy density measurements across 56 dates, while the drone dataset provides a standardized whole-plot overhead perspective at four strategic points in the season. Per-plot drone cover values for all sixteen plots on the four flight dates are provided in Appendix C.

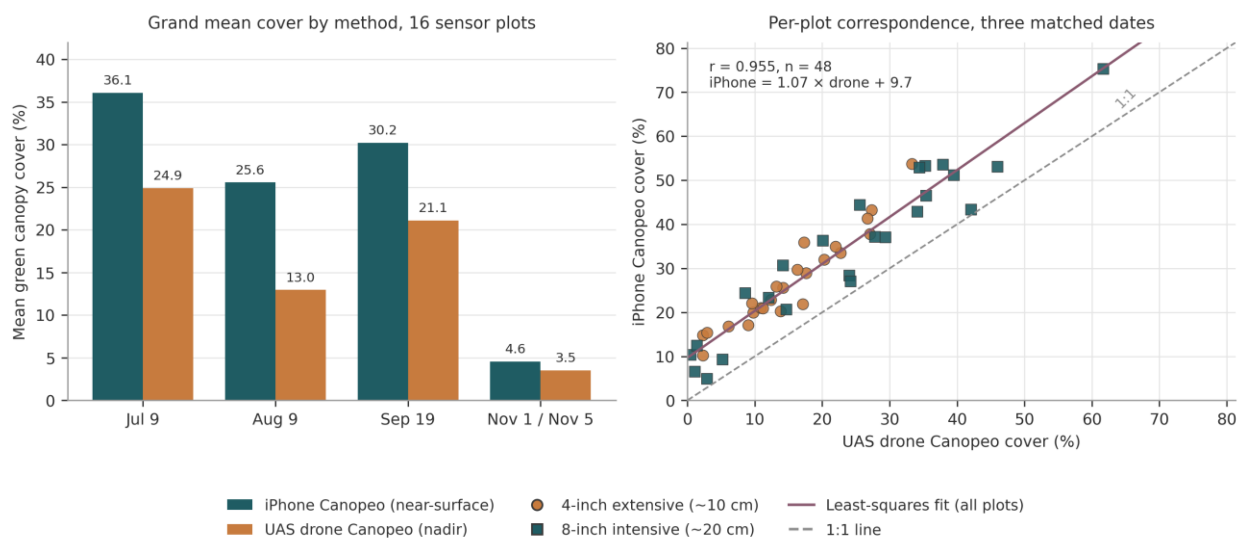

Figure 4.18: Drone (nadir) versus iPhone (near-surface) canopy cover on the four flight dates.

Left: Grand mean by method, showing that the near-surface iPhone imagery recorded systematically higher green cover than the nadir drone imagery on every date.

Right: Per-plot correspondence against the 1:1 line for the three exactly matched dates, showing that the two methods preserve the same relative ordering while the aerial view reads consistently lower. 2025 APD-EGR data analysis by the author (2026).

UAS-Derived NDVI Analysis Across All 72 Plots

Overview

In addition to the RGB-based canopy cover analyses, multispectral UAS imagery from the four flight dates was used to calculate the Normalized Difference Vegetation Index (NDVI) for all 72 plots on the APD-EGR green roof, including the 24 semi-intensive (6-inch) plots that were not part of the 16-plot irrigation and Teros 12 sensor experiment. NDVI data were also generated by Kaden Spencer, who performed the multispectral image processing and NDVI extraction. Imagery was captured with a DJI Mavic 3 Multispectral aircraft (four-band Green, Red, RedEdge, and NIR multispectral camera), radiometrically calibrated before each flight using the onboard light sensor and a Sentera calibration panel. Orthomosaics and the NDVI index were generated in Pix4Dfields at a ground sampling distance of approximately 0.25 cm per pixel, and plot-level mean NDVI values were extracted per plot polygon using QGIS. NDVI is calculated as (NIR − Red) / (NIR + Red) and quantifies vegetation photosynthetic vigor, a distinct dimension of plant performance from the fractional green cover measured by Canopeo. The 72-plot NDVI dataset provides a unique opportunity to compare vegetation health across all three substrate depth categories simultaneously.

Table 4.8 presents mean NDVI by substrate depth category across the four UAS flight dates, covering all 72 plots (24 per depth). NDVI increased with depth overall, but not linearly: the 6-inch semi-intensive plots did not fall midway between the 4-inch and 8-inch plots but instead tracked close to the 8-inch intensive plots on every date. The 8-inch plots exceeded the 4-inch plots significantly on the earlier flights, while the difference narrowed later in the season.

Table 4.8. Mean NDVI by substrate depth category across four UAS flight dates (n = 24 plots per depth).

Blue highlight = 6-inch semi-intensive plots; green highlight = 8-inch intensive plots. Significance of 8-inch vs 4-inch difference: p<0.001, p<0.01, ns = not significant.*

Depth category	**n plots**	**Jul 9**	**Aug 9**	**Sep 19**	**Nov 1**
4-inch extensive	24	0.486	0.525	0.569	0.431
6-inch semi-intensive	24	0.586	0.580	0.602	0.455
8-inch intensive	24	0.597	0.589	0.594	0.445
All 72 plots	**72**	**0.556**	**0.565**	**0.588**	**0.444**
8-inch vs 4-inch difference		*+0.111****	*+0.064***	*+0.025 ns*	*+0.014 ns*

Depth Effect and the Semi-Intensive Finding

NDVI values across all 72 plots and dates ranged from 0.287 to 0.711, with a grand mean of 0.538. The depth effect on NDVI was highly significant during the early- and peak-season flights. Eight-inch plots exceeded 4-inch plots by 0.111 NDVI units on July 9 ($p < 0.001$) and 0.064 units on August 9 ($p = 0.004$), but the difference was not significant by September 19 or November 1. The most notable finding from the full 72-plot dataset is the performance of the 6-inch semi-intensive plots, which achieved NDVI values above the arithmetic midpoint between 4-inch and 8-inch means on all four dates. On July 9, the 6-inch mean NDVI (0.586) was only

0.011 units below the 8-inch mean (0.597) and 0.100 units above the 4-inch mean (0.486). This disproportionate proximity to the deeper category suggests a non-linear relationship between substrate depth and vegetation health, in which much of the benefit of increasing depth is achieved between 5 and 7 inches (the approximate depths of the plots in the 6-inch bed), with diminishing returns thereafter. This finding was only possible because the NDVI analysis encompassed all 72 plots, including the semi-intensive depth category excluded from the sensor experiment. Figure 4.19 plots mean NDVI by depth across the four flight dates (all 72 plots). On every date, the 6-inch plots tracked close to the 8-inch plots and stayed above the 4-to-8-inch midpoint (shaded), showing that most of the depth benefit was reached by 6 inches.

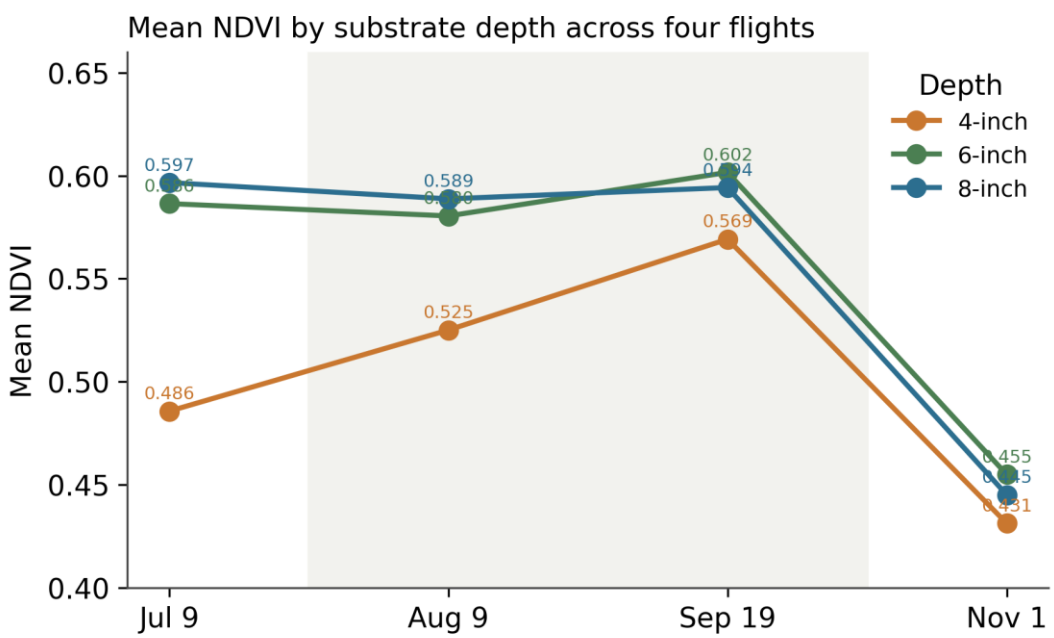

Figure 4.19. Mean NDVI by substrate depth across the four flight dates (all 72 plots). The 6-inch semi-intensive plots tracked close to the 8-inch plots and remained above the 4-to-8-inch midpoint (shaded) on all dates, indicating a non-linear depth response. 2025 APD-EGR data analysis by the author (2026).

NDVI-Canopeo Relationship and Seasonal Sensitivity

For the 16 sensor plots on the three matched flight dates, plot-level NDVI was positively and significantly correlated with drone Canopeo cover ($r = 0.618$, $p < 0.001$, $n = 48$), confirming that the two aerial metrics track the same underlying performance gradient (Figure 4.20). The two Canopeo methods themselves, however, did not agree in magnitude. As Figure 4.21 shows for two contrasting plots on July 9, 2025, the highest-performing plot (8″ P2) and a low-cover 4-inch plot (4″ P3), the ground-based iPhone method read 10 to 18 percentage points higher than the aerial drone method, with the larger gap on the denser plot, because the near-surface oblique view captures canopy structure that the nadir view does not.

These offsets are modest compared with the divergence that emerged when four measures of the same 16 plots were compared over the full season, which constitutes a notable methodological finding of this study (Figure 4.22). The four measures differ in what they quantify: the June and December ocular surveys record total vegetation cover by eye; the iPhone and drone Canopeo analyses record the fraction of visibly green pixels; and NDVI records canopy greenness through the near-infrared and red reflectance bands. These are fundamentally different quantities, so they report different magnitudes even for healthy vegetation. At peak season, ocular total cover was about 82%, whereas iPhone Canopeo green cover reached 36.1% and drone Canopeo 24.9% on the July 9 flight, because green-pixel methods count only the projected area of actively green tissue, not the full ground area a plant occupies.

As the warm-season grasses cured and turned straw-colored through the autumn, the measures diverged further into three distinct tiers. Ocular total cover remained essentially unchanged, easing only from about 82% in June to 78% in December, because the plants were still physically present as standing senesced material. The rescaled NDVI declined only modestly, from about 0.58 at its September peak to 0.44 in November. Both Canopeo green-cover metrics, by contrast, collapsed to under 5% of plot area, because they register only actively green tissue and read straw-colored grass as bare. In effect, the human eye still saw near-complete cover, NDVI still saw substantial greenness, and both Canopeo analyses recorded a near-total loss of green cover: three different answers for the same plots on the same dates.

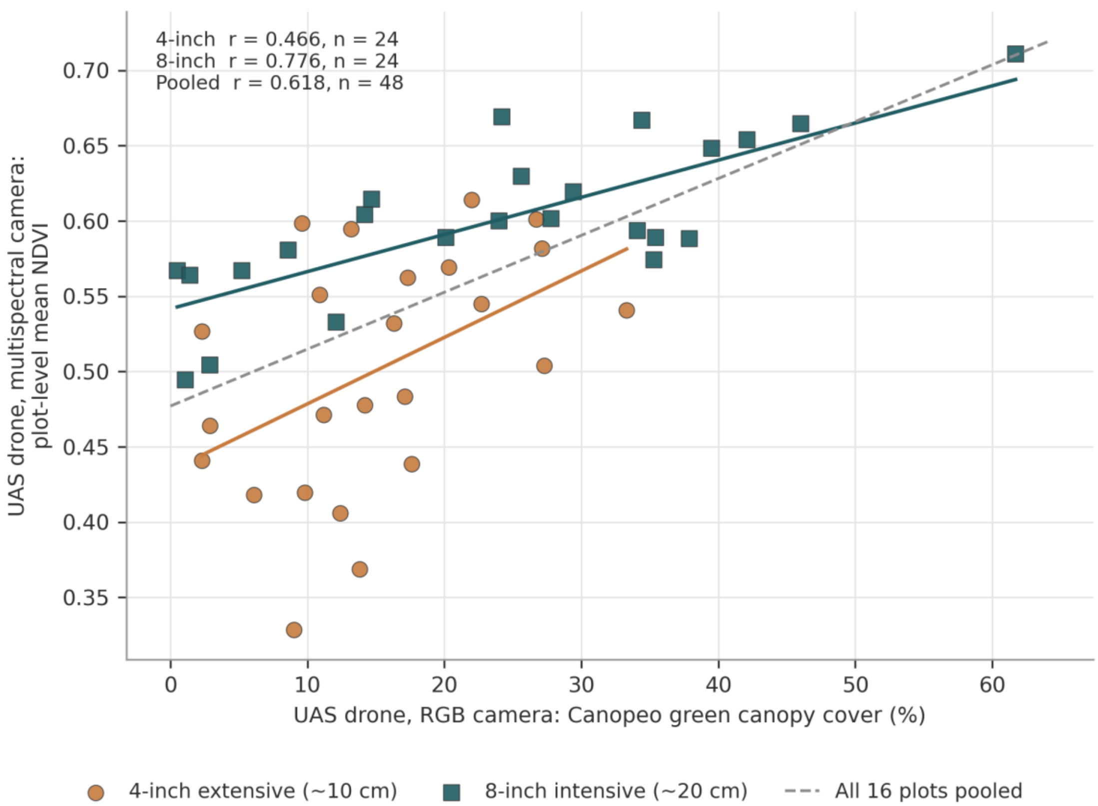

Figure 4.20. Plot-level mean NDVI against drone Canopeo green canopy cover for the 16 sensor plots on the three matched flight dates (n = 48).

Both measures derive from the same UAS flights, NDVI from the multispectral camera and cover from the RGB camera. RGB camera photos were analyzed by Canopeo to extract green canopy cover. Points are separated by substrate depth, with a least-squares fit for each depth and a pooled fit. The relationship is positive at both depths, tighter in the 8-inch intensive plots (~20 cm; $r = 0.776$) than in the 4-inch extensive plots (~10 cm; $r = 0.466$), and pooled $r = 0.618$ ($p < 0.001$). 2025 APD-EGR data analysis by the author (2026).

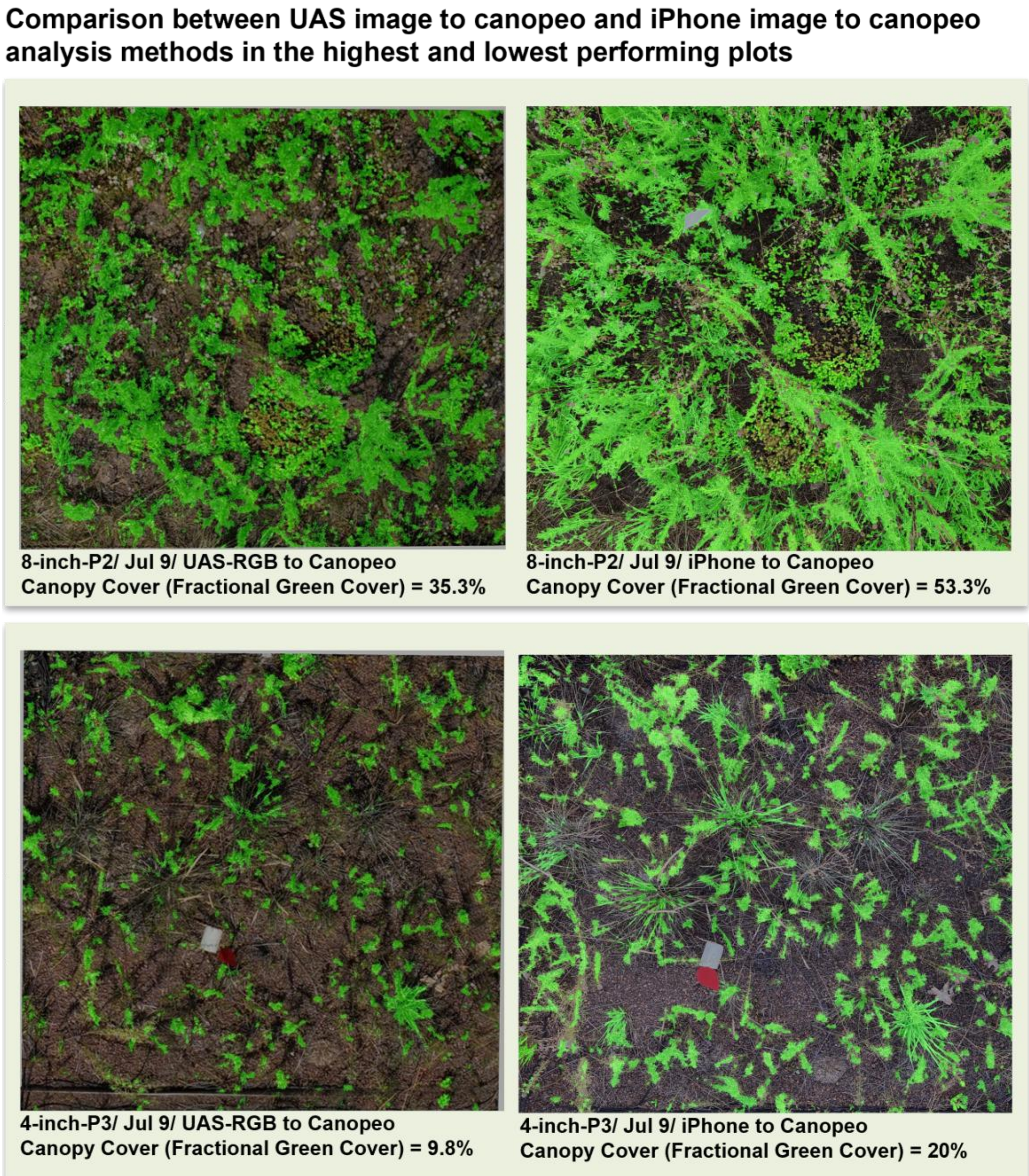

Figure 4.21: Comparison between iPhone to Canopeo versus UAS drone to Canopeo analysis.

On July 9, 2025, for the highest-performing plot (8″ P2) and a low-cover 4-inch plot (4″ P3), the ground-based method read 10 to 18 percentage points higher than the aerial method, with the larger gap on the denser plot. UAS imagery by Kaden Spencer; iPhone photographs by the author; both analyzed by the author in the Canopeo desktop application developed by Patrignani and Ochsner, 2015.

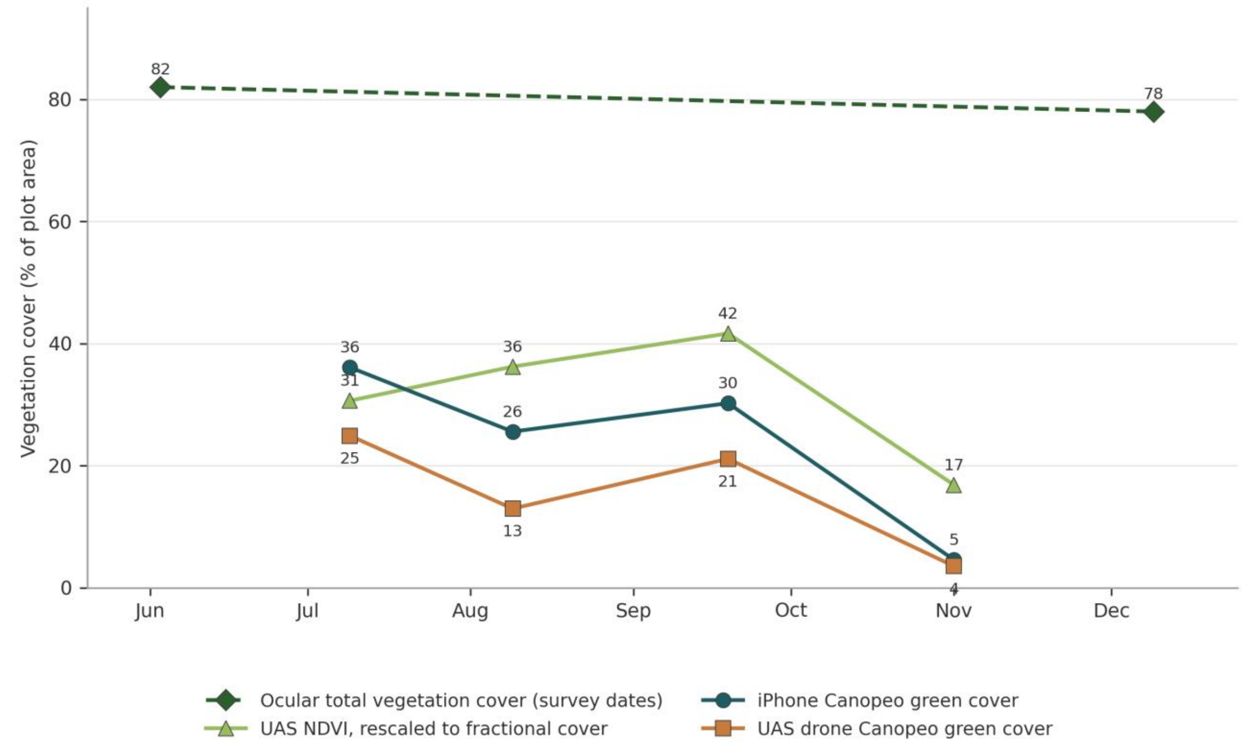

Figure 4.22: Comparison of four vegetation measures on the same 16 sensor plots.

To compare values in the same graph, NDVI was rescaled into fractional vegetation cover using $FVC = ((NDVI - NDVI_{soil}) / (NDVI_{veg} - NDVI_{soil}))^2$, following the squared scaled-NDVI relationship of Carlson and Ripley (1997), computed per plot and then averaged. The endmembers were set to $NDVI_{soil} = 0.20$, the conventional bare-soil threshold (Sobrino, Jiménez-Muñoz, and Paolini 2004), and $NDVI_{veg} = 0.80$, consistent with the value derived from spectral-library vegetation samples by Jiménez-Muñoz et al. (2009).
Ocular surveys by Lee Skabelund and the author; UAS imagery by Kaden Spencer; iPhone photographs and all analysis by the author (2026)

This separation among total physical cover, spectral vigor, and visible-green fraction is itself a finding of this study, and it defines a methodological question that the present dataset can characterize but not settle. The rescaling used in Figure 4.22 illustrates the difficulty. The soil and vegetation endmembers were assumed rather than measured, and no plot in this dataset reached either bound, so the vertical position of the rescaled NDVI series relative to the two Canopeo series should be read as approximate. Determining how these complementary measures should be reconciled and jointly interpreted for late-season vegetation on a mixed warm-season prairie green roof will require dedicated methodological work by specialists in green-fraction image analysis and in multispectral vegetation indices. Until then, the metrics are best interpreted together rather than interchangeably. The ocular survey captures total physical cover, the two Canopeo datasets capture the visible green-cover transition of senescence, and NDVI captures residual photosynthetic activity. No single metric fully describes the seasonal vegetation dynamics of this system, and any assessment of green roof vegetation performance in a warm-season prairie planting should state which of these three properties it is measuring.

Plant Community Composition and Functional Group Cover

Functional Group Cover Across Depth and Community

Figure 4.23 shows functional group cover by depth and plant community from the June 2025 survey. Figure 4.24 shows native grass cover with substrate depth in both communities. Functional group cover revealed three compositional gradients that illuminate the visibly green canopy cover and NDVI findings. First, native grass cover increased strongly and monotonically with substrate depth, rising in the East plots from 25.5% at 4 inches, to 52.2% at 6 inches, and 68.0% at 8 inches, providing the vegetative basis for the substrate depth effect on NDVI and canopy cover. Second, sedum cover was substantially higher in the West plots (31–33% at the deeper depths) than the East plots (11–20% at the same depths), and this plant type's horizontal mat-forming habit explains why West plots registered higher whole-plot cover in the drone imagery despite the East plots supporting more grass cover. Third, bare-soil cover decreased with greater depth, being highest in the 4-inch West plots (50.0%), consistent with their status as the poorest-performing group, and lowest in the 8-inch East plots (10.6%).

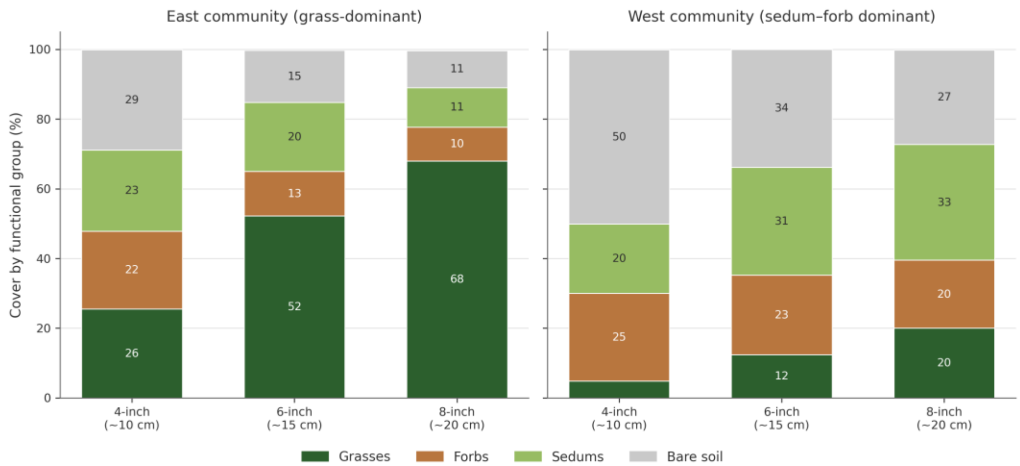

Figure 4.23: Functional group percentage cover by substrate depth and plant community (June 2025 survey). Native grass cover increases with depth in both communities; the West community carries markedly higher sedum and bare-soil cover. Ocular surveys by Lee Skabelund and the author; analysis by the author (2026).

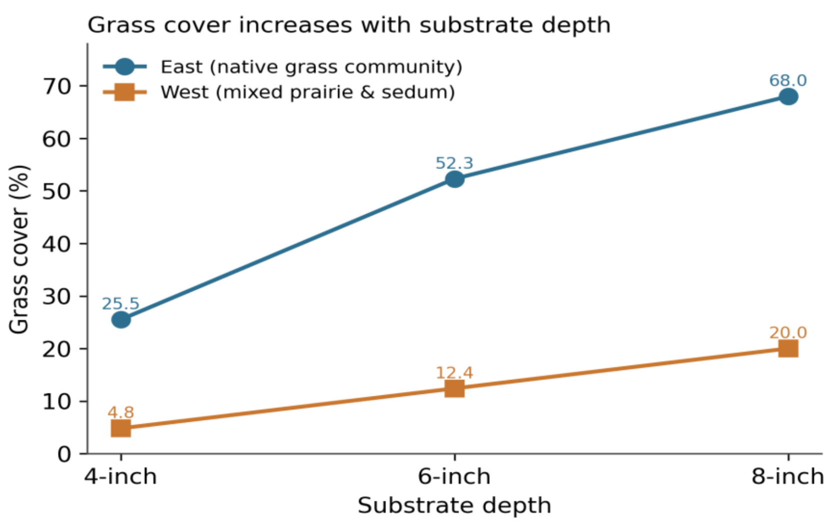

Figure 4.24: Native grass cover as a function of substrate depth for the two plant communities, from the June 2025 vegetation survey.

Native grass cover increased monotonically with depth in both communities. This depth-related increase in grass cover is consistent with, and likely contributes to, the substrate depth effects observed in the season-long NDVI and canopy cover datasets. Ocular surveys by L. Skabelund and the author; analysis by the author (2026).

The consistently lower vegetation cover and higher bare-soil fraction of the west-side plots warrant particular attention, because they reflect the management history of that side of the roof as much as the experimental treatments. The west side did not receive supplemental irrigation during the entire 2022 growing season, and many plants, particularly native grasses, died out as a result (Lee R. Skabelund, personal communication, 2025). This loss of native grasses prompted the reseeding of more than ten forb species together with June grass, primarily on the west side in the seasons that followed, which helps explain the west side's higher prairie forb diversity but markedly lower grass cover relative to the east. The single season without irrigation in 2022 appears to have been the primary driver of the reduced grass cover on the west side. Because this east–west difference reflects a legacy of prior management rather than the imposed treatments, it is reported descriptively and is not analyzed as an experimental factor; the statistical design tests only the three imposed treatments (depth, substrate, and irrigation).

Species Richness and Community Structure

The vegetation survey documented 32 vascular species across the 16 sensor plots over the two 2025 survey dates (7 grasses, 17 forbs, and 8 sedums), and Figure 4.25 shows the constancy of each, defined as the number of plots in which it occurred. The distribution reveals a clear core-and-satellite structure. Three species formed the community core, each occurring in all 16 plots: little bluestem (*Schizachyrium scoparium*), purple prairie clover (*Dalea purpurea*), and *Sedum sexangulare*. That a native grass, a native forb, and an introduced sedum were each equally ubiquitous indicates that both the deep-rooted prairie species and the shallow-rooted succulent groundcover established across the full range of plot conditions. Moss was present in 12 of 16 plots but, as a non-vascular bryophyte, is shown for reference only and excluded from the vascular count.

Below this core, a set of frequent species, Junegrass (14 plots), *Carex* sp. (12), sideoats grama (11), fleabane and small forbs (10 each), and *Sedum album* (8), occupied roughly half or more of the plots, while the remaining species formed a long tail occurring in only one to three plots each. Most forbs and five of the eight sedums fell into this low-constancy group. This concentration of diversity in locally distributed species, rather than in a few dominants, contributes to resilience: the loss of any single rare species has little effect on total cover, while the ubiquitous core maintains the roof's basic vegetative structure. Six further vascular species documented for the planting, including *Coreopsis palmata* and mountain mint, were not recorded in any of the 16 plots in 2025, so the 32 species shown represent the flora actually present in the 16 instrumented plots rather than all of the plant species associated with the EGR as a whole.

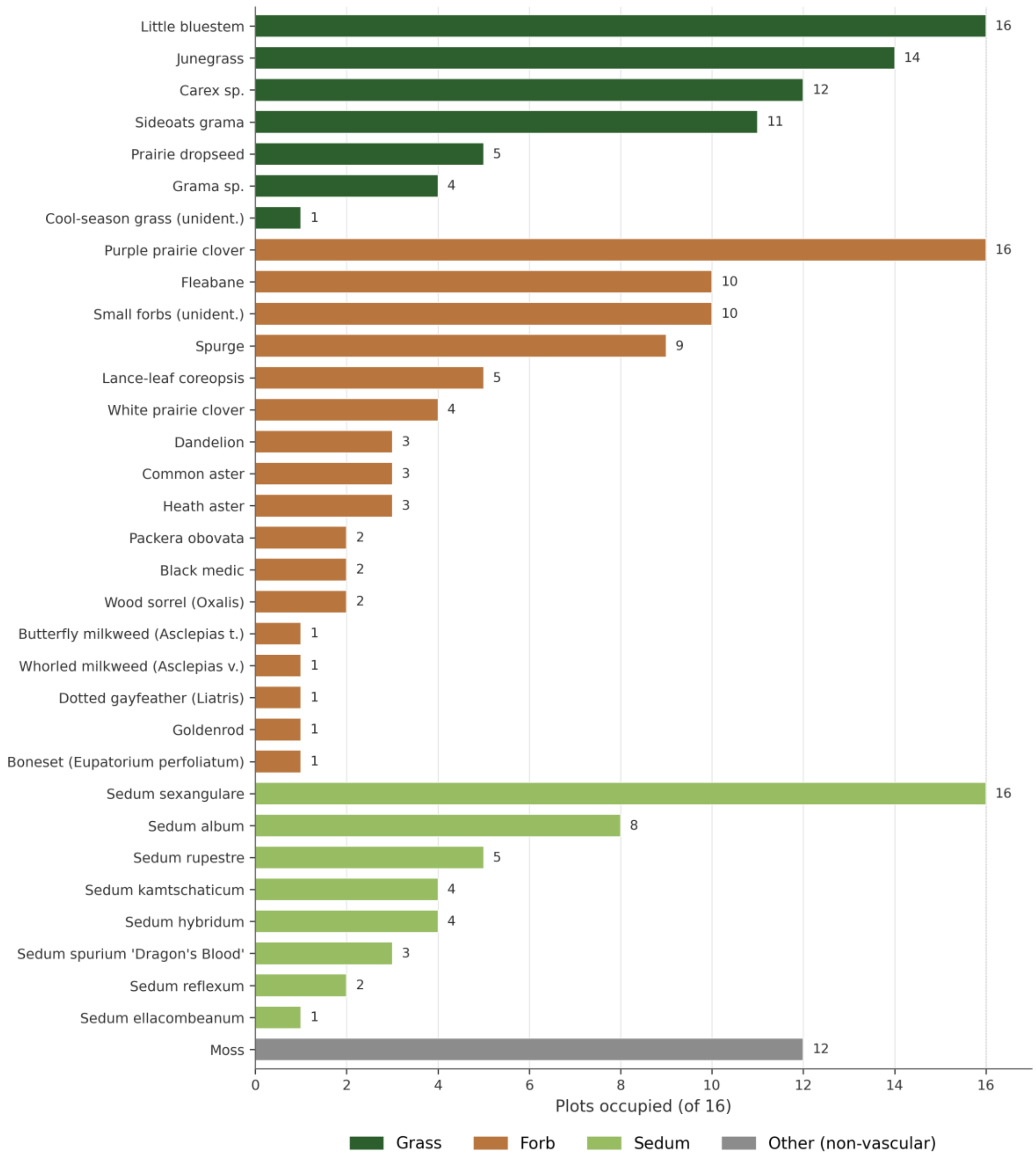

Figure 4.25: Constancy (plots occupied, of 16) for all vascular species recorded in the 2025 surveys.

Little bluestem, purple prairie clover, and *Sedum sexangulare* occurred in all 16 plots. Moss is shown for reference but excluded from the vascular count. Sedum IDs by L. R. Skabelund with botanist J. Taylor (April 2026). APD-EGR 2025 and 2026 field notes analyzed by author (2026).

Grass Height and Vertical Structure

Table 4.9 reports end-of-season little bluestem height by plot, measured November 19, 2025, alongside each plot's seasonal mean canopy cover for comparison. At the close of the growing season, on November 19, 2025, the height of the two dominant native warm-season grasses, little bluestem and sideoats grama, was measured in every plot to add a vertical structural dimension to the horizontal record provided by canopy cover. For each plot, the reported height is the mean of up to three sampled individuals of a given species. Because little bluestem was recorded in all 16 plots in both survey rounds, its height data support the same 2^3 factorial analysis applied to canopy cover, whereas sideoats grama occurred in fewer plots and is treated descriptively.

Table 4.9. End-of-season little bluestem height (cm) by plot, with sample count (n) and seasonal mean canopy cover for comparison.
Height is the mean of up to three sampled individuals per plot, measured November 19, 2025.

Plot	Depth	Substrate	Irrigation	Height (cm)	n	Cover (%)
4″ P1	4″	BuildEx	Less	75.8	3	42.8
4″ P2	4″	Rooflite	More	70.0	3	22.4
4″ P3	4″	Rooflite	Less	64.2	3	17.8
4″ P4	4″	BuildEx	More	96.3	3	35.5
4″ P5	4″	Rooflite	More	102.7	3	32.7
4″ P6	4″	BuildEx	Less	84.0	3	23.7
4″ P7	4″	BuildEx	More	100.8	3	47.0
4″ P8	4″	Rooflite	Less	87.7	3	21.1
8″ P1	8″	Rooflite	Less	84.3	3	15.9
8″ P2	8″	BuildEx	More	71.7	3	64.3
8″ P3	8″	BuildEx	Less	101.0	3	20.7
8″ P4	8″	Rooflite	More	73.2	3	45.0
8″ P5	8″	BuildEx	More	113.7	3	43.7
8″ P6	8″	BuildEx	Less	71.5	2	43.8
8″ P7	8″	Rooflite	More	106.0	3	30.7
8″ P8	8″	Rooflite	Less	73.2	3	44.8

Little bluestem end-of-season height ranged from 64.2 cm (4” P3) to 113.7 cm (8” P5), with a grand mean of 86.0 cm. The factorial analysis of height reproduced the direction of the irrigation and substrate effects seen for canopy cover but reordered their magnitudes and, most importantly, decoupled height from substrate depth. Irrigation produced the largest marginal effect, with more-irrigated plots averaging 91.8 cm against 80.2 cm for less-irrigated plots (a difference of 11.6 cm, $eta^2 = 0.150$), indicating that supplemental water increased both the horizontal and the vertical development of the canopy. Substrate type acted in the same direction as it did for cover, with BuildEx plots slightly taller than Rooflite plots (89.4 versus 82.6 cm). Substrate depth, by contrast, had almost no effect on height (8-inch 86.8 cm versus 4-inch 85.2 cm, a difference of only 1.6 cm, $eta^2 = 0.003$), even though depth was one of the stronger influences on canopy cover. The plant community block showed the largest raw contrast, with the native-grass-dominant East community averaging 93.6 cm against 78.4 cm in the West, consistent with the compositional differences. As with canopy cover, none of the treatment effects (neither substrate depth, substrate type, and irrigation individually nor their combinations) reached statistical significance at the 5% level, given the limited error degrees of freedom. The unexplained plot-to-plot variation was even larger for height than for cover, indicating strong variability among individual plots within the mature planting.

Figure 4.26 shows the marginal mean end-of-season little bluestem height by treatment factor. Irrigation produced the largest effect, with more-irrigated plots taller than less-irrigated plots, and substrate had a smaller effect in the same direction as its effect on cover. Substrate depth, one of the stronger influences on canopy cover, had almost no effect on height. The factors that governed how much the canopy covered were therefore not the same as those that governed how tall it grew.

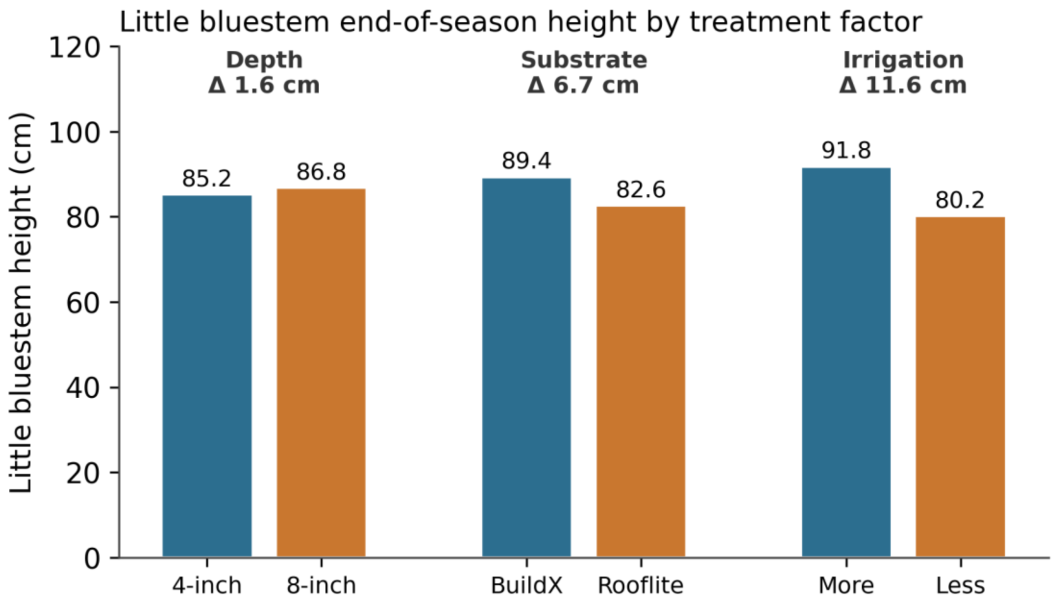

Figure 4.26. Marginal mean end-of-season little bluestem height by treatment factor. Irrigation produced the largest effect and substrate a smaller effect in the same direction as canopy cover, whereas substrate depth, a strong influence on cover, had almost no effect on height. APD-EGR data collected by L. Skabelund and the author in 2025. Analyzed by the author (2026).

Figure 4.27 plots little bluestem height against seasonal mean canopy cover for the 16 plots. The near-flat fit (r = −0.06) and the spread across all four quadrants confirm that the two measures varied independently. The most informative result from the height data is that canopy height and canopy cover are largely independent. Across the 16 plots, little bluestem height showed essentially no correlation with seasonal mean canopy cover (r = -0.06), and a weak inverse relationship with end-of-season cover (r = -0.46). The contrast is clearest at the extremes. The single highest-cover plot, 8” P2 at 64.3% seasonal cover, carried one of the shorter canopies at 71.7 cm, whereas the tallest plots, 8” P5 at 113.7 cm and 8” P7 at 106.0 cm, held only moderate cover of roughly 30 to 44%. Plots therefore tended to be either short and dense or tall and sparse, and a single top-down cover value cannot distinguish between the two structural types. This decoupling reinforces the measurement theme developed in Figure 4.22: because Canopeo registers only the horizontal fraction of green pixels, it does not capture the standing vertical structure that height records, so the two metrics describe complementary rather than redundant dimensions of canopy performance. For green roof evaluation this suggests that cover and height together give a fuller account of the structural and ecosystem-service functions of the vegetation, including rainfall interception, substrate shading, and habitat provision, than either measure alone.

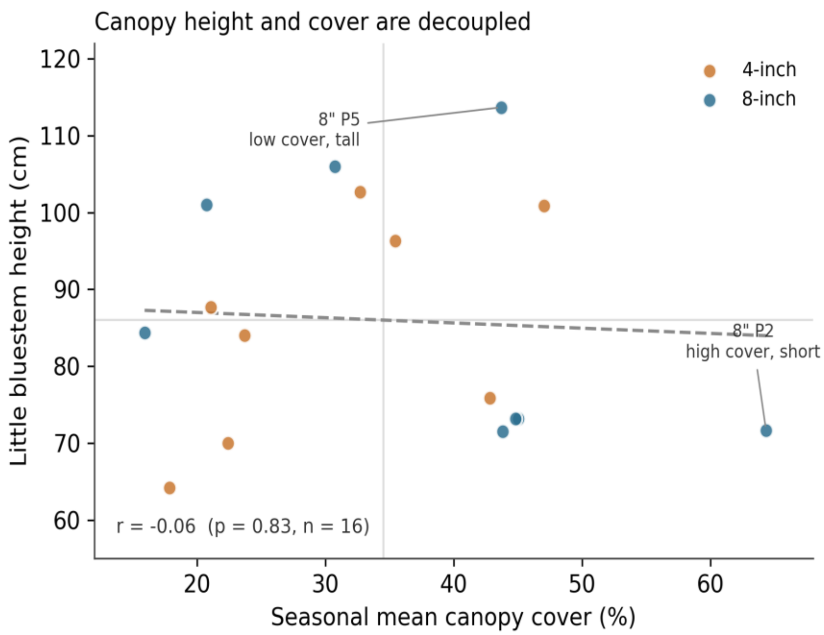

Figure 4.27. End-of-season little bluestem height plotted against seasonal mean canopy cover for all 16 study plots on the APD-EGR.

The near-flat fit (r = -0.06) and the spread of plots across all four quadrants defined by the grand means (grey lines) show that height and cover vary independently: 8" P5 is tall but low in cover, while 8" P2 is short but the highest in cover. APD-EGR data collected by L. Skabelund and the author in 2025. Analyzed by the author (2026).

Sideoats grama (*Bouteloua curtipendula*), the second dominant grass, followed a markedly different distribution and could not be analyzed within the factorial design. It was measured predominantly in the shallow plots, in six of the eight 4-inch plots, and only sparsely in the deep plots, in 8" P3 and 8" P4 alone. Where present it was substantially shorter than little bluestem, averaging approximately 42 cm. This shallow-substrate association is consistent with the vegetation survey, which recorded sideoats grama in nearly all 4-inch plots and in progressively fewer 8-inch plots. Two limitations should be stated explicitly. First, the vegetation survey recorded sideoats grama as present in plot 8" P6 in both the June and December rounds, yet no height sample was taken there, so this plot represents a measurement gap rather than a confirmed absence. Second, the survey distinguishes a separate, unidentified grama entry, recorded as “Grama sp.”, that co-occurs with sideoats grama in four plots (4” P2, 4” P4, 8” P2, and 8” P4) and may represent a second grama species, possibly blue grama, whose identity could not be confirmed from the available records and would require botanical verification. In the three of those plots where a sideoats height was recorded, the measured value could therefore include this unidentified taxon. For these reasons the sideoats grama results are treated as indicative of a shallow-substrate preference rather than as a definitive quantitative comparison.

Chapter Summary

The 2025 growing season data from the APD-EGR experiment provide a multidimensional picture of green roof canopy cover performance under the humid continental climate of the tallgrass prairie ecoregion. Seasonal mean visibly green canopy cover across the 16 sensor-instrumented plots ranged from 15.9% to 64.3%, with the two largest treatment differences attributable to substrate mix (11.4 percentage point marginal effect, BuildEx exceeding Rooflite) and irrigation frequency (11.3 percentage points), followed by substrate depth (8.3 percentage points).

Soil VWC monitoring confirmed that the moisture advantage operated primarily by preventing critically low moisture episodes: less-irrigated 4-inch plots reached mean minimum VWC values near 1.3%, well below the wilting-point zone, during the 39-day irrigation gap of July 2 through August 10. This gap was not a rainless drought, since 108 mm of rain fell during it, but it exposed the shallow substrates' inability to retain frequent light rainfall under high summer evaporative demand, and a plot-level analysis showed that survival through the resulting stress was governed chiefly by plant community rather than by water status.

Substrate temperature data showed that irrigation also provided secondary benefits through evaporative cooling, maintaining substrate temperatures about 0.8 to 1.2°C lower in more-irrigated plots. Across all 16 plots, substrate temperatures remained well below the surface temperatures reported for bare conventional roofing, indicating substantial thermal buffering regardless of treatment, though this study measured substrate rather than air temperature and so did not directly quantify urban heat island mitigation.

The 16-plot drone-Canopeo analysis and 72-plot NDVI analyses corroborated the depth and moisture patterns observed in the iPhone dataset. The NDVI data additionally revealed a non-linear depth response, in which 6-inch semi-intensive plots achieved vegetation health (NDVI) close to that of 8-inch plots.

The vegetation survey documented a diverse, predominantly native plant community comprising 32 vascular species across the 16 plots (7 grasses, 17 forbs, and 8 sedums), with markedly higher species richness in the West plots (mean 14.4 species) than in the East (mean 9.5 species). A comparison of the June and December surveys indicated a stable, persistent community that maintained its core species throughout the season. Species-level identification confirmed eight sedum species across the 16 plots, with somewhat greater per-plot sedum diversity in the West and in the less-irrigated plots (Skabelund and Taylor, field identification, April 2026; Skabelund and Islam field notes, June and December 2025).

End-of-season grass height added a structural dimension, showing that canopy height and cover are largely independent and that the BuildEx and irrigation advantages extend to vertical development. Formal ANOVA did not achieve statistical significance at $\alpha = 0.05$ owing to the limited error degrees of freedom ($df = 8$), but the effect sizes and their directional consistency across multiple response variables support the practical importance of the observed substrate, irrigation, and depth effects.

The Discussion and Conclusions chapter (Chapter 5) contextualizes these findings within the published green roof literature and develops management recommendations for green roof design in the tallgrass prairie ecoregion.

Chapter 5 - Discussion and Conclusion

Discussion of Results

This section interprets the 2025 results in relation to the research questions posed in Chapter 1. I address the two primary questions on canopy cover performance and measurement, followed by the three secondary questions on plant community, resilience, and canopy structure.

Treatment influences on canopy cover, moisture, and temperature

The first primary research question asked how substrate depth, substrate type, and irrigation frequency influence green canopy cover, volumetric water content, and substrate temperature. This question has two parallel answers from two different methods. The clearest result of the study is that substrate type and irrigation frequency were the two dominant controls on seasonal visibly green canopy cover, each producing a marginal effect of about 11 percentage points. In contrast, substrate depth was a secondary influence at about 8 percentage points. Together, these three factors accounted for roughly half of the plot-to-plot variation in green canopy cover, a point discussed further under limitations. The picture differed, however, for vegetation health as measured by NDVI, in the larger 72-plot dataset, which included the 6-inch semi-intensive plots. Substrate depth in this method emerged as a major and statistically significant factor. On the peak-season July flight, mean NDVI rose from 0.486 in the 4-inch plots to 0.586 in the 6-inch plots and 0.597 in the 8-inch plots, a 23% increase from shallowest to deepest, and the depth effect was highly significant (one-way ANOVA, $F = 22.3$, $p < 0.001$, $\eta^2 = 0.39$, $n = 72$).

This contrast likely reflects the difference in statistical power between the two datasets rather than a fundamental difference between the two indicators. Owing to sensor availability, soil moisture and temperature monitoring was installed in only 16 plots: eight extensive (4-inch) and eight intensive (8-inch), and the semi-intensive (6-inch) plots were not instrumented. This left only two replicates per treatment combination and eight error degrees of freedom, so that no effect reached significance in the canopy cover analysis despite substantial effect sizes. The UAS imagery, by contrast, covered all 72 plots, and the resulting NDVI analysis had far greater replication and statistical power, which allowed the substrate depth effect to reach significance. Increasing the number of replicates will provide further accuracy to reveal the answer to the first question.

The substrate result is the most instructive, because it inverts what the laboratory data alone would predict. Rooflite has a higher laboratory water retention capacity, greater porosity, and lower bulk density, properties generally considered favorable for green roof media. Yet the plots built on the denser BuildEx substrate held more water in place throughout the season and supported higher canopy cover. This divergence between laboratory-measured retention and in-place field performance is consistent with the pattern reported for the same roof by Alam et al. (2025) and with the broader observation that laboratory retention tests may not represent the water a substrate actually supplies to plants under rooftop conditions (Szota et al. 2017). The most probable explanation is that the coarser and more porous Rooflite drained more of each water input (rainfall or irrigation) before the vegetation could use it, whereas the finer and denser BuildEx retained a larger fraction within reach of plant roots. The practical implication is that substrate selection for minimally irrigated roofs should weigh in-situ moisture behavior over laboratory retention figures alone.

The moisture record clarifies how these treatments functioned. Irrigation and substrate did not increase cover by maintaining uniformly high moisture; they worked by preventing the shallow substrates from reaching critically low moisture during the season's most demanding period. The 4-inch less-irrigated plots fell to volumetric water content near or below 3% during the 39-day irrigation gap, well into the moisture-stress zone, while the 8-inch plots never approached those minima. Substrate depth, therefore, functioned less as a source of additional cover than as a buffer against extreme low-moisture episodes, a distinction that reframes depth from a growth factor into a risk-reduction factor under minimal irrigation.

Substrate temperature followed the same moisture logic rather than adding an independent effect. Deeper and more frequently irrigated plots ran modestly cooler, by roughly 0.8 to 1.2°C, through greater thermal mass and evaporative cooling. Because the driest plots were also the warmest, heat and moisture stress coincided in the same shallow, less-irrigated plots during the same August window. This coincidence, rather than temperature acting alone, is the most likely explanation for the disproportionate canopy cover decline in those plots. Substrate temperature and moisture cannot be separated in this dataset, since the same water that relieves drought stress also cools the substrate, so the two are best understood as compounding stressors rather than independent influences.

Comparison of ground-based and aerial measurement methods

The second primary research question asked how ground-based and aerial methods compare for assessing vegetation cover, and what each contributes. The three methods used here measured related but distinct properties, and their differences were themselves a finding. Ground-based iPhone Canopeo, captured close to the canopy, recorded systematically higher visibly green cover than UAS/drone Canopeo captured from altitude, because the near-surface view emphasizes the denser canopy interior while the nadir aerial view includes bare-substrate gaps between plants. Despite this difference, the two Canopeo measures agreed closely in relative plot rankings and treatment patterns, indicating that they track the same underlying performance gradient at different absolute scales.

The comparison with multispectral NDVI was more revealing. NDVI, which records photosynthetic vigor rather than the fraction of green pixels, diverged sharply from the Canopeo measures as the season progressed. As the warm-season grasses cured to straw color in autumn, both Canopeo metrics collapsed toward very low values because they register only actively green tissue, while NDVI declined only modestly and the ocular survey continued to record near-complete physical cover. The same plots on the same dates thus returned three different answers depending on what was being measured. The implication for green roof assessment is that these methods are complementary rather than interchangeable: ground-based Canopeo provides a high-frequency record of green-cover dynamics, NDVI captures residual photosynthetic activity that green-pixel methods miss, periodic aerial imagery provides standardized whole-plot coverage, while ocular surveys offer ground truthing. No single metric fully describes the vegetation, and the choice of method materially affects the conclusion drawn, particularly late in the season.

For future research at the APD-EGR, UAS imagery offers the most efficient monitoring approach from a management standpoint, because a single flight covers all 72 plots and simultaneously captures both multispectral imagery for NDVI and RGB imagery that can be processed with Canopeo. This yields two complementary indicators, vegetation health and green-cover fraction, from one data-collection effort. It should be noted that Canopeo consistently returned lower values for the drone imagery than for the ground-based iPhone imagery. The reason needs further exploration. Drone-derived cover values should therefore be interpreted on their own scale rather than compared directly with ground-based values. Concentrating data collection between May and October would best capture the influence of the experimental variables on vegetation, since by late October most of the vegetation loses greenness through normal seasonal senescence rather than treatment effects.

Functional cover composition and its relation to cover and NDVI

The first secondary research question concerned which species were present and how functional cover composition varied with depth and community. The ocular survey recorded 32 vascular species across the 16 plots, comprising 7 grasses, 17 forbs, and 8 sedums, distributed as diverse prairie-like communities rather than a uniform cover plot to plot. Functional composition varied systematically along two axes. Native grass cover rose strongly with substrate depth in both east and west plant communities, from a small fraction of cover on the shallow west beds to the dominant component on the deep east beds. This depth-driven increase in grass cover provides the vegetative basis for the substrate depth effects seen in both the canopy cover and the NDVI datasets, linking the compositional survey to the instrument records. Bare-soil cover ran opposite to grass, highest on the shallow west beds and lowest on the deep east beds, consistent with those groups' respective positions as the poorest and strongest performers for cover.

Plant community and canopy resilience

The second secondary research question asked how community composition affected resilience through peak-summer stress, and what the contrast between the two communities implies for species selection. This produced one of the study's more notable findings. During the August stress period, the grass-dominant east beds lost much of their visible green cover, whereas the sedum-and-forb west beds retained more of theirs, and this difference did not track substrate moisture: some grass-dominant plots lost cover despite adequate moisture, while sedum-and-forb plots held cover under comparable conditions. What governed resilience was therefore composition, not water status. The mechanism was the differing drought and heat response of the functional groups: the warm-season grasses browned under combined heat and moisture stress, while the drought-tolerant sedum component stayed green through the same conditions. The sedum component was present in both communities but was more visible on the west side in 2025, where fewer tall grasses shaded it. The implication for species selection on minimally irrigated prairie green roofs is that including a drought-tolerant, low-growing cover component alongside warm-season grasses provides a visual and functional cover reserve that persists when the grasses brown, buffering the roof's appearance and cover-dependent functions through the most stressful part of the season.

Canopy height and its relation to cover

The third secondary research question asked how end-of-season canopy height relates to horizontal cover, and what the vertical dimension adds. Little bluestem height was essentially uncorrelated with seasonal canopy cover, and if anything, weakly inverse: the highest-cover plots carried moderate-height canopies, while the tallest canopies held only moderate cover. Plots tended to be either short and dense or tall and sparse, so a single top-down cover value cannot distinguish between these structurally different canopies. Height and cover therefore describe complementary rather than redundant dimensions of performance. For green roof evaluation, this means that cover and height together give a fuller account of the vegetation's structural and functional roles, including rainfall interception, substrate shading, and habitat provision, than cover alone. The irrigation and substrate advantages that raised cover also extended to height, but substrate depth, a strong influence on cover, had almost no effect on height, reinforcing that the two measures respond differently to the treatments.

Conclusion and Practical Applications

Under minimal supplemental irrigation on a mature tallgrass-prairie green roof, canopy cover was governed primarily by substrate type and irrigation frequency, with substrate depth acting as a secondary buffer against extreme low-moisture episodes. The most consequential finding for practice is that the denser Build-X substrate, despite a lower laboratory field capacity (13.0% versus 15.0% for Rooflite; Table 3.5), supported about 11 percentage points more visibly green canopy cover than the more porous Rooflite in the field (40.2% versus 28.8%), which cautions against selecting green roof media on laboratory retention figures alone (Decker 2021). The 39-day irrigation gap showed that the limiting factor for shallow extensive beds was not the amount of rainfall but the substrate's inability to store frequent light rain under high summer evaporative demand, so that supplemental irrigation functions chiefly as a hedge against this storage limitation rather than as a substitute for absent rain.

Several practical applications follow. First, irrigation for extensive roofs in this climate should be triggered by measured substrate moisture rather than by recent rainfall, since the occurrence of rain proved a poor proxy for substrate moisture adequacy in shallow media. What mattered was the amount and timing of each event: in the shallow, less-irrigated beds, rain events below roughly 0.15 inch produced little or no measurable gain in substrate moisture, and events of about 0.25 inch or more were needed to recharge the profile meaningfully, though even those gains dissipated within a few days under high summer evaporative demand. This is why frequent light rain during the 39-day gap did not sustain the shallow plots. Second, where minimal irrigation is intended, greater substrate depth is valuable less for added growth than for its capacity to buffer against the low-moisture extremes that drive irreversible cover loss. Second, where minimal irrigation is intended, greater substrate depth is valuable less for added growth than for its capacity to buffer against the low-moisture extremes that drive irreversible cover loss. Third, planting design should pair warm-season grasses with a drought-tolerant, low-growing cover component such as hardy *Sedum spp.*, which sustains cover and its associated functions through the peak-stress period when the grasses brown. Finally, a mature, eight-year planting that regreened widely after severe transient stress is an encouraging signal for the resilience of established prairie green roofs under minimal management. These findings are offered as a contribution to the longer-term study of the APD-EGR and as provisional guidance for comparable continental climates, subject to limitations now discussed.

Limitations and Gaps

Several limitations constrain the strength of my thesis conclusions as well as the methods that produced them. The foremost limitation is statistical. The fully instrumented design provided only two replicates per treatment combination, leaving eight error degrees of freedom, so that no treatment effect reached statistical significance at the conventional $\alpha = 0.05$ level even though several of the effect sizes were sizeable. The results are therefore interpreted as directional evidence supported by effect size and consistency across multiple response variables, not as statistically confirmed effects. The two replicates in each cell corresponded to the east and west sides of the roof, which differ in pre-existing plant community; that community difference was described rather than modeled, and it is one source of the substantial plot-to-plot variation that the three treatments left unexplained.

The design was also observational in an important respect. Substrate depth, substrate type, and plant community were pre-existing features of the green roof as established between fall 2017 and summer 2018, not conditions randomly assigned for this experiment, and only irrigation frequency was imposed as an independent factor in 2025. The study therefore reflects the behavior of a single mature roof under one season's weather and irrigation protocols. Another limitation is the length of this study. Through a single growing season study, it is difficult to generalize green roof behavior.

Method limitations qualify several measures. Canopeo classifies cover from the fraction of green pixels, so it registers species-specific stress coloration, whereby some plants change color rather than die, as a loss of cover; this contributed to the divergence between Canopeo and both NDVI and ocular cover observations late in the season, and it means Canopeo values track visible greenness rather than total living cover. Because temperature and moisture were confounded across the plots, their separate contributions to cover decline could not be isolated.

Finally, in an in-situ mature green roof, multiple variables play together to influence vegetation health and behavior, including green canopy cover. Identifying the impact of each of them separately is quite challenging compared to the controlled green roof research approaches. However, the vegetation behavior in actual in-situ green roofs is also different from the controlled green roofs. Though there are methodological challenges in in-situ green roof research, this study prioritized understanding the in-situ green roof behavior.

New Questions and Future Directions

Each of the following questions arises directly from a limitation above and defines a direction for the continued study of the APD-EGR and comparable roofs.

Questions arising from the measurement limitations:

1. How do species-specific stress responses, in which plants change color rather than die, bias green-pixel cover estimates, and can a combined use of Canopeo, NDVI, and ocular survey be calibrated into a single reconciled measure of late-season cover for mixed warm-season prairie roofs?
2. How do substrate depth and treatment effects express in the ~6-inch semi-intensive beds, which the NDVI data indicated achieve vegetation health close to that of the 8-inch beds, and would extending sensor instrumentation and ground-based cover measurement to those beds confirm the non-linear depth response suggested by the aerial data?

Questions arising from the design and replication limitations:

3. Would the directional substrate, irrigation, and depth effects observed here reach statistical significance under a design with greater replication, and do they persist across multiple growing seasons with differing rainfall patterns?
4. Because the substrate paradox rests on in-situ moisture behavior rather than laboratory retention, what physical mechanism, such as the rate at which each substrate drains and releases water to roots, produces the field advantage of the denser BuildEx substrate?

Questions arising from the thermal and community limitations:

5. How does substrate thermal buffering translate into roof-surface and near-surface air temperature effects, which this study did not measure, and what is the actual contribution of a minimally irrigated prairie green roof in this climate to mitigate the urban heat island effect?
6. Which specific drought-tolerant species contributes most to covering resilience through peak stress, and what species combinations best sustain cover on minimally irrigated beds of each depth?

Questions arising from observation of other K-State green roofs:

1. How do the vegetation cover and green canopy cover respond to even more stress on APD-EGR given some other nearby green roofs at K-State are managed entirely without irrigation?
2. Why does a larger portion of grass disappear on the west side plots due to no irrigation in 2022, whereas nearby extensive plots have vegetation without any supplemental irrigation?
3. Can green roof plants in the Flint Hills ecoregion be trained over time to adapt to more stress by gradually reducing the irrigation frequency
4. How can an automated alert system be developed to notify when to irrigate?
5. How do substrate depth and substrate type impact stormwater retention on these experimental green roofs?

Answering these questions would extend the single-season baseline established here toward the long-term understanding of substrate, irrigation, and species selection needed to design and manage low-input green roofs in the tallgrass prairie ecoregion.

References

Abass, F., L. H. Ismail, I. A. Wahab, and A. A. Elgadi. 2020. "A Review of Green Roof: Definition, History, Evolution and Functions." IOP Conference Series: Materials Science and Engineering 713 (1): 012048. https://iopscience.iop.org/article/10.1088/1757-899X/713/1/012048

Akther, M., J. He, A. Chu, J. Huang, and B. van Duin. 2018. "A Review of Green Roof Applications for Managing Urban Stormwater in Different Climatic Zones." Sustainability 10 (8): 2864. https://doi.org/10.3390/su10082864.

Alam, M. M. L. 2022. "Climate Change Mitigation Potential of Green Roofs: Exploring Urban Heat Island Indicators and a Green Roof's Capacity to Sequester Carbon in the Flint Hills Ecoregion." PhD Dissertation, Kansas State University. https://krex.k-state.edu/items/5d4f9c9a-ee32-4d66-9c88-4148c0ebc966

Alam, M. M. L., L. R. Skabelund, C. W. Rice, J. S. Lin, and J. Ha. 2025. "How Effective Are Green Roofs as Building Carbon Sinks? Empirical Evidence Linking Substrate, Depth, and Vegetation Dynamics in the U.S. Great Plains." Journal of Environmental Management 396: 128117. https://doi.org/10.1016/j.jenvman.2025.128117

Alam, M. M. L., L. R. Skabelund, M. D. Gibson, and J. Lee. 2026. "Assessing Seasonal Thermal Performance of a Mid-Continental USA Green Roof System under Real-World Conditions: Moisture-Driven Thermodynamic Implications for Building Energy Performance." Energy and Buildings 364: 117607. 10.1016/j.enbuild.2026.117607

Alam, M. M. L., L. Skabelund, J. Lin, and J. Ha. 2024. "Investigating the Climate Mitigation Performance of a Green Roof System in the Flint Hills Ecoregion, USA." Journal of Living Architecture 11 (1). https://doi.org/10.46534/jliv.2023.11.01.001

Allen, R. G., L. S. Pereira, D. Raes, and M. Smith. 1998. Crop Evapotranspiration: Guidelines for Computing Crop Water Requirements. FAO Irrigation and Drainage Paper 56. Rome: Food and Agriculture Organization of the United Nations. https://www.fao.org/4/X0490E/x0490e00.htm

ASTM International. 2019. ASTM E2399/E2399M-19: Standard Test Method for Maximum Media Density for Dead Load Analysis of Vegetative (Green) Roof Systems. West Conshohocken, PA: ASTM International. https://doi.org/10.1520/E2399_E2399M-19.

Bates, A. J., J. P. Sadler, and R. Mackay. 2013. "Vegetation Development over Four Years on Two Green Roofs in the UK." Urban Forestry & Urban Greening 12 (1): 98-108. https://doi.org/10.1016/j.ufug.2012.12.003

Berardi, U., A. GhaffarianHoseini, and A. GhaffarianHoseini. 2014. "State-of-the-Art Analysis of the Environmental Benefits of Green Roofs." Applied Energy 115: 411-428. https://doi.org/10.1016/j.apenergy.2013.10.047.

Bergstedt, J., L. Westerberg, and P. Milberg. 2009. "In the Eye of the Beholder: Bias and Stochastic Variation in Cover Estimates." Plant Ecology 204 (2): 271-283. https://doi.org/10.1007/s11258-009-9590-7.

Bevilacqua, P., D. Mazzeo, R. Bruno, and N. Arcuri. 2017. "Surface Temperature Analysis of an Extensive Green Roof for the Mitigation of Urban Heat Island in Southern Mediterranean Climate." Energy and Buildings 150: 318-327. 10.1016/j.enbuild.2017.05.081

Bevilacqua, P., J. Coma, G. Pérez, C. Chocarro, A. Juárez, C. Solé, and L. F. Cabeza. 2015. "Plant Cover and Floristic Composition Effect on Thermal Behaviour of Extensive Green Roofs." Building and Environment 92: 305-316. https://doi.org/10.1016/j.buildenv.2015.04.026

Butler, C., E. Butler, and C. M. Orians. 2012. "Native Plant Enthusiasm Reaches New Heights: Perceptions, Evidence, and the Future of Green Roofs." Urban Forestry & Urban Greening 11 (1): 1-10. https://doi.org/10.1016/j.ufug.2011.11.002.

Cantor, S. L. 2008. Green Roofs in Sustainable Landscape Design. W. W. Norton. https://wwnorton.com/books/Green-Roofs-in-Sustainable-Landscape-Design/

Cao, R., and J. S. MacIvor. 2024. "Automation of Green Roof Plant Cover Measurements Using Machine Learning and a Comparison of Digital and Thermal Imaging Techniques." Applied Vegetation Science 27 (2): e12790. https://doi.org/10.1111/avsc.12790.

Carlson, T. N., and D. A. Ripley. 1997. "On the Relation between NDVI, Fractional Vegetation Cover, and Leaf Area Index." Remote Sensing of Environment 62 (3): 241-252. https://doi.org/10.1016/S0034-4257(97)00104-1.

Cascone, S. 2019a. "Green Roof Design: State of the Art on Technology and Materials." Sustainability 11 (11): 3020. https://doi.org/10.3390/su11113020.

Cascone, S., J. Coma, A. Gagliano, and G. Pérez. 2019b. "The Evapotranspiration Process in Green Roofs: A Review." Building and Environment 147: 337-355. https://doi.org/10.1016/j.buildenv.2018.10.024.

Chen, C.-F. 2013. "Performance Evaluation and Development Strategies for Green Roofs in Taiwan: A Review." Ecological Engineering 52: 51-58. https://doi.org/10.1016/j.ecoleng.2012.12.083

Conn, R., J. Werdin, J. P. Rayner, and C. Farrell. 2020. "Green Roof Substrate Physical Properties Differ between Standard Laboratory Tests Due to Differences in Compaction." Journal of Environmental Management 261: 110206. https://doi.org/10.1016/j.jenvman.2020.110206.

Daubenmire, R. F. 1959. "A Canopy-Coverage Method of Vegetational Analysis." Northwest Science 33: 43-64.

De Stefano, A., B. Fowers, and B. A. Mealor. 2021. “Comparison of Visual Estimation and LinePoint Intercept Vegetation Survey Methods on Annual Grass–Invaded Rangelands of Wyoming.” Invasive Plant Science and Management 14 (4): 240-252. https://doi.org/10.1017/inp.2021.36.

Decker, A. B. 2021. “An Experimental Design to Assess Soil-Plant-Water Relations on a Kansas Green Roof.” PhD Dissertation, Kansas State University. https://krex.k-state.edu/items/1c9e06c0-bd56-4e43-9714-04aa861590ef

Decker, A., L. R. Skabelund, Y. Gao, and P. Shrestha. 2022. “Investigating Extensive Green Roof Native Plant Growth over a Four-Year Period in the Central Great Plains.” Paper presented at the Cities Alive Green Roof and Wall Conference, Philadelphia, PA.

DeNardo, J. C., A. R. Jarrett, H. B. Manbeck, D. J. Beattie, and R. D. Berghage. 2005. “Stormwater Mitigation and Surface Temperature Reduction by Green Roofs.” Transactions of the ASAE 48 (4): 1491-1496. https://doi.org/10.13031/2013.19181

Dunnett, N. 2006. “Greening Rooftops for Biodiversity: Reconciling Aesthetics with Ecology.” In Cities Alive Conference Proceedings, 1-12. https://www.osti.gov/etdeweb/biblio/20861946

Dunnett, N., A. Nagase, R. Booth, and P. Grime. 2008. “Influence of Vegetation Composition on Runoff in Two Simulated Green Roof Experiments.” Urban Ecosystems 11 (4): 385-398. https://doi.org/10.1007/s11252-008-0064-9

Dunnett, N., and A. Nolan. 2004. “The Effect of Substrate Depth and Supplementary Watering on the Growth of Nine Herbaceous Perennials in a Semi-Extensive Green Roof.” Acta Horticulturae 643: 305-309. https://doi.org/10.17660/ActaHortic.2004.643.40

Dunnett, N., and N. Kingsbury. 2008. Planting Green Roofs and Living Walls. 2nd Edition. Timber Press.

Durhman, A. K., D. B. Rowe, and C. L. Rugh. 2007. “Effect of Substrate Depth on Initial Growth, Coverage, and Survival of 25 Succulent Green Roof Plant Taxa.” HortScience 42 (3): 588-595. https://doi.org/10.21273/HORTSCI.42.3.588.

Dvorak, B. 2015. “Eco-Regional Green Roof Case Studies.” In Green Roof Ecosystems, edited by R. K. Sutton, 391-421. Springer. https://link.springer.com/chapter/10.1007/978-3-319-14983-7_16

Dvorak, B., and A. Volder. 2010. “Green Roof Vegetation for North American Ecoregions: A Literature Review.” Landscape and Urban Planning 96 (4): 197-213. https://doi.org/10.1016/j.landurbplan.2010.04.009.

Dvorak, B., and L. R. Skabelund. 2021. “Green Roofs in Tallgrass Prairie Ecoregions.” In Ecoregional Green Roofs: Theory and Application in the Western USA and Canada, edited by B. Dvorak, 1st ed., 83-139. Springer. https://link.springer.com/chapter/10.1007/978-3-030-58395-8_3

Farrell, C., X. Q. Ang, and J. P. Rayner. 2013. "Water-Retention Additives Increase Plant Available Water in Green Roof Substrates." Ecological Engineering 52: 112-118. https://doi.org/10.1016/j.ecoleng.2012.12.098.

Francis, R. A., and J. Lorimer. 2011. "Urban Reconciliation Ecology: The Potential of Living Roofs and Walls." Journal of Environmental Management 92 (6): 1429-1437. https://doi.org/10.1016/j.jenvman.2011.01.012

Garadnai, and M. Kertész. 2017. "Comparing the Accuracy of Three Non-Destructive Methods in Estimating Aboveground Plant Biomass." Community Ecology 18 (1): 56-62. https://doi.org/10.1556/168.2017.18.1.7.

Getter, K. L., and D. B. Rowe. 2006. "The Role of Extensive Green Roofs in Sustainable Development." HortScience 41 (5): 1276-1285. https://www.plantsatwork.org.uk/images/PDFs/23279834_-_HortScience_The_Role_of_Extensive_Green_Roofs_in_Sustainable_Development.pdf

Getter, K. L., D. B. Rowe, J. A. Andresen, and I. S. Wichman. 2011. "Seasonal Heat Flux Properties of an Extensive Green Roof in a Midwestern U.S. Climate." Energy and Buildings 43 (12): 3548-3557. https://doi.org/10.1016/j.enbuild.2011.09.018

Gillman, W., R. Jenkins, J. Owen, and J. Schmidt. 2026. "Soil, Water, and Plant Relations in Green Roof Management." NRES Capstone Project, Natural Resources and Environmental Sciences Program, Kansas State University, Manhattan, KS.

Hatton, T. J., N. E. West, and P. S. Johnson. 1986. "Relationships of the Error Associated with Ocular Estimation and Actual Total Cover." J. of Range Management 39 (1): 91-92. https://doi.org/10.2307/3899697

Herman, R. 2003. "Green Roofs in Germany: Yesterday, Today and Tomorrow." First North American Green Roof Conference. Chicago, IL. https://www.osti.gov/etdeweb/biblio/20398172

Hoffman, L., and W. McDonough. 2005. Green Roofs: Ecological Design and Construction. Schiffer Publishing.

Iwata, T., R. Shimoda, T. Takahashi, and K. Umeki. 2025. "Evaluating Native Grassland Species for Application in Extensive Green Roofs in Japan." Environments 12 (10): 345. https://doi.org/10.3390/environments12100345

Jim, C. Y., and S. W. Tsang. 2011. "Biophysical Properties and Thermal Performance of an Intensive Green Roof." Building and Environment 46 (6): 1263-1274. https://doi.org/10.1016/j.buildenv.2010.12.013

Jiménez-Muñoz, J. C., J. A. Sobrino, A. Plaza, L. Guanter, J. Moreno, and P. Martínez. 2009. "Comparison between Fractional Vegetation Cover Retrievals from Vegetation Indices and Spectral Mixture Analysis: Case Study of PROBA/CHRIS Data over an Agricultural Area." *Sensors* 9 (2): 768-793. https://doi.org/10.3390/s90200768.

Karachaliou, P., M. Santamouris, and H. Pangalou. 2016. "Experimental and Numerical Analysis of the Energy Performance of a Large Scale Intensive Green Roof System Installed on an Office Building in Athens." Energy and Buildings 114: 256-264. https://doi.org/10.1016/j.enbuild.2015.04.055

Kazemi, F., and R. Mohorko. 2017. "Review on the Roles and Effects of Growing Media on Plant Performance in Green Roofs in World Climates." Urban Forestry & Urban Greening 23: 13-26. https://doi.org/10.1016/j.ufug.2017.02.006

Kirkham, M. B. 2014. Principles of Soil and Plant Water Relations. 2nd ed. Amsterdam: Academic Press.

Köhler, K. K. Y. Liu, and B. Rowe. 2007. "Green Roofs as Urban Ecosystems: Ecological Structures, Functions, and Services." BioScience 57 (10): 823-833. https://doi.org/10.1641/B571005.

Kotsiris, G., P. A. Nektarios, and A. T. Paraskevopoulou. 2012. "Lavandula angustifolia Growth and Physiology Is Affected by Substrate Type and Depth When Grown under Mediterranean Semi-Intensive Green Roof Conditions." HortScience 47 (2): 311-317. DOI: 10.21273/HORTSCI.47.2.311

Ksiazek-Mikenas, K., V. B. Chaudhary, D. J. Larkin, and K. A. Skogen. 2021. "A Habitat Analog Approach Establishes Native Plant Communities on Green Roofs." Ecosphere 12 (9): e03754. https://doi.org/10.1002/ecs2.3754.

Lee, L. S. H., and C. Y. Jim. 2018. "Thermal-Cooling Performance of Subtropical Green Roof with Deep Substrate and Woodland Vegetation." Ecological Engineering 119: 8-18. https://doi.org/10.1016/j.ecoleng.2018.05.014.

Leotta, L., S. Toscano, and D. Romano. 2023. "Which Plant Species for Green Roofs in the Mediterranean Environment?" Plants 12 (23): 3985. https://doi.org/10.3390/plants12233985.

Li, W. C., and K. K. A. Yeung. 2014. "A Comprehensive Study of Green Roof Performance from Environmental Perspective." International Journal of Sustainable Built Environment 3 (1): 127-134. https://doi.org/10.1016/j.ijsbe.2014.05.001

Liu, J., P. Shrestha, L. R. Skabelund, T. Todd, A. Decker, and M. B. Kirkham. 2019. "Growth of Prairie Plants and Sedums in Different Substrates on an Experimental Green Roof in Mid-Continental USA." Science of the Total Environment 697: 134089. https://doi.org/10.1016/j.scitotenv.2019.134089

Liu, K., and J. Minor. 2005. "Performance Evaluation of an Extensive Green Roof." In Greening Rooftops for Sustainable Communities, 1-11. Washington, DC, May 5-6, 2005. https://nrc-publications.canada.ca/eng/view/object/?id=e10a2c46-5c45-4a9e-8625-d7b0ea46e847

Lönnqvist, J., G. T. Blecken, and M. Viklander. 2021. "Vegetation Cover and Plant Diversity on Cold Climate Green Roofs." Journal of Urban Ecology 7 (1): juaa035. https://doi.org/10.1093/jue/juaa035

Lu, J., J. G. Yuan, J. Z. Yang, A. K. Chen, and Z. Y. Yang. 2015. "Effect of Substrate Depth on Initial Growth and Drought Tolerance of Sedum lineare in Extensive Green Roof System." Ecological Engineering 74: 408-414. https://doi.org/10.1016/j.ecoleng.2014.11.018.

Lundholm, J. T., and E. A. Walker. 2018. "Evaluating the Habitat-Template Approach Applied to Green Roofs." Urban Naturalist, Special Issue No. 1: 39-51. https://www.eaglehill.us/URNAonline/articles/URNA-sp1/13-Lundholm.shtml

Lundholm, J. T., J. S. MacIvor, Z. MacDougall, and M. Ranalli. 2010. "Plant Species and Functional Group Combinations Affect Green Roof Ecosystem Functions." PLoS ONE 5 (3): e9677. https://doi.org/10.1371/journal.pone.0009677.

Lykhovyd, P., R. Vozhehova, S. Lavrenko, and N. Lavrenko. 2022. "The Study on the Relationship between Normalized Difference Vegetation Index and Fractional Green Canopy Cover in Five Selected Crops." The Scientific World Journal 2022: 8479424. https://doi.org/10.1155/2022/8479424

MacIvor, J. S., and J. Lundholm. 2011. "Performance Evaluation of Native Plants Suited to Extensive Green Roof Conditions in a Maritime Climate." Ecological Engineering 37 (3): 407-417. https://doi.org/10.1016/j.ecoleng.2010.10.004

- MacIvor, J. S., L. Margolis, C. L. Puncher, and B. J. C. Matthews. 2013. "Decoupling Factors Affecting Plant Diversity and Cover on Extensive Green Roofs." Journal of Environmental Management 130: 297-305. DOI: 10.1016/j.jenvman.2013.09.014

Marouli, C., P. Savvidou, M. Koutsokali, P. Papadopoulou, A. Misseyanni, G. Tsiliki, and D. Georgas. 2022. "Plant Growth on a Mediterranean Green Roof: A Pilot Study on Influence of Substrate Depth, Substrate Composition, and Type of Green Roof." Frontiers in Sustainable Cities 3: 796441. https://doi.org/10.3389/frsc.2021.796441

Morrison, L. W. 2016. "Observer Error in Vegetation Surveys: A Review." Journal of Plant Ecology 9 (4): 367-379. https://doi.org/10.1093/jpe/rtv077.

Muratet, A., M. Barra, L. Hardion, and F. Chiron. 2024. "Origins and Drivers of Roof Plant Assemblages: Designing Green Roofs for Biodiversity Conservation." Urban Forestry & Urban Greening 94: 128247. https://doi.org/10.1016/j.ufug.2024.128247

Nagase, A., and N. Dunnett. 2010. "Drought Tolerance in Different Vegetation Types for Extensive Green Roofs: Effects of Watering and Diversity." Landscape and Urban Planning 97 (4): 318-327. https://doi.org/10.1016/j.landurbplan.2010.07.005

Nawaz, R., A. McDonald, and S. Postoyko. 2015. “Hydrological Performance of a Full-Scale Extensive Green Roof Located in a Temperate Climate.” Ecological Engineering 82: 66-80. https://doi.org/10.1016/j.ecoleng.2014.11.061.

Ndayambaje, P., J. S. MacIvor, and M. W. Cadotte. 2024. “Plant Diversity on Green Roofs: A Review of the Ecological Benefits, Challenges, and Best Management Practices.” Nature-Based Solutions 6: 100162. https://doi.org/10.1016/j.nbsj.2024.100162.

Nektarios, P. A. 2018. “Green Roofs: Irrigation and Maintenance.” In Nature Based Strategies for Urban and Building Sustainability, 75–84. Butterworth-Heinemann. https://doi.org/10.1016/B978-0-12-812150-4.00007-0

Nektarios, P. A., I. Amountzias, I. Kokkinou, and N. Ntoulas. 2011. “Green Roof Substrate Type and Depth Affect the Growth of the Native Species Dianthus fruticosus under Reduced Irrigation Regimens.” HortScience 46 (8): 1208-1216. https://doi.org/10.21273/HORTSCI.46.8.1208.

Oberndorfer, E., J. Lundholm, B. Bass, R. R. Coffman, H. Doshi, N. Dunnett, S. Gaffin, M. Köhler, K. K. Y. Liu, and B. Rowe. 2007. "Green Roofs as Urban Ecosystems: Ecological Structures, Functions, and Services." *BioScience* 57 (10): 823–833. https://doi.org/10.1641/B571005.

Ondoño, S., J. J. Martínez-Sánchez, and J. L. Moreno. 2016. “The Composition and Depth of Green Roof Substrates Affect the Growth of Silene vulgaris and Lagurus ovatus Species and the C and N Sequestration under Two Irrigation Conditions.” Journal of Environmental Management 166: 330-340. https://doi.org/10.1016/j.jenvman.2015.08.045.

Osmundson, T. H. 1999. Roof Gardens: History, Design, and Construction. W. W. Norton.

Papafotiou, M., N. Pergialioti, L. Tassoula, I. Massas, and G. Kargas. 2013. “Growth of Native Aromatic Xerophytes in an Extensive Mediterranean Green Roof as Affected by Substrate Type and Depth and Irrigation Frequency.” HortScience 48 (10): 1327-1333. https://doi.org/10.21273/HORTSCI.48.10.1327.

Patrignani, A., and T. E. Ochsner. 2015. “Canopeo: A Powerful New Tool for Measuring Fractional Green Canopy Cover.” Agronomy Journal 107 (6): 2312-2320. https://doi.org/10.2134/agronj15.0150

Peck, S. W. 2008. Award-Winning Green Roof Designs: Green Roofs for Healthy Cities. Schiffer.

Pérez, G., C. Chocarro, A. Juárez-Escario, and J. Coma. 2020. “Evaluation of the Development of Five Sedum Species on Extensive Green Roofs in a Continental Mediterranean Climate.” Urban Forestry & Urban Greening 48: 126566. https://doi.org/10.1016/j.ufug.2019.126566.

Pettorelli, N., J. O. Vik, A. Mysterud, J.-M. Gaillard, C. J. Tucker, and N. C. Stenseth. 2005. "Using the Satellite-Derived NDVI to Assess Ecological Responses to Environmental Change." Trends in Ecology & Evolution 20 (9): 503-510. https://doi.org/10.1016/j.tree.2005.05.011.

Rivière, L., S. Meeûs, and G. Mahy. 2024. "Stress Tolerant Species Are Keys to Plant Communities Success on Extensive Green Roof." Urban Ecosystems 27: 591-600. https://doi.org/10.1007/s11252-023-01479-w.

Rodrigues, M., P. Arsénio, and T. A. do Paço. 2024. "The Use of Drought-Tolerant Vegetation on Green Roofs: A Method for the Digital Photographic Monitoring of Its Development." Horticulturae 10 (1): 106. https://doi.org/10.3390/horticulturae10010106.

Rouse, J. W., R. H. Haas, J. A. Schell, and D. W. Deering. 1974. "Monitoring Vegetation Systems in the Great Plains with ERTS." In Proceedings of the Third Earth Resources Technology Satellite-1 Symposium, vol. 1, 309–317. NASA SP-351. Washington, DC: NASA. https://ntrs.nasa.gov/citations/19740022614

Rowe, D. B., M. R. Kolp, S. E. Greer, and K. L. Getter. 2014. "Comparison of Irrigation Efficiency and Plant Health of Overhead, Drip, and Sub-Irrigation for Extensive Green Roofs." Ecological Engineering 64: 306-313. https://doi.org/10.1016/j.ecoleng.2013.12.052

Santamouris, M. 2014. "Cooling the Cities – A Review of Reflective and Green Roof Mitigation Technologies to Fight Heat Island and Improve Comfort in Urban Environments." Solar Energy 103: 682-703. https://doi.org/10.1016/j.solener.2012.07.003.

Schramm, P. 1990. "Prairie Restoration: A Twenty-Five Year Perspective on Establishment and Management." In Proceedings of the Twelfth North American Prairie Conference, 12:169–177. University of Northern Iowa.

Schroll, E., J. G. Lambrinos, and D. Sandrock. 2011. "An Evaluation of Plant Selections and Irrigation Requirements for Extensive Green Roofs in the Pacific Northwestern United States." HortTechnology 21 (3): 314-322. DOI: 10.21273/HORTTECH.21.3.314

Shafique, M., R. Kim, and M. Rafiq. 2018. "Green Roof Benefits, Opportunities and Challenges: A Review." Renewable and Sustainable Energy Reviews 90: 757-773. https://doi.org/10.1016/j.rser.2018.04.006

Shrestha, P. 2019. "Assessment of First-Year Survival, Growth, and Physiological Performance of Seven Species of Graminoids within Two Substrate Types on a Green Roof in the Flint Hills Ecoregion." Master's Thesis, Kansas State University. https://krex.k-state.edu/items/df568e1c-f785-4f27-b610-1131bc1da639

Sims, A. W., C. E. Robinson, C. C. Smart, J. A. Voogt, G. J. Hay, J. T. Lundholm, B. Powers, and D. M. O'Carroll. 2016. "Retention Performance of Green Roofs in Three Different Climate Regions." Journal of Hydrology 542: 115-124. https://doi.org/10.1016/j.jhydrol.2016.08.055.

Skabelund, L. R., A. Decker, T. Moore, P. Shrestha, and J. L. Bruce. 2017. "Monitoring Two Large-Scale Prairie-Like Green Roofs in Manhattan, Kansas." In Cities Alive Green Roof and Wall Conference Proceedings. Seattle, WA. Green Roofs for Healthy Cities. https://www.k-state.edu/greenroofs/images/pdf_docs/CitiesAlive2017_Skabelund_Decker_Paper13Sep2017.pdf

Skabelund, L. R., and M. M. L. Alam. 2020. "Kansas State University Memorial Stadium Green Roofs Methods." Landscape Performance Series. Landscape Architecture Foundation. https://doi.org/10.31353/cs1691.

Skabelund, L. R., K. DiGiovanni, and O. Starry. 2015. "Monitoring Abiotic Inputs and Outputs." In Green Roof Ecosystems, edited by R. K. Sutton. Ecological Studies 223. Springer. https://doi.org/10.1007/978-3-319-14983-7_2

Skabelund, L. R., Y. Gao, J. H. Taylor, N. Laney, E. Musoke-Flores, M. M. L. Alam, and A. Decker. 2022. "Dominant Vegetation Types on Two Steep-Slope Prairie-Like Green Roofs (Kansas/USA)." In Cities Alive Green Roof and Wall Conference Proceedings. Philadelphia, PA. Green Roofs for Healthy Cities.

Snodgrass, E. C., and L. L. Snodgrass. 2006. Green Roof Plants: A Resource and Planting Guide. Timber Press.

Sobrino, J. A., J. C. Jiménez-Muñoz, and L. Paolini. 2004. "Land Surface Temperature Retrieval from LANDSAT TM 5." *Remote Sensing of Environment* 90 (4): 434–440. https://doi.org/10.1016/j.rse.2004.02.003.

Solcerova, A., F. van de Ven, M. Wang, M. Rijsdijk, and N. van de Giesen. 2017. "Do Green Roofs Cool the Air?" Building and Environment 111: 249-255. https://doi.org/10.1016/j.buildenv.2016.10.021.

Soni, L., C. Farrell, T. D. Fletcher, and C. Szota. 2025. "Climate Is More Important than Green Roof Design for Rainfall Retention and Plant Drought Stress in Temperate and SemiArid Climates." Urban Water Journal 22 (7): 761-776. https://doi.org/10.1080/1573062X.2025.2509071.

Soulis, K. X., N. Ntoulas, P. A. Nektarios, and G. Kargas. 2017. "Runoff Reduction from Extensive Green Roofs Having Different Substrate Depth and Plant Cover." Ecological Engineering 102: 80-89. https://doi.org/10.1016/j.ecoleng.2017.01.031

Steinauer, E. M., and S. L. Collins. 1996. "Prairie Ecology: The Tallgrass Prairie." In Prairie Conservation: Preserving North America's Most Endangered Ecosystem, 39–52. Island Press.

Sutton, R. K., J. A. Harrington, L. Skabelund, P. MacDonagh, R. R. Coffman, and G. Koch. 2012. "Prairie-Based Green Roofs: Literature, Templates, and Analogs." Journal of Green Building 7 (1): 143-172. https://doi.org/10.3992/jgb.7.1.143

Szota, C., T. D. Fletcher, C. Desbois, J. P. Rayner, N. S. G. Williams, and C. Farrell. 2017. "Laboratory Tests of Substrate Physical Properties May Not Represent the Retention Capacity of Green Roof Substrates In Situ." Water 9 (12): 920. https://doi.org/10.3390/w9120920.

Técher, D. 2022. "Using Superpixel- or Pixel-Based Segmentation for Efficient Green Roof Digital Image Classification and Rapid Estimation of Plant Species Cover." Urban Forestry & Urban Greening 76: 127722. https://doi.org/10.1016/j.ufug.2022.127722.

Thuring, C. E., R. D. Berghage, and D. J. Beattie. 2010. "Green Roof Plant Responses to Different Substrate Types and Depths under Various Drought Conditions." HortTechnology 20 (2): 395-401. https://doi.org/10.21273/HORTTECH.20.2.395

Todeschini, C. C., and A. G. Fett-Neto. 2025. "Life at the Top: Extensive Green Roof Plant Species and Their Traits for Urban Use." Plants 14 (5): 735. https://doi.org/10.3390/plants14050735

Tomasella, M., E. De Nardi, F. Petruzzellis, S. Andri, M. Castello, and A. Nardini. 2022. "Green Roof Irrigation Management Based on Substrate Water Potential Assures Water Saving without Affecting Plant Physiological Performance." Ecohydrology 15 (4): e2428. https://doi.org/10.1002/eco.2428.

Tucker, C. J. 1979. "Red and Photographic Infrared Linear Combinations for Monitoring Vegetation." Remote Sensing of Environment 8 (2): 127-150. https://doi.org/10.1016/0034-4257(79)90013-0.

Vacek, P., K. Struhala, and L. Matějka. 2017. "Life-Cycle Study on Semi Intensive Green Roofs." Journal of Cleaner Production 154: 203-213. https://doi.org/10.1016/j.jclepro.2017.03.188

Van der Merwe, D., L. R. Skabelund, P. Blackmore, A. J. Sharda, and D. Bremer. 2017. "Characterizing Green Roof Vegetation Using Color-Infrared and Thermal Sensors." Paper presented at the 15th Annual Cities Alive Green Roof and Wall Conference, Seattle, WA. Green Roofs for Healthy Cities. https://www.kstate.edu/greenroofs/images/pdf_docs/CitiesAlive2017_VanDerMerwe_Skabelund_Paper_22Aug2017.pdf

Van Mechelen, C., T. Dutoit, and M. Hermy. 2015. "Adapting Green Roof Irrigation Practices for a Sustainable Future: A Review." Sustainable Cities and Society 19: 74–90. https://doi.org/10.1016/j.scs.2015.07.007

Vandegrift, D. A., D. B. Rowe, B. M. Cregg, and D. Liang. 2019. "Effect of Substrate Depth on Plant Community Development on a Michigan Green Roof." Ecological Engineering 138: 264-273. https://doi.org/10.1016/j.ecoleng.2019.07.032.

VanWoert, N. D., D. B. Rowe, J. A. Andresen, C. L. Rugh, and L. Xiao. 2005. "Watering Regime and Green Roof Substrate Design Affect Sedum Plant Growth." HortScience 40 (3): 659–664. https://doi.org/10.21273/HORTSCI.40.3.659.

Vaz Monteiro, M., T. Blanuša, A. Verhoef, M. Richardson, P. Hadley, and R. W. F. Cameron. 2017. “Functional Green Roofs: Importance of Plant Choice in Maximising Summertime Environmental Cooling and Substrate Insulation Potential.” Energy and Buildings 141: 56-68. https://doi.org/10.1016/j.enbuild.2017.02.011.

Veihmeyer, F. J., and A. H. Hendrickson. 1931. "The Moisture Equivalent as a Measure of the Field Capacity of Soils." *Soil Science* 32 (3): 181-194. https://www.ovid.com/jnls/soilsci/fulltext/00010694-193109000-00003~the-moisture-equivalent-as-a-measure-of-the-field-capacity.

Xu, T., J. Sathaye, H. Akbari, V. Garg, and S. Tetali. 2012. “Quantifying the Direct Benefits of Cool Roofs in an Urban Setting: Reduced Cooling Energy Use and Lowered Greenhouse Gas Emissions.” Building and Environment 48: 1-6. https://doi.org/10.1016/j.buildenv.2011.08.011

Young, T., D. D. Cameron, J. Sorrill, T. Edwards, and G. K. Phoenix. 2014. “Importance of Different Components of Green Roof Substrate on Plant Growth and Physiological Performance.” Urban Forestry & Urban Greening 13 (3): 507-516. https://doi.org/10.1016/j.ufug.2014.04.007

Zhang, H., S. Lu, X. Fan, J. Wu, Y. Jiang, L. Ren, J. Wu, and H. Zhao. 2021. “Is Sustainable Extensive Green Roof Realizable without Irrigation in a Temperate Monsoonal Climate? A Case Study in Beijing.” Science of the Total Environment 753: 142067. https://doi.org/10.1016/j.scitotenv.2020.142067

Zhang, X., L. Shen, V. W. Y. Tam, and W. W. Y. Lee. 2012. “Barriers to Implement Extensive Green Roof Systems: A Hong Kong Study.” Renewable and Sustainable Energy Reviews 16 (1): 314-319. https://doi.org/10.1016/j.rser.2011.07.157

Appendix A - APD-EGR Study Plots and Plot Registry

Appendix Table A.1: Plot registry for the 16 APD-EGR instrumented plots.

Showing treatment assignments, plant community, site plot number, and logger/port for each of the 16 plots.

Plot	Depth	Substrate	Irrigation	Community	Plot no.	Logger/port
4″ P1	4″	BuildEx	Less	East	3 (403)	03500 / P4
4″ P2	4″	Rooflite	More	West	4 (404)	07870 / P4
4″ P3	4″	Rooflite	Less	East	10 (410)	03500 / P3
4″ P4	4″	BuildEx	More	West	9 (409)	07870 / P3
4″ P5	4″	Rooflite	More	East	15 (415)	03500 / P2
4″ P6	4″	BuildEx	Less	West	16 (416)	07870 / P2
4″ P7	4″	BuildEx	More	East	22 (422)	03500 / P1
4″ P8	4″	Rooflite	Less	West	21 (421)	07870 / P1
8″ P1	8″	Rooflite	Less	East	3 (803)	03504 / P4
8″ P2	8″	BuildEx	More	West	4 (804)	03501 / P4
8″ P3	8″	BuildEx	Less	East	10 (810)	03504 / P3
8″ P4	8″	Rooflite	More	West	9 (809)	03501 / P3
8″ P5	8″	BuildEx	More	East	15 (815)	03504 / P2
8″ P6	8″	BuildEx	Less	West	16 (816)	03501 / P2
8″ P7	8″	Rooflite	More	East	22 (822)	03504 / P1
8″ P8	8″	Rooflite	Less	West	21 (821)	03501 / P1

Source: Created by Author from synthesizing previous plot registry files and data logger output files. Note: K = BuildEx, R = Rooflite; "Less" = less-irrigated (approximately 12 gallons per plot over the season), "More" = more-irrigated (approximately 72 gallons per plot over the season).

Appendix B - Plot-Level Canopy Cover (iPhone Canopeo)

Fractional green canopy cover was measured on 56 dates between June 30 and November 5, 2025. Overhead (nadir) photographs of each plot were captured with an iPhone 11 Pro Max or iPhone 12 Pro from a ladder, cropped immediately for quality control, and later analyzed with the Canopeo Desktop application (Patrignani and Ochsner, 2015). Table B-1 gives the per-plot seasonal summary; Tables B-2 and B-3 give daily records for 4- and 8-inch plots, respectively.

Appendix Table B.1. Seasonal-mean, minimum, and maximum APD-EGR canopy cover (%) and seasonal area under the cover curve (AUC, %·day) for each plot, 56 measurement dates.

Plot	Substrate	Irrigation	Community	Seasonal mean	Min	Max	AUC
4″ P1	BuildEx	Less	East	42.8	6.0	73.2	4,246
4″ P2	Rooflite	More	West	22.4	1.7	34.2	2,629
4″ P3	Rooflite	Less	East	17.8	6.5	29.5	2,036
4″ P4	BuildEx	More	West	35.5	9.5	48.7	4,262
4″ P5	Rooflite	More	East	32.7	2.9	52.9	3,234
4″ P6	BuildEx	Less	West	23.7	6.1	34.8	2,720
4″ P7	BuildEx	More	East	47.0	1.0	65.1	4,733
4″ P8	Rooflite	Less	West	21.1	0.2	33.3	2,278
8″ P1	Rooflite	Less	East	15.9	0.1	35.1	1,308
8″ P2	BuildEx	More	West	64.3	5.7	77.9	7,569
8″ P3	BuildEx	Less	East	20.7	0.5	38.3	1,788
8″ P4	Rooflite	More	West	45.0	6.5	61.4	4,726
8″ P5	BuildEx	More	East	43.7	0.9	74.0	3,923
8″ P6	BuildEx	Less	West	43.8	17.9	61.3	4,961

Plot	Substrate	Irrigation	Community	Seasonal mean	Min	Max	AUC
8″ P7	Rooflite	More	East	30.7	0.7	54.8	2,475
8″ P8	Rooflite	Less	West	44.8	6.9	57.7	5,513

Source: Canopeo_Cover_56_Day_Analysis_Ready.csv (Author). Grand mean of 16 plot means = 34.5%; lowest plot 8″ P1 (15.9%), highest plot 8″ P2 (64.3%).

Appendix Table B.2. Daily APD-EGR canopy cover (%) for the eight 4-inch (~10 cm) plots across all 56 measurement dates.

Date	P1	P2	P3	P4	P5	P6	P7	P8
Jun 30	73.2	15.4	24.9	33.7	45.3	24.7	63.7	20.7
Jul 3	58.2	11.6	19.4	31.1	35.0	21.2	52.0	15.2
Jul 4	58.0	13.8	25.0	32.0	48.1	21.5	55.5	18.1
Jul 5	64.5	14.6	29.5	35.6	50.6	24.8	54.5	19.5
Jul 6	66.0	18.5	28.2	37.6	52.9	26.3	64.2	24.1
Jul 7	57.4	17.5	22.5	32.8	35.1	23.5	41.1	21.3
Jul 8	67.2	18.5	25.8	34.9	48.5	25.5	59.9	22.7
Jul 9	53.7	17.1	20.0	28.9	33.5	22.8	43.2	20.3
Jul 10	44.2	17.9	14.5	31.6	36.5	18.7	56.3	20.7
Jul 11	25.8	17.5	13.3	31.7	38.3	18.7	37.3	14.1
Jul 12	42.1	17.1	15.0	29.5	26.2	15.8	49.4	18.0
Jul 13	55.0	19.8	18.7	36.2	41.7	23.9	58.7	22.1
Jul 14	51.9	20.3	17.0	34.5	37.7	23.6	57.4	22.1
Jul 15	39.3	18.7	15.0	32.8	27.9	21.0	47.5	20.7
Jul 16	28.8	18.0	14.2	30.4	43.1	18.8	44.0	16.2
Jul 17	41.3	20.0	14.9	32.6	33.3	20.1	47.1	19.6
Jul 18	51.3	22.0	18.4	35.1	43.0	25.0	45.4	19.1
Jul 19	52.5	24.4	17.3	38.7	39.3	25.5	56.9	24.2

Date	P1	P2	P3	P4	P5	P6	P7	P8
Jul 20	51.3	22.3	18.3	38.0	33.7	26.6	52.6	22.8
Jul 21	53.7	25.1	18.3	40.2	35.7	27.0	51.0	23.5
Jul 22	56.7	26.5	19.5	43.7	39.0	30.7	58.9	26.6
Jul 23	59.5	27.1	21.2	42.5	42.7	32.2	60.8	27.4
Jul 24	58.2	28.1	22.5	46.9	44.9	34.3	56.7	26.9
Jul 25	55.2	26.8	22.5	40.7	41.5	32.3	54.7	27.7
Jul 27	61.7	28.9	22.2	43.1	49.5	34.8	61.8	30.6
Jul 28	61.9	31.0	18.1	42.5	45.5	29.4	65.1	30.4
Jul 29	53.7	30.7	13.9	40.6	41.1	22.2	65.1	27.8
Jul 30	42.2	26.3	14.6	35.8	34.9	20.0	51.2	21.4
Jul 31	42.8	24.0	11.8	27.0	24.3	15.7	38.6	17.3
Aug 1	52.3	26.4	15.0	34.0	34.3	24.0	56.1	24.1
Aug 2	45.2	23.0	15.7	32.7	30.0	25.9	43.1	18.2
Aug 5	49.9	25.9	17.4	36.3	29.3	27.8	48.4	21.8
Aug 6	42.2	27.3	15.8	34.7	28.8	26.2	42.3	25.4
Aug 7	35.8	25.0	16.8	36.5	32.4	22.3	45.7	21.4
Aug 9	14.8	25.6	10.2	32.0	25.9	15.4	35.9	16.8
Aug 11	20.5	26.9	16.8	36.9	33.8	22.7	51.5	23.6
Aug 12	33.2	34.1	19.6	46.0	40.2	30.0	61.7	32.9
Aug 13	34.1	34.2	19.9	46.1	38.3	30.6	63.1	33.3
Aug 14	32.3	31.9	19.8	45.6	39.1	30.6	60.9	31.1
Aug 15	24.1	24.0	18.7	37.5	30.2	28.6	43.5	21.8
Aug 16	33.5	33.1	18.0	44.0	35.7	27.9	63.2	32.1
Aug 23	41.3	32.6	21.2	48.7	39.6	29.2	57.9	30.0

Date	P1	P2	P3	P4	P5	P6	P7	P8
Aug 25	29.2	28.8	16.1	37.8	23.8	18.7	51.9	22.6
Aug 28	15.0	22.2	12.7	38.2	35.0	10.7	42.8	9.4
Sep 7	33.0	17.5	17.4	31.1	16.5	21.3	34.5	18.1
Sep 8	44.8	26.4	16.8	29.4	18.3	21.6	45.5	24.6
Sep 9	39.9	20.8	22.1	41.8	22.6	31.3	33.7	17.4
Sep 12	33.8	17.5	16.6	28.2	14.1	20.4	27.3	14.9
Sep 14	36.7	18.6	13.4	24.6	12.3	17.5	28.2	14.8
Sep 17	35.0	17.9	17.6	28.5	17.9	18.4	28.6	13.3
Sep 19	41.3	21.9	21.0	37.8	22.1	29.7	34.9	20.9
Sep 24	33.1	19.9	17.2	35.2	16.0	25.2	24.6	13.1
Sep 28	24.2	15.3	14.0	28.0	14.6	18.3	16.5	9.8
Oct 1	21.4	16.2	15.5	33.9	16.2	21.4	17.8	10.5
Oct 19	18.8	20.5	11.2	30.0	13.3	17.8	22.4	17.5
Nov 5	6.0	1.7	6.5	9.5	2.9	6.1	1.0	0.2

Source: Canopeo_Cover_56_Day_Analysis_Ready.csv (Author). Columns show data for APD-EGR plots P1–P8 within the 4-inch bed.

Appendix Table B.3. Daily canopy cover (%) for the eight 8-inch (~20 cm) plots across all 56 measurement dates.

Date	P1	P2	P3	P4	P5	P6	P7	P8
Jun 30	28.7	74.2	32.5	61.4	71.9	61.3	54.8	57.7
Jul 3	22.7	64.7	32.5	50.5	61.1	50.8	36.9	55.2
Jul 4	28.4	66.9	38.3	53.1	70.1	49.3	42.9	45.5
Jul 5	22.7	64.7	37.9	54.7	66.1	53.1	43.3	46.9
Jul 6	35.1	70.2	36.6	59.1	74.0	56.8	49.5	50.6
Jul 7	29.4	61.0	28.6	54.6	50.5	49.4	40.5	46.7
Jul 8	32.5	66.2	35.3	55.3	73.3	52.5	46.2	48.8
Jul 9	23.3	53.3	28.4	53.5	53.1	46.5	37.1	42.9
Jul 10	22.6	59.8	23.4	51.5	55.5	40.5	43.7	43.4
Jul 11	12.3	49.6	34.3	48.8	47.1	41.2	28.4	32.1
Jul 12	18.6	57.0	25.5	47.5	57.0	36.7	41.2	40.4
Jul 13	24.5	63.8	24.4	50.1	61.3	44.9	41.9	42.2
Jul 14	23.6	61.5	24.3	51.4	55.1	44.6	43.9	42.3
Jul 15	15.8	49.8	14.7	48.8	51.3	40.3	34.6	38.5
Jul 16	9.4	52.5	16.6	48.3	59.5	38.5	30.3	29.8
Jul 17	14.9	56.3	23.3	42.1	46.5	41.1	36.5	36.1
Jul 18	13.9	57.6	29.5	49.1	59.1	45.9	30.8	38.0
Jul 19	22.0	65.5	18.7	48.6	57.3	47.3	43.8	45.8
Jul 20	15.3	61.0	21.0	48.9	49.6	53.0	34.1	41.3
Jul 21	16.3	60.3	22.3	41.9	51.5	40.7	36.8	43.2
Jul 22	24.8	67.0	24.8	50.3	55.6	51.2	43.3	49.5
Jul 23	24.8	69.6	22.6	53.2	55.1	48.9	44.0	50.7

Date	P1	P2	P3	P4	P5	P6	P7	P8
Jul 24	23.9	67.4	33.7	49.6	62.6	49.7	43.8	49.6
Jul 25	21.7	67.0	20.0	48.2	47.0	51.2	40.7	48.9
Jul 27	29.3	72.3	34.9	55.9	68.2	57.7	46.0	51.6
Jul 28	32.9	75.5	36.2	57.6	67.8	54.7	53.4	54.6
Jul 29	30.0	76.4	34.1	56.0	66.3	52.6	52.3	50.6
Jul 30	18.9	66.2	24.7	42.4	44.4	40.8	35.0	41.5
Jul 31	11.1	63.8	17.8	33.7	30.2	33.6	29.6	42.5
Aug 1	17.8	68.3	24.1	44.8	50.4	43.3	40.5	43.3
Aug 2	10.9	61.1	23.8	47.3	32.6	46.1	25.8	36.2
Aug 5	10.7	64.3	15.7	49.6	38.8	45.4	24.8	41.5
Aug 6	11.6	60.6	19.8	44.8	41.6	45.1	27.3	43.0
Aug 7	9.7	62.8	19.4	44.4	26.1	38.5	25.0	39.5
Aug 9	6.5	52.9	10.3	44.4	27.0	30.7	24.4	36.3
Aug 11	8.9	64.9	23.2	50.5	42.6	46.7	27.6	43.8
Aug 12	22.1	76.6	27.2	56.7	50.3	50.4	45.5	51.6
Aug 13	20.5	77.3	27.9	56.4	54.6	50.9	44.5	53.2
Aug 14	18.4	76.7	24.4	51.0	49.0	49.4	37.3	50.0
Aug 15	9.8	63.9	13.9	41.1	34.9	41.8	20.4	41.4
Aug 16	22.4	77.4	26.1	53.9	46.8	49.6	42.9	51.4
Aug 23	16.2	70.8	14.4	51.3	35.7	47.9	26.9	48.4
Aug 25	9.6	71.1	11.0	44.9	34.8	35.6	25.4	43.5
Aug 28	3.7	63.7	2.4	44.2	35.6	30.5	16.6	36.0
Sep 7	5.0	75.4	7.0	31.2	15.6	33.5	11.9	49.9
Sep 8	10.1	77.9	9.7	33.7	22.5	42.1	18.7	52.3

Date	P1	P2	P3	P4	P5	P6	P7	P8
Sep 9	5.0	72.0	14.4	42.8	25.9	51.6	9.3	50.0
Sep 12	2.2	70.9	4.8	23.8	12.0	24.1	5.9	49.7
Sep 14	1.9	68.9	4.2	23.8	13.0	31.3	7.2	52.7
Sep 17	2.6	71.1	1.9	31.8	11.4	49.4	5.3	45.7
Sep 19	4.9	75.3	12.4	37.0	20.6	43.3	9.3	51.2
Sep 24	2.4	70.4	6.1	30.7	13.3	40.4	5.0	49.5
Sep 28	1.5	62.0	5.1	19.6	13.2	24.8	2.5	46.2
Oct 1	2.0	57.4	8.0	26.6	15.8	36.8	3.1	46.5
Oct 19	4.7	43.0	6.9	22.9	14.3	31.2	1.3	43.6
Nov 5	0.1	5.7	0.5	6.5	0.9	17.9	0.7	6.9

Source: Canopeo_Cover_56_Day_Analysis_Ready.csv (Author). Columns show data for APD-EGR plots P1–P8 within the 8-inch bed.

Appendix C - UAS Drone Canopy Cover and NDVI

Aerial imagery of the APD-EGR was acquired on four flight dates (July 9, August 9, September 19, and November 1, 2025) with a DJI Mavic 3 Multispectral aircraft flown by Kaden Spencer (Graduate Research Assistant, Department of Agronomy, Kansas State University). Two distinct analyses were derived from these flights, by different analysts.

The drone canopy cover values in Tables C-1 and C-4 were produced by the author from the RGB orthomosaics supplied by Kaden Spencer. Each 1 m × 1 m plot was cropped manually from the orthomosaic in Adobe Photoshop and saved in a structured folder hierarchy of one parent folder per flight date, with subfolders by depth, each containing eight named plot images. Each set was then batch-analysed in the Canopeo Desktop application to generate fractional green canopy cover, mirroring the procedure used for the iPhone imagery.

The NDVI values in Tables C-2 and C-3 were produced by Kaden Spencer, who processed the four-band imagery (green, red, red-edge, near-infrared) in Pix4Dfields and extracted per-plot mean NDVI in QGIS.

Drone cover values run systematically lower than the iPhone measurements, by approximately 9 to 13 percentage points on the three exactly matched dates, because the nadir view from altitude captures the full plot, including bare-substrate gaps. NDVI covers all 72 roof plots and therefore resolves the 6-inch (~15 cm) semi-intensive bed that was excluded from the sensor experiment.

Appendix Table C.1. Drone-derived canopy cover (%) for the sixteen instrumented plots on four flight dates.

Plot	Substrate	Irrigation	Community	Jul 9	Aug 9	Sep 19	Nov 1
4″ P1	BuildEx	Less	East	33.3	2.3	26.7	5.2
4″ P2	Rooflite	More	West	9.0	14.2	17.1	2.6
4″ P3	Rooflite	Less	East	9.8	2.3	10.9	2.1
4″ P4	BuildEx	More	West	17.6	20.3	27.1	3.0
4″ P5	Rooflite	More	East	22.7	13.2	9.6	0.7
4″ P6	BuildEx	Less	West	12.4	2.9	16.3	1.7
4″ P7	BuildEx	More	East	27.3	17.3	22.0	2.2
4″ P8	Rooflite	Less	West	13.8	6.1	11.2	0.6
8″ P1	Rooflite	Less	East	12.1	1.1	2.9	0.1

Plot	Substrate	Irrigation	Community	Jul 9	Aug 9	Sep 19	Nov 1
8″ P2	BuildEx	More	West	35.3	34.4	61.7	12.0
8″ P3	BuildEx	Less	East	24.0	0.5	1.4	0.0
8″ P4	Rooflite	More	West	37.9	25.6	29.4	3.2
8″ P5	BuildEx	More	East	46.0	24.2	14.7	0.3
8″ P6	BuildEx	Less	West	35.4	14.2	42.1	12.1
8″ P7	Rooflite	More	East	27.8	8.6	5.2	0.4
8″ P8	Rooflite	Less	West	34.1	20.1	39.5	10.3
4-inch mean				18.2	9.8	17.6	2.3
8-inch mean				31.6	16.1	24.6	4.8
All 16 plots				24.9	13.0	21.1	3.5

Source: UAS_Drone_Canopeo_4Flights_Analysis_Ready_CORRECTED.csv. Imagery acquired by K. Spencer (Department of Agronomy, KSU); plot cropping and Canopeo analysis by the author. The July 9 values for the eight 4-inch plots were corrected against the raw Canopeo export in August 2026; all other values are unchanged.

Appendix Table C.2. Mean NDVI by substrate depth for each flight date, including all 72 roof plots and the arithmetic 4-to-8-inch midpoint.

Flight date	4-inch	4–8 midpoint	6-inch	8-inch	All 72 plots
Jul 9	0.486	0.541	0.586	0.597	0.556
Aug 9	0.525	0.557	0.580	0.589	0.565
Sep 19	0.569	0.582	0.602	0.594	0.588
Nov 1	0.431	0.438	0.455	0.445	0.444

Source: NDVI_Datain_4_Flights.csv (imagery, multispectral processing, and NDVI extraction by K. Spencer, Department of Agronomy, KSU). On every date the 6-inch mean exceeds the 4-to-8-inch midpoint, indicating a non-linear depth response.

Appendix Table C.3. Per-plot mean NDVI for all 72 roof plots on four flight dates. Plot identifiers begin with the depth bed (4xx = 4-inch, 6xx = 6-inch, 8xx = 8-inch).

Plot	Depth	Jul 9	Aug 9	Sep 19	Nov 1	Plot	Depth	Jul 9	Aug 9	Sep 19	Nov 1
401	4″	0.612	0.547	0.572	0.437	613	6″	0.676	0.663	0.646	0.451
402	4″	0.529	0.500	0.595	0.455	614	6″	0.641	0.656	0.618	0.450
403	4″	0.541	0.527	0.601	0.458	615	6″	0.577	0.569	0.564	0.423
404	4″	0.328	0.478	0.484	0.347	616	6″	0.535	0.547	0.612	0.445
405	4″	0.407	0.502	0.504	0.348	617	6″	0.564	0.551	0.624	0.461
406	4″	0.571	0.626	0.628	0.459	618	6″	0.629	0.616	0.647	0.491
407	4″	0.605	0.661	0.635	0.478	619	6″	0.581	0.598	0.653	0.503
408	4″	0.496	0.603	0.620	0.481	620	6″	0.487	0.478	0.551	0.389
409	4″	0.439	0.569	0.582	0.449	621	6″	0.512	0.499	0.567	0.427
410	4″	0.420	0.441	0.551	0.394	622	6″	0.608	0.607	0.593	0.462
411	4″	0.463	0.454	0.551	0.412	623	6″	0.581	0.582	0.585	0.470
412	4″	0.408	0.401	0.444	0.348	624	6″	0.567	0.562	0.517	0.449
413	4″	0.500	0.512	0.536	0.387	801	8″	0.571	0.512	0.509	0.419
414	4″	0.511	0.559	0.579	0.410	802	8″	0.593	0.531	0.541	0.414
415	4″	0.545	0.595	0.598	0.433	803	8″	0.533	0.494	0.504	0.388
416	4″	0.406	0.464	0.532	0.431	804	8″	0.574	0.667	0.711	0.560
417	4″	0.468	0.491	0.581	0.445	805	8″	0.594	0.669	0.684	0.556
418	4″	0.604	0.616	0.692	0.569	806	8″	0.648	0.676	0.615	0.493
419	4″	0.455	0.486	0.537	0.453	807	8″	0.626	0.642	0.608	0.467

Plot	Depth	Jul 9	Aug 9	Sep 19	Nov 1	Plot	Depth	Jul 9	Aug 9	Sep 19	Nov 1
420	4″	0.379	0.397	0.507	0.380	808	8″	0.610	0.659	0.662	0.532
421	4″	0.369	0.418	0.471	0.375	809	8″	0.588	0.630	0.620	0.449
422	4″	0.504	0.562	0.614	0.461	810	8″	0.600	0.567	0.564	0.420
423	4″	0.523	0.582	0.625	0.469	811	8″	0.647	0.575	0.596	0.430
424	4″	0.577	0.611	0.622	0.471	812	8″	0.643	0.551	0.577	0.439
601	6″	0.655	0.609	0.610	0.461	813	8″	0.679	0.646	0.642	0.450
602	6″	0.572	0.523	0.558	0.420	814	8″	0.670	0.645	0.630	0.460
603	6″	0.569	0.506	0.582	0.443	815	8″	0.664	0.669	0.614	0.455
604	6″	0.518	0.596	0.614	0.448	816	8″	0.589	0.604	0.654	0.515
605	6″	0.616	0.636	0.641	0.492	817	8″	0.621	0.643	0.684	0.527
606	6″	0.592	0.617	0.600	0.511	818	8″	0.550	0.572	0.565	0.437
607	6″	0.632	0.657	0.630	0.496	819	8″	0.473	0.480	0.473	0.326
608	6″	0.616	0.655	0.654	0.481	820	8″	0.418	0.426	0.477	0.287
609	6″	0.589	0.655	0.660	0.492	821	8″	0.594	0.589	0.648	0.516
610	6″	0.555	0.467	0.555	0.428	822	8″	0.602	0.581	0.567	0.393
611	6″	0.596	0.540	0.580	0.406	823	8″	0.651	0.624	0.611	0.429
612	6″	0.608	0.541	0.577	0.418	824	8″	0.581	0.474	0.505	0.320

Source: NDVI_Datain_4_Flights.csv (K. Spencer, Department of Agronomy, KSU). NDVI = (NIR − Red)/(NIR + Red). Range across all plots and dates: 0.287–0.711; grand mean 0.538.

Appendix Table C.4. Drone and iPhone Canopeo cover (%) on the three exactly matched dates, with the offset between methods.

Plot	Jul 9 drone	Jul 9 iPhone	Diff.	Aug 9 drone	Aug 9 iPhone	Diff.	Sep 19 drone	Sep 19 iPhone	Diff.
4″ P1	33.3	53.7	20.4	2.3	14.8	12.5	26.7	41.3	14.6
4″ P2	9.0	17.1	8.1	14.2	25.6	11.4	17.1	21.9	4.8
4″ P3	9.8	20.0	10.2	2.3	10.2	7.9	10.9	21.0	10.1
4″ P4	17.6	28.9	11.3	20.3	32.0	11.7	27.1	37.8	10.7
4″ P5	22.7	33.5	10.8	13.2	25.9	12.7	9.6	22.1	12.5
4″ P6	12.4	22.8	10.4	2.9	15.4	12.5	16.3	29.7	13.4
4″ P7	27.3	43.2	15.9	17.3	35.9	18.6	22.0	34.9	12.9
4″ P8	13.8	20.3	6.5	6.1	16.8	10.7	11.2	20.9	9.7
8″ P1	12.1	23.3	11.2	1.1	6.5	5.4	2.9	4.9	2.0
8″ P2	35.3	53.3	18.0	34.4	52.9	18.5	61.7	75.3	13.6
8″ P3	24.0	28.4	4.4	0.5	10.3	9.8	1.4	12.4	11.0
8″ P4	37.9	53.5	15.6	25.6	44.4	18.8	29.4	37.0	7.6
8″ P5	46.0	53.1	7.1	24.2	27.0	2.8	14.7	20.6	5.9
8″ P6	35.4	46.5	11.1	14.2	30.7	16.5	42.1	43.3	1.2
8″ P7	27.8	37.1	9.3	8.6	24.4	15.8	5.2	9.3	4.1
8″ P8	34.1	42.9	8.8	20.1	36.3	16.2	39.5	51.2	11.7
Mean	24.9	36.1	11.2	13.0	25.6	12.6	21.1	30.2	9.1

Sources: UAS_Drone_Canopeo_4Flights_Analysis_Ready_CORRECTED.csv and Canopeo_Cover_56_Day_Analysis_Ready.csv. Both cover datasets were analysed by the author in Canopeo Desktop. Diff. = iPhone minus drone, in percentage points. Across all 48 matched observations the mean offset is 11.0 percentage points, and the offset increases with canopy density ($r = 0.478$, $p < 0.001$). The November 1 flight is omitted because the nearest ground-based measurement was November 5.

UAS Equipment and Processing

Aircraft: DJI Mavic 3 Multispectral (Enterprise), carrying an integrated four-band multispectral camera (green, red, red-edge, near-infrared) and a 20-megapixel RGB camera. Radiometric calibration used the onboard sunlight sensor together with a Sentera reflectance panel imaged before each flight. Flights were flown at approximately 25 ft (~7.6 m) above ground level on sunny, clear-sky, low-wind days for consistent illumination. Image stitching and orthomosaic generation were performed in Pix4Dfields. The ground sampling distance was 0.25 cm/pixel for both the RGB and multispectral orthomosaics, a resolution that resolved individual plant structures within each plot.

Division of work. Flight planning, flight operation, radiometric calibration, orthomosaic generation, NDVI calculation, and per-polygon NDVI extraction were carried out by Kaden Spencer. Plot-level cropping of the RGB orthomosaics and all Canopeo analysis of the resulting plot images were carried out by the author.

Appendix D - Teros 12 Soil Moisture and Temperature Values for Each Substrate Type

Appendix Table D.1. Seasonal-mean and minimum volumetric water content (%) and seasonal-mean substrate temperature (°C) for each of the 16 APD-EGR plots.

Plot	Substrate	Irrigation	Community	Mean VWC	Min VWC	Mean temp
4″ P1	BuildEx	Less	East	12.1	2.7	23.8
4″ P2	Rooflite	More	West	18.8	8.8	24.6
4″ P3	Rooflite	Less	East	9.9	0.1	25.2
4″ P4	BuildEx	More	West	14.1	4.4	23.8
4″ P5	Rooflite	More	East	14.1	2.8	24.3
4″ P6	BuildEx	Less	West	10.8	1.6	24.6
4″ P7	BuildEx	More	East	12.1	2.7	23.8
4″ P8	Rooflite	Less	West	13.1	3.5	25.2
8″ P1	Rooflite	Less	East	10.3	6.3	24.0
8″ P2	BuildEx	More	West	14.4	7.0	23.9
8″ P3	BuildEx	Less	East	14.6	7.1	23.6
8″ P4	Rooflite	More	West	10.4	6.1	24.3
8″ P5	BuildEx	More	East	15.0	7.6	22.6
8″ P6	BuildEx	Less	West	10.1	5.7	24.0
8″ P7	Rooflite	More	East	9.3	4.9	23.6
8″ P8	Rooflite	Less	West	11.4	6.0	24.6

Source: TEROS 12 data as saved in the APD-EGR data logger files z6-03500 and z6-07870 (4-inch, East and West) and z6-03501 and z6-03504 (8-inch, West and East), calibrated with the substrate-specific equations in Appendix E. Note that the deeper plots typically maintained higher minimum VWC, the buffering mechanism behind the depth effect.

Appendix E - Sensor Calibration (Substrate-Specific TEROS 12)

Appendix Table E.1. Final calibration equations converting raw TEROS 12 output (x, in millivolts) to volumetric water content (VWC, $m^3\ m^{-3}$).

Substrate	Calibration equation	Fit
BuildEx (3rd order)	$VWC = -39.34620275 + 0.05185726x - 2.27550613\times10^{-5}x^2 + 3.33651882\times10^{-9}x^3$	$R^2 = 0.948$
Rooflite (2nd order)	$VWC = -2.16239357 + 0.00160120x - 2.47285241\times10^{-7}x^2$	$R^2 = 0.996$

Source: APD-EGR substrate-specific calibration, 27 May 2025; full-precision refit with support from Andres Patrignani (15 July 2025). The Rooflite third-order coefficient is zero by design.

Appendix F - Substrate Physical and Hydraulic Properties

The operative physical and hydraulic properties below were measured in 2025 on undisturbed cores and entered into ZENTRA Cloud; they govern the irrigation trigger and the interpretation of the moisture record. The 8% VWC irrigation threshold corresponds to 50% depletion of plant-available water capacity (PAWC) and is therefore not arbitrary.

Appendix Table F.1. Operative substrate physical and hydraulic properties (based on May 2025 APD-EGR soil samples and A. Patrignani K-State Soil-Water Lab measurements).

Property	Rooflite	BuildEx	Units
Particle density	1.83	2.01	g cm^{-3}
Bulk density	0.84	1.24	g cm^{-3}
Field capacity (10 kPa)	0.150	0.130	m^3 m^{-3}
Wilting point (1.5 MPa)	0.016	0.029	m^3 m^{-3}
Plant-available water capacity	0.134	0.100	m^3 m^{-3}
Irrigation threshold (50% PAWC)	0.083	0.080	m^3 m^{-3}
Porosity (computed)	54.3	38.4	%

Source: May 2025 K-State Agronomy Soil-Water Laboratory, undisturbed 100 cm^3 cores.

Appendix Table F.2. Three independent bulk-density determinations. These are different quantities and should not be conflated; the 2025 undisturbed-core values are operative.

Determination	BuildEx	Rooflite
Decker (2021), ASTM E2399, never-installed material	1.47	0.98
May 2025 undisturbed 100 cm^3 cores (operative)	1.24	0.84
NRES Capstone sampling (Apr 2026), 128 cm^3 tins	1.01	0.89

Sources: Decker (2021); K-State Agronomy Soil-Water Lab data (Andres Patrignani, personal communication, 2025); K-State Soil Testing Laboratory (per Gillman et al. 2026). ASTM E2399 reports a packed maximum for dead-load estimation, not in-place density.

Appendix G - Substrate Chemistry

Eight (8) composite substrate samples (two substrates × East/West × 4-inch/8-inch) were submitted to the Kansas State University Soil Testing Laboratory (Order 60602) May 21, 2025. Particle-size fractions are reported for the less-than-2-mm fraction and sum to 100%; coarse material greater than 2 mm is reported separately, so the basis must always be stated.

Appendix Table G.1. Substrate chemistry and texture, K-State Soil Testing Laboratory (2025).

Property	**BuildEx**	**Rooflite**
Sand (of <2 mm fraction)	88.2%	85.5%
Silt / clay (<2 mm)	7.0% / 4.8%	10.0% / 4.5%
Coarse >2 mm (whole sample)	21.4%	43.9%
Sand (whole-sample basis)	69.3%	47.8%
Organic matter (loss on ignition)	2.05%	2.67%
Total carbon	1.28%	1.61%
pH	7.97	7.93
Electrical conductivity	0.63 dS m^{-1}	0.64 dS m^{-1}

Source: KSU Soil Testing Laboratory, Order 60602 (2025). Note that on a whole-sample basis, these values corroborate the coarser texture of Rooflite reported by Decker (2021).

Appendix H - Irrigation Water Quality

Three water samples were analyzed by the KSU Soil Testing Laboratory (Order 60649). Irrigation drew from the on-site cistern. The 2022 cistern sample had been refrigerated in a single-use plastic bottle for more than three years before analysis and returned the highest values in the batch; it does not characterize the water applied in 2025 and is reported only for completeness.

Appendix Table H.1. Irrigation water quality, KSU Soil Testing Laboratory (2025).

Parameter	2022 cistern	2025 cistern (applied)	2025 spigot
pH	—	6.99	7.24
Electrical conductivity (mS cm^{-1})	0.09	0.03	0.04
Total dissolved solids (mg L^{-1})	62.0	17.8	31.2
Total nitrogen (ppm)	2.88	0.55	0.76
Total phosphorus (ppm)	—	0.02	0.06
Zinc (ppm)	4.83	1.58	2.31

Source: K-State Soil Testing Laboratory, Order 60649. Salinity load is negligible. Sodium was not measured, so the sodium adsorption ratio was not computed and sodicity was not assessed. Cistern zinc (1.58 ppm) is below the FAO continuous-irrigation guideline of 2.0 mg L^{-1}.

Appendix I - Irrigation Event Log

Supplemental irrigation was applied from the on-site cistern at approximately 6.5 gallons per plot per event. "More-only" events watered the 36 more-irrigated plots; "all" events watered all 72 plots. Over the season the more-irrigated plots received twelve events (~78 gal/plot) and the less-irrigated plots four events (~26 gal/plot), a 3:1 ratio. The central event of the experiment was the 39-day interval (July 2 to August 10) during which the less-irrigated plots received no supplemental water.

Appendix Table I.1. Supplemental irrigation events, 2025 growing season, with cumulative water applied to each treatment group.

#	Date	Event type	Plots	Cum. more (gal)	Cum. less (gal)	Notes
1	Jun 30	More only	36	6.5	0	First event; forecast >90 °F
2	Jul 2	All 72	72	13.0	6.5	VWC trigger; both groups watered
3	Jul 15	More only	36	19.5	6.5	39-day gap, day 13
4	Jul 27	More only	36	26.0	6.5	Peak summer heat; gap day 25
5	Aug 6	More only	36	32.5	6.5	August stress; gap day 35
6	Aug 10	All 72	72	39.0	13.0	39-day gap ends
7	Aug 15	More only	36	45.5	13.0	5-day gap
8	Aug 17	All 72	72	52.0	19.5	Intensive intervention
9	Aug 23	More only	36	58.5	19.5	6-day gap
10	Aug 28	All 72	72	65.0	26.0	Last all-plots event
11	Sep 15	More only	36	71.5	26.0	Less-irrigated rain-only hereafter
12	Oct 2	More only	36	78.0	26.0	Final event before senescence

Source: 2021–2025 Irrigation Log, APD-EGR Research Team OneDrive files. Cumulative volumes are per plot within each treatment group.

Appendix J - Vegetation Survey

The vegetation of the mature planting (installed 2017–2018) was surveyed on June 3 and December 9, 2025, using expert-guided ocular estimation (Daubenmire method adapted), with species identification by educator and Professional Landscape Architect Lee R. Skabelund. Cover was recorded by functional group as a range and reduced to a midpoint. A species was counted as present if observed on either date. The community is diverse and predominantly native prairie. A total of 32 vascular species were recorded in the 16 sensor plots across the two survey dates (7 grasses, 17 forbs, and 8 sedums).

Appendix Table J.1. Percent cover by functional group and bed, June 3, 2025.

Functional group	8″ East	8″ West	6″ East	6″ West	4″ East	4″ West
Grasses	68.0	20.0	52.2	12.4	25.5	4.8
Forbs	9.7	19.5	12.8	22.8	22.3	25.2
Sedums	11.3	33.2	19.8	31.0	23.3	19.9
Bare soil +	10.6	27.1	14.9	33.8	28.8	50.0

Source: APDesign Plant Survival Survey (June & December 2025), Comparison sheet.

Appendix Table J.2. Species pool recorded in the vegetation survey, by functional group.

Plant species names follow field identifications; sedums were recorded as observed morphotypes and were not identified to the species level.

Group	Species recorded
Grasses (7)	Little bluestem (*Schizachyrium scoparium*), sideoats grama (*Bouteloua curtipendula*), June grass (*Koeleria macrantha*), prairie dropseed (*Sporobolus heterolepis*), *Carex sp.*, an unidentified *Grama sp.*, and a cool-season grass.
Forbs (17)	Purple prairie clover (*Dalea purpurea*), white prairie clover (*Dalea candida*), *Packera obovata*, fleabane, spurge, lance-leaf coreopsis (*Coreopsis lanceolata*), *Asclepias tuberosa* and *A. verticillata*, *Liatris punctata*, common aster, heath aster, goldenrod, wood sorrel (*Oxalis*), boneset (*Eupatorium perfoliatum*), managed ruderal plants (dandelion and black medic), and small unidentified forbs.
Sedums (8)	*Sedum sexangulare*, *S. album*, *S. rupestre*, *S. kamtschaticum*, *S. hybridum*, *S. spurium* 'Dragon's Blood', *S. reflexum*, and *S. ellacombeanum*. Initially recorded as two morphotypes (Sedum A, Sedum B) and resolved to eight species through field verification (L. R. Skabelund with botanist J. Taylor, April 2026). *S. sexangulare* occurred in all 16 plots; the remaining sedums occurred in one to eight plots each. All sedums in the original planting are non-native.

Source: APDesign Research Team - Plant Survival Survey field notes, 2025 and 2026.

Appendix K - Plant Height Data

End-of-season canopy height was measured on November 19, 2025 as the distance from the substrate surface to the top of the plant, living or senesced. Three little bluestem stems were measured per plot; the per-plot means are reported below. Sideoats grama, present mainly in shallow plots, averaged about 42 cm and is descriptive only.

Appendix Table K.1. Mean end-of-season little bluestem height (cm) by plot, with treatment (supplemental irrigation) and plant community location (east or west).

Plot	Substrate	Irrigation	Community	Mean height (cm)
4″ P1	BuildEx	Less	East	75.8
4″ P2	Rooflite	More	West	70.0
4″ P3	Rooflite	Less	East	64.2
4″ P4	BuildEx	More	West	96.3
4″ P5	Rooflite	More	East	102.7
4″ P6	BuildEx	Less	West	84.0
4″ P7	BuildEx	More	East	100.8
4″ P8	Rooflite	Less	West	87.7
8″ P1	Rooflite	Less	East	84.3
8″ P2	BuildEx	More	West	71.7
8″ P3	BuildEx	Less	East	101.0
8″ P4	Rooflite	More	West	73.2
8″ P5	BuildEx	More	East	113.7
8″ P6	BuildEx	Less	West	71.5
8″ P7	Rooflite	More	East	106.0
8″ P8	Rooflite	Less	West	73.2

Source: Plant Height Data for Experimental Plots (November 19, 2025). Key Findings: Grand mean 86.0 cm; range 64.2 cm (4" P3) to 113.7 cm (8" P5). Marginal means: irrigation More 91.8 / Less 80.2; substrate BuildEx 89.3 / Rooflite 82.7; depth 8" 86.8 / 4" 85.2; community East 93.6 / West 78.5. Height is essentially uncorrelated with seasonal cover.

Appendix L - Statistical Output (Analysis of Variance)

The primary analysis is a balanced 2^3 factorial ANOVA of seasonal-mean canopy cover, with substrate depth, substrate type, and irrigation frequency as treatment factors. The two replicates in each treatment cell correspond to the east and west sides of the roof, so the error term (df = 8) represents the within-cell east–west variation. Because the design is balanced, the sums of squares are independent. The pre-existing east-west difference in plant community is described qualitatively rather than entered as a factor in this model. No factor reaches significance at $\alpha = 0.05$; with only 8 error degrees of freedom, the design would need an effect of roughly 30 percentage points to reach significance, so the interpretation rests on the size and directional consistency of the effects rather than on significance.

Appendix Table L.1. Analysis of variance for seasonal-mean canopy cover (%).

The two replicates per cell correspond to the east and west sides of the roof; the error term represents within-cell east–west plant community variation.

Source	df	SS	MS	F	p	η^2
Depth	1	272.5	272.5	1.666	0.233	0.098
Substrate mix	1	518.3	518.3	3.169	0.113	0.186
Irrigation	1	514.0	514.0	3.143	0.114	0.185
Depth × Substrate	1	22.2	22.2	0.136	0.722	0.008
Depth × Irrigation	1	43.5	43.5	0.266	0.620	0.016
Substrate × Irrigation	1	49.9	49.9	0.305	0.596	0.018
Depth × Substrate × Irrigation	1	51.5	51.5	0.315	0.590	0.019
Error (east–west within cell)	8	1308.4	163.5			0.471
Total	**15**	**2780.3**				

Source: Computed from Canopeo_Cover_56_Day_Analysis_Ready.csv. Substrate and irrigation are co-leading ($\eta^2 \approx 0.186$ and 0.185); depth is secondary ($\eta^2 = 0.098$); all examined interactions are deemed to be negligible ($\eta^2 < 0.02$). Residuals meet the normality assumption (Shapiro-Wilk $W = 0.938$, $p = 0.329$).

Appendix Table L.2. Marginal APD-EGR treatment means for seasonal canopy cover (%).

Factor (level 1 vs level 2)	Level 1	Level 2
Depth: 4-inch vs 8-inch	30.4	38.6
Substrate: Rooflite vs BuildEx	28.8	40.2
Irrigation: Less vs More	28.8	40.2
Community: East vs West	31.4	37.6

Source: Canopeo_Cover_56_Day_Analysis_Ready.csv. The area-under-the-curve ANOVA yields the same ordering and comparable effect sizes (Chapter 4).

Appendix M - Artificial Intelligence Use Acknowledgement

This study used three artificial intelligence tools. Their roles are described here in the interest of transparency.

Claude (Anthropic)

The Professional version of Claude, using the Opus 4.8 model, was used for statistical data analysis, figure generation, and writing support throughout the study. The pre-trained model was supplied with project-specific context through the "Claude Projects" workspace, into which the author uploaded the study's data files and reference documents. These included the 57-day Canopeo green-cover data, the 2021–2025 irrigation log, the Kansas Mesonet weather comparison (Manhattan versus Ekdahl, prepared by NRES students), volumetric water content and substrate temperature data from the dataloggers, the APD-EGR plot layout with substrate depth, type, and irrigation treatments, NDVI data from four drone flights over 72 plots, drone-derived green-cover data for the sixteen 4-inch and 8-inch plots, and the 2025 plant-survival survey.

Two dissertations and one thesis (Decker 2021; Alam 2022; Shrestha 2019) and previously published articles on Kansas State University's green roofs were also uploaded to provide context for the study.

Statistical analyses and graphs were produced from the uploaded data through iterative prompting, and statistical results were re-run multiple times to check the replicability of the process. A cross-check using conventional statistical software, such as Python or R, was not performed within the timeframe of this study and would strengthen future work. All AI-assisted analysis and text were reviewed, verified, and interpreted by the author, who takes full responsibility for the content of this thesis.

Consensus

Consensus, an AI-based scholarly literature search engine, was connected to the Claude platform through Claude's connector feature. It was used to support the literature review by locating relevant peer-reviewed sources.

Grammarly

Grammarly was used for grammar, spelling, and clarity editing of the written text only. It was not used to generate content.

Appendix N - UAS and iPhone Images

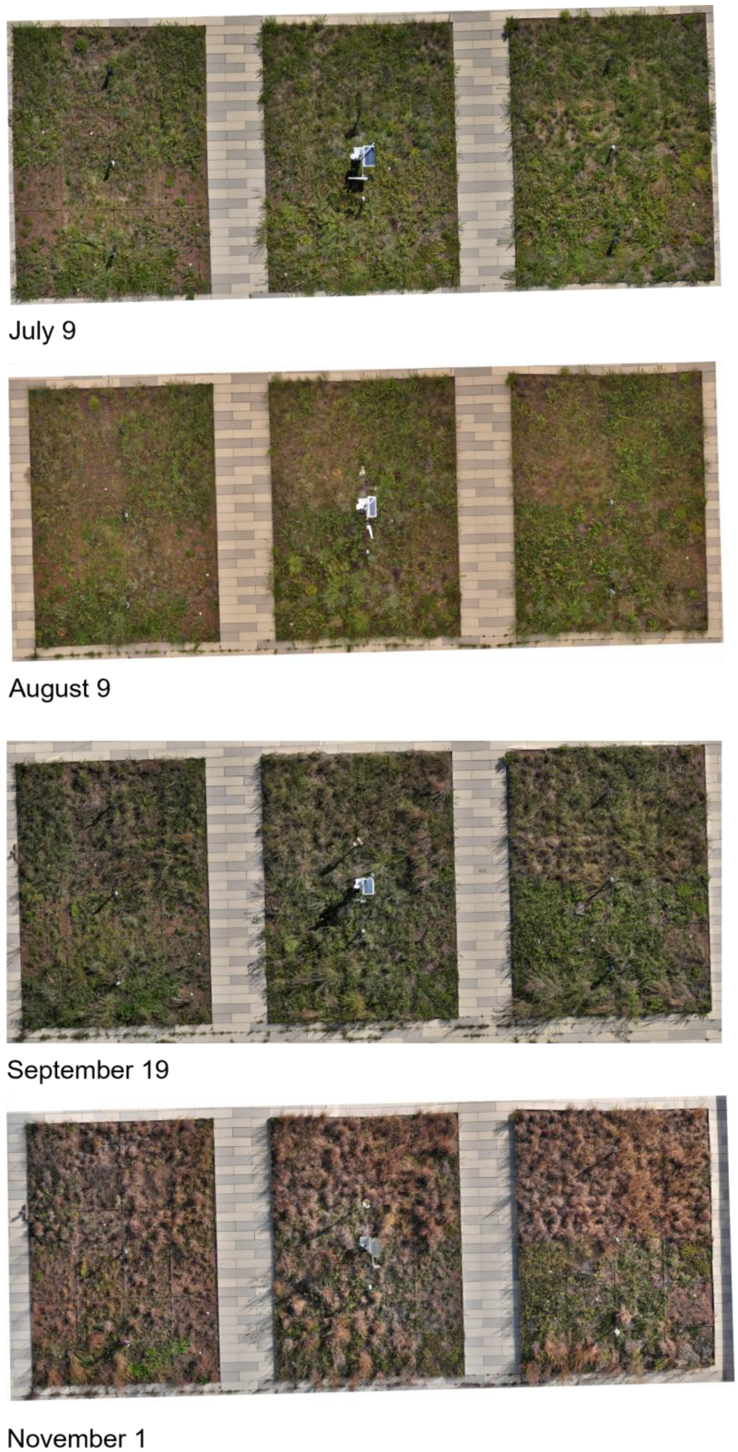

Appendix Figure N.1. UAS RGB images of APD-EGR Plots in July, August, September, and November 2025.

(Images taken and prepared by Kaden Spencer, 2025)

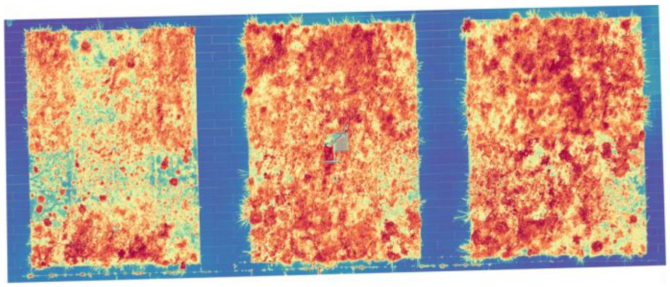

July 9

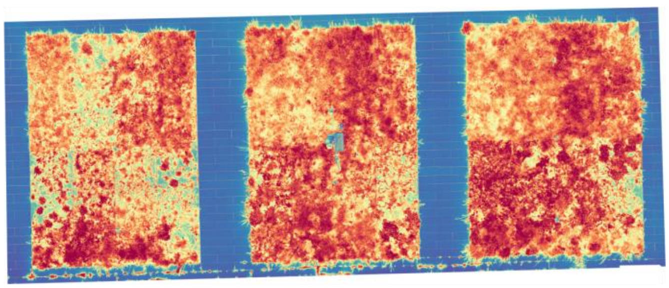

August 9

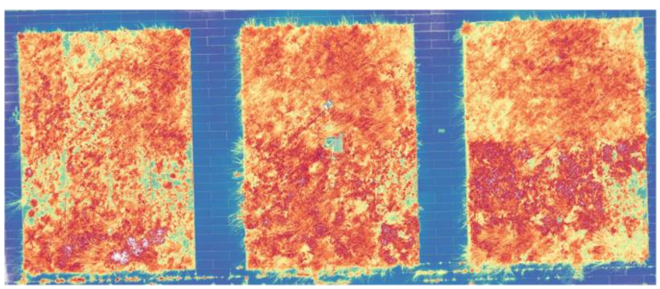

September 19

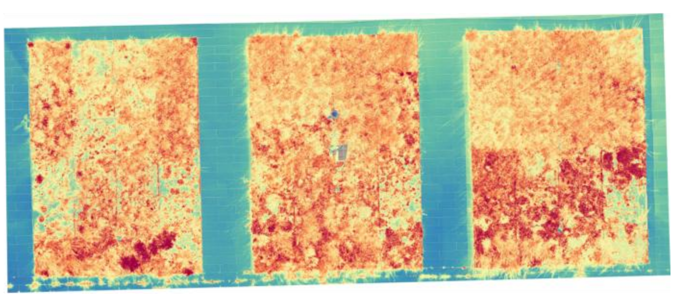

November 1

Appendix Figure N.2. NDVI images of APD-EGR Plots.

(Images taken and prepared by Kaden Spencer, 2025)

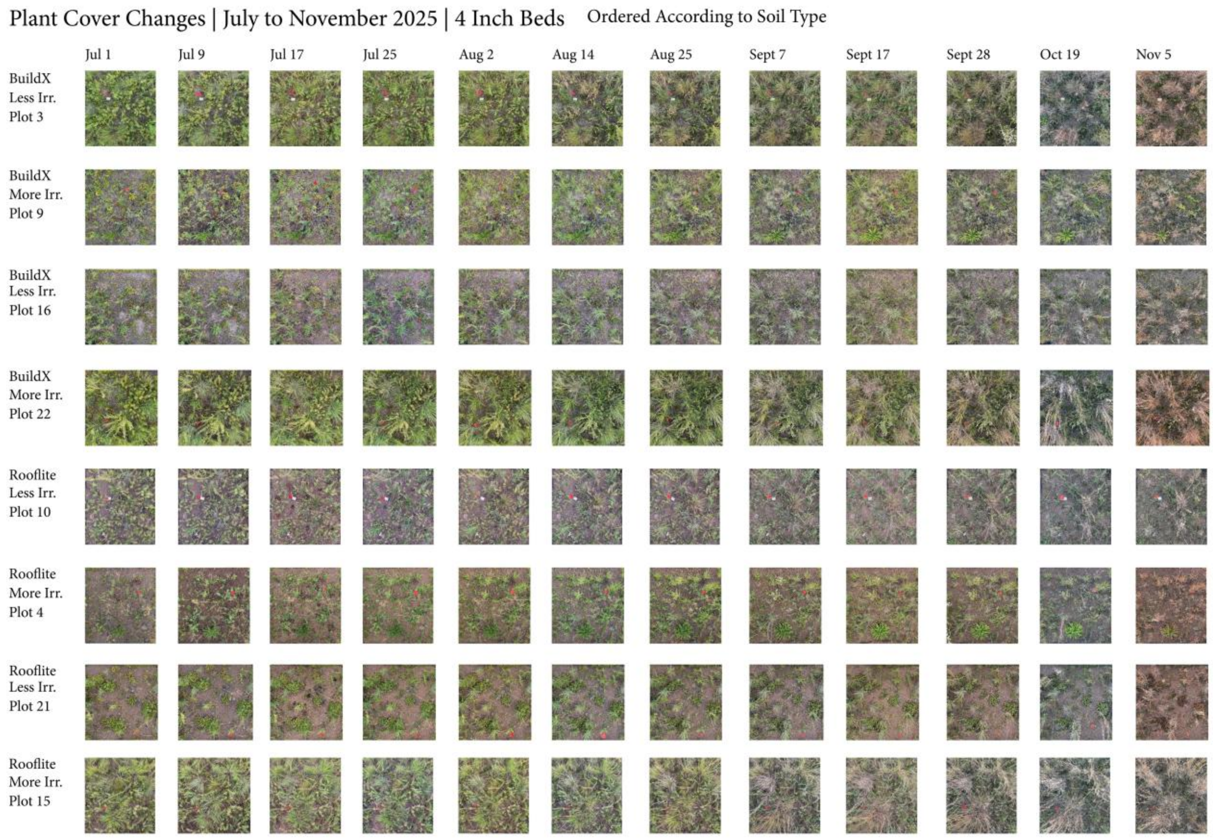

Appendix Figure N.3. iPhone photos of APD-EGR 4-inch beds.

12 days were selected from 56 days to give an overview of how greenness changed on each of the sixteen experimental plots over the season (Photographed by the author, 2025).

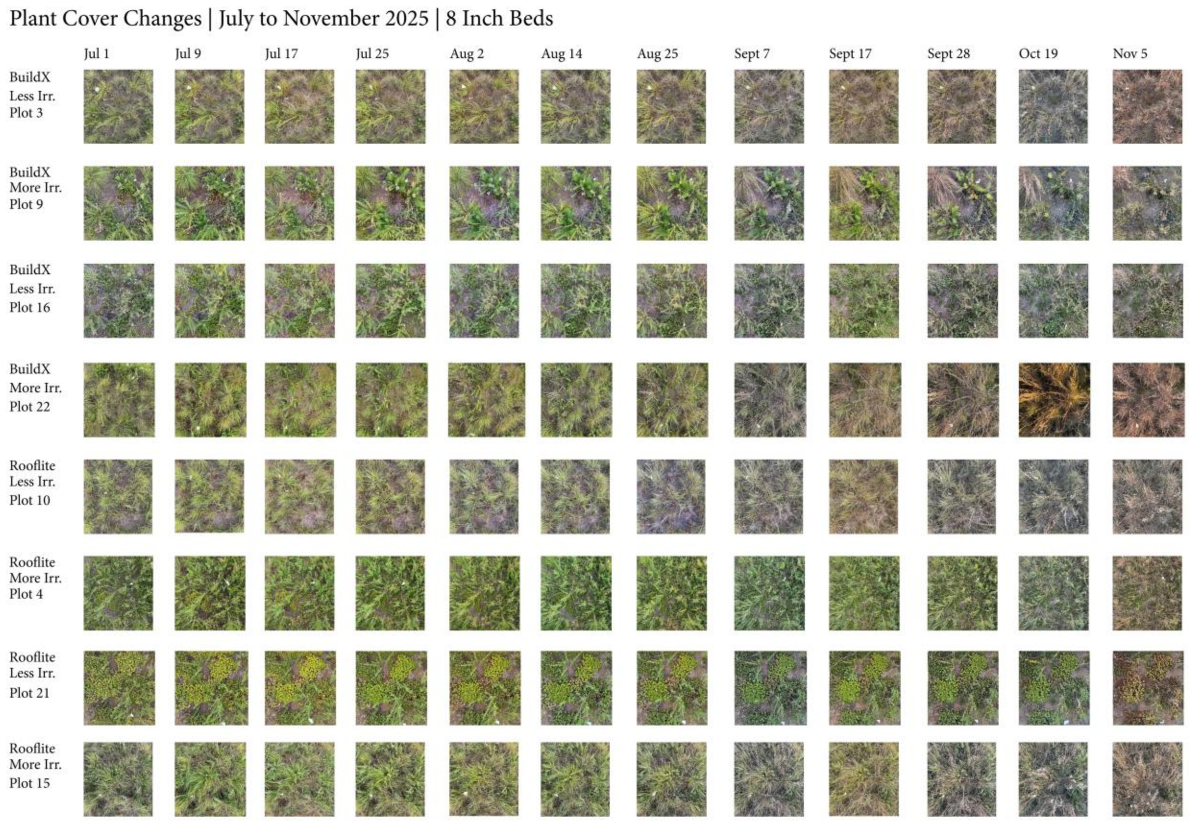

Appendix Figure N.4. iPhone photos of APD-EGR 8-inch beds.

(Photographed by the author, 2025)